

# **New insights into drivers and passengers of tree architecture**

## **Dissertation**

to attain the doctoral degree Doctor of Philosophy (Ph.D.)  
of the Faculty of Forest Sciences and Forest Ecology  
Georg-August-Universität Göttingen

Submitted by

**Yonten Dorji**

Born on November 10, 1983 in Wangdue Phodrang, Bhutan

Göttingen, January 2023

1<sup>st</sup> Referee: **Professor Dr. Dominik Seidel**

2<sup>nd</sup> Referee: **Professor Dr. Holger Kreft**

.....

Additional members of the exam committee:

**Professor Dr. Peter Annighöfer**

Date of Oral examination: **May 2, 2023**



# Table of Contents

List of abbreviations.....	iv
Summary .....	v
Zusammenfassung .....	vii
<b>CHAPTER 1</b> .....	<b>1</b>
1.1 Background of the Study .....	1
1.2 Drivers and Passengers of tree architecture .....	2
1.3 Objectives and Scope of the Dissertation.....	4
1.4 State-of-Art Overview of Laser Scanning Systems.....	5
1.4.1 Uses of Laser Scanning (LiDAR) .....	5
1.4.2 Workings of Light Detection and Ranging techniques (LiDAR).....	6
1.4.3 Mobile Laser Scanning (MLS) overview.....	7
1.4.4 Terrestrial Laser Scanning (TLS) overview .....	8
1.5 Point Cloud Processing and Quantitative Structure Modelling (QSM).....	9
1.6 Fractal analysis and Box-dimension ( $D_b$ ) approach.....	10
1.7 Xylem pressure as a unit for Hydraulic vulnerability .....	12
1.8 Research Study sites .....	12
1.9 References:.....	14
<b>CHAPTER 2</b> .....	<b>20</b>
<b>Response of Beech (<i>Fagus sylvatica</i> L.) Trees to Competition - New Insights from Using Fractal Analysis.....</b>	<b>20</b>
2.1 Introduction .....	22
2.2 Materials and Methods .....	24
2.2.1 Study Sites and Objects .....	24
2.2.2 Laser Scanning.....	26
2.2.3 Point Cloud Processing and Quantitative Structure Models.....	27
2.2.4 Box-dimension, Intercept and Self-Similarity .....	29
2.2.5 Calculation of Competitive Pressure.....	31
2.2.6 Statistical Analysis .....	31
2.3 Results .....	32
2.4 Discussion.....	35
2.5 Conclusions.....	37
2.6 References:.....	39
<b>CHAPTER 3</b> .....	<b>42</b>

<b>Three-dimensional Quantification of Tree Architecture from Mobile Laser Scanning and Geometry Analysis .....</b>	<b>42</b>
3.1 Introduction .....	44
3.2 Materials and Method.....	47
3.2.1 Study site.....	47
3.2.2 Mobile Laser scanning.....	48
3.2.3 Data Collection .....	49
3.2.4 Species information (origin, latitudinal range, and seed dispersal strategy) .....	49
3.2.5 Scan data post-processing .....	50
3.2.6 Statistical analysis .....	51
3.2.7 Fractal analysis with box-dimension .....	52
3.2.8 Topological measure of geometry.....	53
3.3 Results .....	53
3.4 Discussion.....	59
3.5 Conclusion .....	63
3.6 References.....	65
<b>CHAPTER 4 .....</b>	<b>69</b>
<b>Insights into the Relationship Between Hydraulic Safety, Hydraulic Efficiency and Tree Structural Complexity from Terrestrial Laser Scanning and Fractal Analysis .....</b>	<b>69</b>
4.1 Introduction .....	71
4.2 Materials and Methods.....	73
4.2.1 Study site.....	73
4.2.2 Terrestrial LiDAR.....	76
4.2.3 Point Cloud Processing and Quantitative Structure Models (QSM).....	77
4.2.4 Box-dimension ( $D_b$ ).....	78
4.2.5 Xylem pressure measurement ( $P_{12}$ , $P_{50}$ , $P_{88}$ ).....	80
4.2.6 Wood anatomy and hydraulic efficiency .....	81
4.2.7 Statistical Analysis.....	82
4.3 Results .....	82
4.4 Discussion.....	88
4.5 Conclusion .....	91
4.6 References.....	93
<b>CHAPTER 5 .....</b>	<b>98</b>
<b>Synthesis.....</b>	<b>98</b>
5.1 The role of competition on the tree architecture complexity .....	98

5.2	The relation between the tree architecture and solar light angle, seed dispersal strategy, and tree growth performance .....	100
5.2.1	Tree architecture and solar light angle.....	100
5.2.2	Tree architecture and Seed dispersal strategy .....	102
5.2.3	Tree architecture complexity and tree growth performance.....	102
5.3	The linkage between tree architecture and hydraulic vulnerability .....	104
5.4	Limitations of LiDAR systems.....	108
5.5	Conclusion and outlook.....	109
5.6	References.....	112
	<b>List of Tables .....</b>	<b>115</b>
	<b>List of Figures.....</b>	<b>115</b>
	<b>Acknowledgment.....</b>	<b>119</b>
	<b>Curriculum Vitae.....</b>	<b>120</b>

## List of abbreviations

3D	Three-dimensional
ALS	Airborne Laser Scanning (scanner)
CCSA	Cumulative Crown Surface Area
CSA	Crown Surface Area
CV	Crown Volume
$D_b$	Box dimension
$D_h$	Hydraulically-weighted average vessel diameter
DBH/dbh	Diameter at breast height
DevEx	Deviation Explained
EDF	Effective Degrees of Freedom
GAM	Generalized Additive Modeling
GNSSs	Global Navigation Satellite Systems
GPS	Global Positioning System
INSS	Inertial Navigation Systems
IMU	Inertial measurement unit
$K_s$	Specific Hydraulic Conductivity
Ksat	Initial conductivity at full saturation
Laser	Light amplification by stimulated emission of radiation
LiDAR	Light Detection and Ranging
Masl	Meters above sea level
MLS	Mobile Laser Scanning (Scanner)
n.a	Not Available
N.S/ n.s	Non-Significant
$P_{50}$	Water potential at 50% loss of conductivity
QSM	Quantitative Structure Model
Rel.Hmaxarea	Relative height of the maximum horizontal crown area
$S_{50}$	Slope of the vulnerability curve
SLAM	Simultaneous Localization and Mapping
TLS	Terrestrial Laser Scanning (Scanner)
TTH	Total Tree Height

## Summary

Individual tree architecture and species composition perform a critical role in many ecological processes and resources a forest offers, such as wood value, biodiversity, and ecosystem stability. The structure and dynamics of a forest are determined by its individual trees' architecture and growth patterns. In turn, the interaction of ecological parameters and genomic structural components contributes to the architecture and growth of trees. However, understanding how tree structure develops and adapts in response to various factors, such as competition, drought stress, sunlight angle, and resource utilization, is still scarce. Several theories and models exist in advocating and disseminating the concerns and issues about this discipline. However, many aspects are still unknown due to the scarcity of data. Therefore, the scope and aim of this dissertation are to look into the drivers and passengers of tree architecture from empirical evidence.

We quantitatively analyzed the three-dimensional architecture of the trees using LiDAR (light detection and ranging) and fractal geometry approaches. The combination of LiDAR technology and fractal analysis has made it possible to give a holistic, in-depth analysis of tree architecture. Hence providing an avenue to empirically draw links between the trees' architecture (and the complexity of this architecture) and several ecosystem functions, which were not possible in the past. In this thesis, we present three independent papers (chapters 2 to 4) related to exploring the drivers and passengers of tree architecture as follows.

In the first study, we explored the intricate 3D structure of 24 beech (*Fagus sylvatica* L.) trees that grew amid various levels of competitive pressure using 3D LiDAR data from the German Biodiversity Exploratories. We developed robust quantitative structure models (QSMs) of each tree to understand their branching patterns. The box-dimension ( $D_b$ ) method from fractal analysis was used to quantify the architectural complexity and self-similarity of the trees. The findings showed that the competition appears to significantly influence the branching structure of trees, as demonstrated by the strong responses exhibited by various tree architectural measures. A new metric presented here, the 'D<sub>b</sub>-Intercept' (intercept of the regression used to derive the box-dimension), showed the most robust response to competition, with a correlation coefficient of -0.78.

In the second study, we sought to determine whether (i) latitudinal adaptations of crown shape result from distinctive solar inclination angles at a species' origin? (ii)



structural variances in trees are associated with seed dispersal methods? and (iii) tree structural complexity is linked with tree growth performance? We scanned 473 trees using MLS (mobile laser scanning) to obtain 3D data for each tree. The arboretum's environmental conditions were the same for all the tree species being investigated, although coming from different latitudinal regions. Then, applying fractal analysis and the box-dimension method, the tree's structural complexity was quantified. Also, the topological measurement of a tree's top-heaviness (Rel.Hmaxarea) was derived. We observed that trees from higher latitudes had significantly less top-heavy geometry than those from lower latitudes. Therefore, to some extent, a tree species' crown form appears to be influenced by solar elevation angles at the species' origin. Additionally, we revealed that tree species with wind-dispersed seeds had higher tree architectural complexity than those with seeds dispersed by animals ( $p < 0.001$ ). Furthermore, tree structural complexity was positively associated with the trees' radial growth increment ( $p < 0.001$ ).

In the third study, we used terrestrial laser scanning (TLS) to scan 71 trees of 19 species and generated 3D attributes of each tree. We constructed QSMs to characterize their branching patterns. Additionally, the box-dimension approach from fractal analysis was used to assess the overall structural complexity of the trees. The pressures inducing 12%, 50%, and 88% losses of stem hydraulic conductance ( $P_{12}$ ,  $P_{50}$ ,  $P_{88}$ ) of all the concerned trees were measured. Our findings revealed that the tree's structural complexity ( $D_b$ ) relates significantly to xylem safety ( $p < 0.001$ ). The branching geometry also showed significant results relating to xylem pressure ( $p < 0.01$ ). We further observed a close relationship between specific hydraulic conductivity ( $K_s$ ) of the branches and  $D_b$ , while the hydraulically-weighted vessel diameter was also related to  $D_b$  at marginal significance.

Finally, we also conclude that using 3D data from LiDAR in combination with geometrical analysis, including fractal analysis, is a promising tool to investigate tree architecture relating it to ecosystem functionality.

**Keywords:** Tree architecture, LiDAR, Fractal analysis, Box-dimension, Competition, Seed dispersal strategy, Sunlight angle, Tree growth, Climate Change, Xylem pressure, Hydraulic vulnerability.

## Zusammenfassung

Die Architektur und die Artenzusammensetzung der Bäume spielen eine entscheidende Rolle für viele ökologische Prozesse und Ressourcen eines Waldes, wie z. B. den Holzwert, die Artenvielfalt und die Stabilität des Ökosystems. Die Struktur und die Dynamik eines Waldes werden durch die Architektur und die Wachstumsmuster der einzelnen Bäume bestimmt. Das Zusammenspiel von ökologischen Parametern und genomischen Strukturkomponenten trägt wiederum zur Architektur und zum Wachstum der Bäume bei. Das Verständnis dafür, wie sich die Baumstruktur als Reaktion auf verschiedene Faktoren wie Konkurrenz, Trockenstress, Sonneneinstrahlung und Ressourcennutzung entwickelt und anpasst, ist jedoch noch wenig ausgeprägt. Daher ist es Ziel dieser Dissertation, die Treiber und abhängigen Größen der Baumarchitektur anhand empirischer Daten zu untersuchen.

Wir haben die 3D (dreidimensionale) Architektur der Bäume mit Hilfe von LiDAR (Light Detection and Ranging) und fraktaler Geometrie quantitativ analysiert. Die Fortschritte bei der dreidimensionalen Modellierung der Baumarchitektur auf der Grundlage der LiDAR-Technologie und die Anwendung der Fraktalanalyse haben eine eingehende Analyse der Baumarchitektur ermöglicht und damit eine Möglichkeit geschaffen, empirisch Zusammenhänge zwischen der strukturellen Komplexität der Bäume und verschiedenen Ökosystemfunktionen herzustellen, die in der Vergangenheit nicht möglich waren. In dieser Studie werden drei unabhängige Arbeiten (Kapitel 2 bis 4) vorgestellt, die sich mit der Erforschung der Triebkräfte und abhängigen Größen der Baumarchitektur befassen (siehe unten).

In der ersten Studie untersuchten wir die komplexe 3D-Struktur von 24 Buchen (*Fagus sylvatica* L.), die unter unterschiedlichem Konkurrenzdruck wuchsen, anhand von 3D-LiDAR-Daten. Wir entwickelten robuste quantitative Strukturmodelle (QSMs) für jeden Baum, um ihre Verzweigungsmuster zu verstehen. Die box-Dimension ( $D_b$ )-Methode aus der Fraktalanalyse wurde verwendet, um die architektonische Komplexität und Selbstähnlichkeit der Bäume zu quantifizieren. Die Ergebnisse zeigten, dass der Wettbewerb die Verzweigungsstruktur der Bäume erheblich zu beeinflussen scheint, wie die starken Reaktionen verschiedener Baumarchitekturmaße zeigen. Eine neue, hier vorgestellte Metrik, der " $D_b$ -Intercept" (Achsenabschnitt der zur Ableitung der Box-Dimension verwendeten Regression), zeigte mit einem Korrelationskoeffizienten von -0,78 die stärkste Reaktion auf den Wettbewerb.

In der zweiten Studie wollten wir herausfinden, ob (i) Anpassungen der Kronenform an den Sonnenstand im Herkunftsgebiet einer Art, beschrieben durch den Breitenkreis, nachweisbar sind, (ii) ob strukturelle Unterschiede in Bäumen mit den Methoden der Samenverbreitung zusammenhängen? und (iii) ob die strukturelle Komplexität von Bäumen mit der Wachstumsleistung von Bäumen zusammenhängt? Wir haben 473 Bäume mit MLS (Mobile Laser Scanning) gescannt, um für jeden Baum 3D-Daten zu erhalten. Die Umweltbedingungen im Arboretum waren für alle untersuchten Baumarten gleich, auch wenn ihre Arten ursprünglich aus unterschiedlichen Breitengraden stammten. Anschließend wurde mit Hilfe der Fraktalanalyse und der Box-Dimension-Methode die strukturelle Komplexität jedes Baumes quantifiziert. Außerdem wurde das topologische Maß der Kopflastigkeit eines Baumes (Rel.Hmaxarea) abgeleitet. Wir stellten fest, dass Bäume aus höheren Breitengraden eine deutlich weniger kopflastige Geometrie aufwiesen als Bäume aus niedrigeren Breitengraden. Die Kronenform einer Baumart scheint also bis zu einem gewissen Grad von ihrer Heimatumgebung beeinflusst zu werden. Darüber hinaus zeigte sich, dass Baumarten mit Samen, die durch Wind verbreitet werden, eine höhere architektonische Komplexität aufweisen als Baumarten mit Samen, die durch Tiere verbreitet werden ( $p < 0,001$ ). Darüber hinaus stand die strukturelle Komplexität der Bäume in einem positiven Zusammenhang mit dem radialen Wachstumszuwachs der Bäume ( $p < 0,001$ ). In der dritten Studie scanneten wir mit terrestrischem Laserscanning (TLS) 71 Bäume von 19 Arten und erstellten 3D-Attribute von jedem Baum. Wir konstruierten QSMs, um ihre Verzweigungsmuster zu charakterisieren. Zusätzlich wurde der Ansatz der Box-Dimensionen aus der Fraktalanalyse verwendet, um die strukturelle Gesamtkomplexität der Bäume zu bewerten. Bei allen betroffenen Bäumen wurden die Drücke gemessen, die zu einem Verlust der hydraulischen Leitfähigkeit des Stammes von 12 %, 50 % und 88 % führen ( $P_{12}$ ,  $P_{50}$ ,  $P_{88}$ ). Unsere Ergebnisse zeigten, dass die strukturelle Komplexität des Baumes ( $D_b$ ) signifikant mit der Xylemsicherheit zusammenhängt ( $p < 0,001$ ). Die Verzweigungsgeometrie zeigte ebenfalls signifikante Ergebnisse in Bezug auf den Xylemdruck ( $p < 0,01$ ). Darüber hinaus wurde eine enge Beziehung zwischen der spezifischen hydraulischen Leitfähigkeit ( $K_s$ ) der Äste und  $D_b$  festgestellt, während der hydraulisch gewichtete Gefäßdurchmesser ebenfalls mit  $D_b$  in Verbindung gebracht wurde, allerdings mit marginaler Signifikanz.

Abschließend kommen wir zu dem Schluss, dass die Verwendung von 3D-Daten aus LiDAR in Kombination mit geometrischer Analyse, einschließlich Fraktalanalyse, ein vielversprechendes Instrument zur Untersuchung der Baumarchitektur darstellt.

**Schlüsselwörter:** Baumarchitektur, LiDAR, Fraktalanalyse, Box Dimension, Wettbewerb, Samenausbreitungsstrategie, Sonneneinstrahlungswinkel, Baumwachstum, Klimawandel, Xylemdruck, Hydraulische Anfälligkeit.

# CHAPTER 1

---

## Introduction

### 1.1 Background of the Study

Leonardo da Vinci was a pioneer in the study of tree architecture and shape. He observed that the cross-sectional area of branches remained consistent throughout the branching orders of trees (Da Vinci, 1967; Richter, 1970). Later, Hallé & Oldeman (1970) detailed the "concept of tree architecture" and its significance to the study of ecology and the growth mechanism of trees. They developed 23 different and distinct tree architecture models, often known as "genetic blueprints," to elucidate tree structure and form. These models are considered a universal representation of tree growth for a wide range of species (Hallé et al. 1978).

The organization and function of a forest ecosystem are ultimately determined by the species composition and structure of its individual trees (West et al., 2009; Price et al., 2012; Seidel et al., 2019a). The structural traits and species composition of a stand directly influence a variety of ecological activities and services provided by a forest, which include timber (Ishii et al., 2004), habitat range (MacArthur & MacArthur, 1961), aesthetic value (Ribe et al., 2009), carbon storage (Calders et al., 2022), and ecosystem strength (Neill & Puettmann, 2013). Additionally, the diversity of tree species in forest stands results in variations in tree crown measures and sunlight interceptions, which impacts the forest's ecosystem growth and general vitality (Sterck et al., 2001). Thus, tree architecture and growth study are relevant to many fields, including phylogeny and taxonomy, ecological modeling, tree physiology, remote sensing of landscapes, and carbon stock estimates for climate change adaptation and mitigation measures (Malhi et al., 2018).

Until recent times, when the somewhat qualitative structural models of the past could not meet the requirements of current science, extremely labour- and time-intensive approaches were utilized to investigate tree structure in depth (Bentley et al., 2013). Conventional measures of tree architectural attributes, such as height (Sterck & Bongers,

2001), stem DBH (Gering & May, 1995), or crown base height (Sprinz & Burkhardt, 1987), among many others, were used to evaluate tree structure and shape quantitatively. Lately, using three-dimensional data derived from state-of-art laser scanning technology (LiDAR), tree structural attributes such as tree crown volume, crown surface area, crown radius, and a detailed branching pattern with branch angles, lengths, and volumes have been derived (Tao et al., 2015; Dorji et al., 2020; Neudam et al., 2022) with levels of accuracy greater than the most prominent allometric models used worldwide (Liang et al., 2014; Newnham et al., 2015; Demol et al., 2022). In reality, LiDAR is transforming how we observe trees (Gonzalez de Tanago et al., 2018) by enabling a detailed tree structure analysis. Consequently, this has given a way to examine and comprehend how tree architecture varies in response to diverse elements, including competition, drought, light availability, and seed distribution strategy, which will be empirically explored in the entire scope of this thesis.

This dissertation's primary scopes are outlined in Chapter 1, which serves as the introduction. It also offers a comprehensive theoretical foundation and the driving force behind this dissertation study. The fundamental theories of tree architecture are discussed, along with the preamble to the drivers and passengers of tree structure complexity. At the outset, I would like to clarify that we are not the first to propound and test the theories of the study mentioned here. However, we used new techniques (TLS and MLS) and approaches (fractal geometry) to empirically analyze and gain insights into the relationship between tree structural complexity and the influencing key parameters. The workings of the LiDAR devices used here for the field studies are briefly discussed, i.e., the TLS (Terrestrial Laser Scanning) and MLS (Mobile Laser Scanning). Also covered in the first chapter are the methods and approaches used in obtaining the 3D model of the tree architecture through Point Cloud Processing and Quantitative Structure Modelling. Further, the fractal analysis (box-dimension and self-similarity) used to quantify the structural complexity of the trees is discussed in detail.

## **1.2 Drivers and Passengers of tree architecture**

Tree architecture and shape span from narrow, post-like forms to enormous, spreading, multilayered crowns (Beech et al., 2017), and it is unlikely that any two trees on the planet, even within a species, are identical in terms of all aspects of their architecture (Seidel et al., 2019b). Tree growth and form are not stochastic (Valladares & Niinemets,

2007); it is decided by the tree's response to various abiotic and biotic factors (Lang et al., 2010) within the context of its genetic makeup (Wu & Hinckley, 2001; Burkardt et al., 2021). Tree growth and form are determined by several environmental factors such as latitude and solar angle (Oker-Blom & Kellomäki, 1982; Kuuluvainen, 1992), soil (Zeide & Gresham, 1991), seed dispersal strategy (Malhi et al., 2018; Dorji et al., 2021), wind (De Langre, 2008; Nishimura & Setoguchi, 2011), temperature (Niinemets & Kull, 1995; Went, 1953; Moles et al., 2014) availability of water resources (Archibald & Bond, 2003; Scharnweber et al., 2011), competitions (Muth & Bazzaz, 2003; Juchheim et al., 2017b), slope exposition (Johnson et al., 2019), pest and diseases (Setiawan et al., 2014), anthropogenic activities (Schaberg et al., 2008), and altitude (Nishimura & Setoguchi, 2011) amongst many others. However, most studies mentioned above are based on theories and model simulations and less on empirical evidence. For example, pioneering studies of crown shape evolution were carried out by Iwasa, Cohen, and Leon (1985) using light competition interaction models. Also, the popular theory that sun-light angle influences the type of crown shape of the trees according to their latitude is based on ecological modelling and simulations by Kuuluvainen (1992) and subsequently corroborated by many other studies later (Niinemets & Kull, 1995; Valladares & Niinemets, 2007). Similarly, there has been limited research to date that has looked at the connection between tree architectural complexity and seed dispersion technique.

As a consequence of climate change, the occurrence of severe droughts is increasing in several parts of the world (Trenberth et al., 2014; Settele et al., 2014). While forest systems are susceptible to a variety of severe climatic conditions, drought and its concomitant disruptions have the largest impact worldwide (Reichstein et al., 2013). Tree mortality is most likely linked to a plant's inability to control its hydraulic network, especially the xylem structural adjustments that require new growth (McDowell & Allen, 2015; Rowland et al., 2015; Choat et al., 2018). Hence investigating the adaptative scope of these attributes is critical for anticipating future responses of trees to climate change. Therefore, this study also examined how tree architectural complexity affects susceptibility to drought stress.

This dissertation delves into the drivers and passengers of tree architecture using new methodologies, i.e., LiDAR technology (light detection and ranging) and fractal geometry. We contend that characterizing tree architecture may be done effectively and comprehensively using three-dimensional data from laser scanning, especially when used in

conjunction with cutting-edge tools for evaluating geometry, such as the box-dimension approach. To measure complexity and relate it to a variety of functional patterns of trees and forests, geometrical traits and structural complexity can be reduced to a single number and applied to individual trees or even to entire forest stands. This opens up new perspectives on how terrestrial ecosystems' structure and function are related.

### **1.3 Objectives and Scope of the Dissertation**

The first paper's detailed scope and intent are outlined in chapter 2 of the dissertation. The aim was to understand how tree architecture changes in response to competition. Precisely, we investigated the response of beech (*Fagus Sylvatica*. L) trees to competitive pressures.

The objective and hypothesis of the first paper of the dissertation are as follows:

i. Examine the efficacy and implications of fractal analytic measures to gain new insights into the effects of competition on tree architecture. To elaborate, use the box dimension ( $D_b$ ), the self-similarity approach from fractal analysis, and conventional measures of tree architecture to analyze the effect of competition on the architectural changes of beech (*Fagus sylvatica* L.) trees.

We hypothesize that there is a strong effect of competition on the tree's structural complexity. To be precise, competition affects the a) internal branching patterns (detailed branch numbers, angles, and length) and also b) tree structural complexity represented by fractal measures (box-dimension and self-similarity)

The second paper's purpose and intent are outlined in Chapter 3 of the dissertation. We scanned 473 trees with MLS and acquired 3D data for each tree. To quantify the architectural complexity of the tree, we employed fractal analysis and a topological measure of geometry to investigate the link to various parameters.

The objective and hypothesis of the second paper are as follows:

ii. Quantify the three-dimensional attribute of tree architecture and explore the relationship between seed dispersal strategy and tree structural complexity. Also, use  $D_b$  to observe the link between tree structure complexity ( $D_b$ ) and tree growth performance (represented by DBH). Furthermore, to empirically address the popular Kuuluvainen's theory of tree crown shape depending on the latitude of a species' home range owing to different sunlight angles. Here, we use the tree crown geometry metric (Relative height of the maximum horizontal crown area [Rel.Hmaxarea]) of the trees.



We hypothesize that tree structural complexity is related to its seed dispersal strategy, where the complexity of wind-dispersed trees would show higher complexity than that of animal-dispersed trees. Also, higher tree growth performance would show higher tree structural complexity and vice versa. Furthermore, we hypothesize that trees from various latitudes display crown morphologies corresponding to adaptations to the environment in their home range latitude.

The third paper's purpose and aim are drafted in chapter 4, i.e., to explore the relationship between drought stress and tree structural complexity.

3. explore the relationship between drought stress and tree structural complexity. We used terrestrial laser scanning (TLS) to scan 71 trees of 18 species and generated 3D attributes of each tree. Then the measures of xylem safety ( $P_{12}$ ,  $P_{50}$ ,  $P_{88}$ ), specific hydraulic conductivity ( $K_s$ ), and hydraulically-weighted vessel diameter ( $D_h$ ) were obtained and related to tree structural complexity ( $D_b$ ).

The objective and hypothesis of the third paper are as follows:

**iii.** Study and evaluate the relationship between hydraulic safety, hydraulic efficiency and the tree's structural complexity. Find out which specific traits of the tree's structural complexity are sensitive to drought exposure.

We hypothesize that the tree's structural complexity directly relates to hydraulic vulnerability. Furthermore, the branching network of the tree is significantly affected when it is exposed to drought.

Finally, in Chapter 5, the synopsis of the dissertation synthesizes all of the other/previous chapters (Chapters 2 to 4). Furthermore, the analytic techniques are assessed to pinpoint issues regarding the fractal nature of tree design and the usage of TLS and MLS to analyze architecture complexity. Limitations and considerations are also covered. An overall conclusion is drawn, signifying this study's relevance to science and the world with the broader framework. Future study exploration possibilities are also highlighted with possibilities of new tools.

## **1.4 State-of-Art Overview of Laser Scanning Systems**

### **1.4.1 Uses of Laser Scanning (LiDAR)**

The best way to measure forest structural attributes is with high-quality 3D data from LiDAR (Potter, 2019). There are three types of LiDAR systems: Airborne (ALS), Terrestrial tripod-based (TLS), and Mobile (MLS). These systems have evolved in the last two

decades and are now used to accurately and efficiently measure various aspects of forest structure, making them a valuable tool in forestry. LiDAR technology is used in forest inventory to measure various characteristics, such as volume (Astrup et al., 2014), biomass (Hackenberg et al., 2015), canopy height (Bayer et al., 2013), and canopy openness (Juchheim et al., 2017a). It is also used in forest operations (Liang et al., 2018), for monitoring landslides (Travelletti et al., 2008), estimating afforestation and secondary succession (Janus & Bozek, 2018), mapping urban forests (Holopainen et al., 2013), wildlife habitats and forest fires (Kelly & Di Tommaso, 2015).

Laser scanners can retrieve detailed forest information without being destructive and invasive (Malhi et al., 2018). While LiDAR equipment is costly, it performs quick and efficient data collection and can easily compensate for the cost incurred (Williams et al., 2013).

Airborne laser scanning has the potential to cover vast and rugged terrain (Williams et al., 2013). It can create 3D models of large forest areas with rapidity and high efficiency (Akay et al., 2009).

Since 2002, terrestrial laser scanning (TLS) has been used in forestry (Hopkinson et al., 2004). The use of TLS has made it possible to accurately and efficiently map forest structures in great detail, which was not possible before (Malhi et al., 2018). TLS can provide high-resolution data on tree attributes, particularly in the understory vegetation where other methods, such as ALS, are limited (Simonse et al., 2003).

The development of MLS (mobile laser scanning) technology has made it easier and more efficient to survey forests, as it does not require the use of bulky accessories like TLS (Bauwens et al., 2016). MLS can quickly acquire high-quality data (Qian et al., 2016). Additionally, MLS can measure the detailed under-the-canopy structures, which is not possible with ALS (Williams et al., 2013).

In our study here, we used Mobile Laser Scanning and Terrestrial Laser Scanning to investigate the drivers and passengers of tree architecture since we were interested in small-scale architectural differences of individual trees.

#### ***1.4.2 Workings of Light Detection and Ranging techniques (LiDAR)***

LiDAR technology can measure and model the dimensions of forest structures (Potter, 2019). LiDAR sensors are mounted on platforms that are either stationary (Terrestrial LiDAR) or moving (ALS, MLS) during the application process (Lin et al., 2010). To determine the distance between a target object and the device employed, forward and re-

turning pulse laser light is used (Dubayah & Drake, 2000). By integrating information from the LiDAR instrument's Inertial measurement unit (IMU) and, in some cases, additional Global Navigation Satellite Systems (GNSSs) with light pulses, this technique produces three-dimensional information on the object of interest (Qian et al., 2016), so-called point clouds. Every point in the point cloud will have three-dimensional spatial coordinates, if needed, referenced to global coordinate systems or another reference of choice (Rieg et al., 2014). Consequently, an accurate 3D model of the real world is created.

### **1.4.3 Mobile Laser Scanning (MLS) overview**

There are different terminologies for the Slam-based Mobile Laser scanning systems used by the scientific community, and this, in particular, has to be brought into accordance (Gollob et al., 2020). The different names used are WLS: Wearable laser scanning (Cabo et al. 2018), MTLs: Mobile terrestrial laser scanning (Méndez et al., 2014), HMLS: Handheld mobile laser scanner (Vatandaslar et al. 2020), HLS: Hand-held laser scanner (Oveland et al., 2018), PLS: Personnel laser scanning (Chen et al. 2019). We have used the term Mobile Laser scanning (MLS) in our study.

The MLS device used here is GeoSLAM ZEB-HORIZON (Geoslam Zebedee Horizon, Geoslam Ltd., UK 2019), primarily focused on accurate 3D measurement and mapping of the environment without a need for GPS signal and provides a rapid and simple means of capturing 3D point cloud data. It saves the time required to set up a scanner and data registration associated with the traditional terrestrial laser scanning method and is therefore considered highly efficient. The maximum range of the ZEB horizon is 100 m, with a recommendation of fewer than 50 meters to ensure good point density. The field view of the MLS is 360° horizontal and 270° vertical. It uses a laser with a wavelength of 903 nm and scans at the rate of 300,000 points per second. The scan range noise is  $\pm 30$  mm. The scanner continuously records the surroundings as it moves around using the SLAM-Algorithm (Simultaneous Locating and Mapping).



**Figure 1.1** Hand-held mobile scanning device (ZEB HORIZON, GeoSLAM, 2019) used in this study.

#### **1.4.4 Terrestrial Laser Scanning (TLS) overview**

We also used the Faro Focus M70 Terrestrial Laser Scanner (Faro Technologies Inc., Lake Mary, FL, USA) to obtain detailed 3D point cloud data of study trees. TLS was used in our studies 1 and 3 (**Chapter 2 and Chapter 4**). The instrument uses laser light with a 1550 nm wavelength for scanning the environment up to a distance of 70 m, covering a field of view of  $300^{\circ} \times 360^{\circ}$  with a resolution of 0.03 degrees resulting in 10,240 points per  $360^{\circ}$ . The scanner was set up on a tripod at 1.3 meters and levelled horizontally using a bubble level.

Scanning was carried out during a dry period with no wind when the trees were in leafless condition to guarantee the best visibility of the entire wooden tree crown. We performed a multi-scan procedure of all trees, with four to six scans for every tree. We scanned each tree from four corner points with the tree always in the centre, also referred to as a corner set-up in the literature (Zande et al. 2008). One or two additional scans were performed if corner-views seemed incapable of capturing the entire crown due to self-shading. During scanning, we applied the instrument's standard filters (clear contour and clear sky). After that, Faro Scene (Faro Technologies Inc., Lake Mary, FL, USA) automatically recorded, processed, and transferred the scan data as a single xyz-files. The generated 3D image of each tree is a composite of millions of 3D measuring points, producing a precise and detailed replica of our study trees in the field. Therefore,

with the TLS method, each study tree was made accessible as 3D high-resolution point clouds depicting the actual tree (e.g., two samples in Figure 4.3 of Chapter 4)



**Figure 1.2** A tripod-mounted Faro Focus 3D TLS (Faro Focus M70 Terrestrial Laser Scanner) that is placed 1.3 meters above the ground at the Stutel-Arboretum.

## **1.5 Point Cloud Processing and Quantitative Structure Modelling (QSM)**

It was necessary to manually segregate the research trees from the rest of the forest using the point cloud of a study tree and its environment. Leica Cyclone Software was used to do this manually (Leica Geosystems, Heerbrugg, Switzerland). Using the free and open-source CloudCompare software (version 2.10.1, available at <https://www.danielgm.net/cc/>), each tree was manually separated from the background throughout the scan. CompuTree software (Version 5.0, CompuTree Group; [http://computree.onf.fr/?page\\_id=42](http://computree.onf.fr/?page_id=42)) was then used to generate quantitative structure models (QSM) for all study trees. A QSM model depicts the tree point cloud constructed from cylinders of diverse diameters and lengths. We applied the same QSM-parameter configurations for all trees to ensure the reproducibility of our observations. Clustering tolerance was set at 1 cm, with a maximum of 600-point clusters containing at least 400 points each. If fewer clusters are found, the software will automatically modify them.

To ensure greater reliability of our findings, we decided to use identical QSM-parameter values across all trees. We are unaware of any method enabling less biased quality control for the quantitative structure models. For all trees, we used QSM models to acquire detailed information on the branching architecture of the trees. We obtained the i) total branch volume, ii) total branch length, iii) mean branch angle up to 3<sup>rd</sup> order of branches, iv) mean branch length up to 3<sup>rd</sup> order of branches, and v) mean branch volume up to 3<sup>rd</sup> order of branches. An exemplary tree QSM with a cylindrical demonstration of branching patterns is depicted in Figure 4.2 of chapter 4).

## **1.6 Fractal analysis and Box-dimension ( $D_b$ ) approach**

To ascertain the overall structural complexity of each tree, we applied an algorithm created in Mathematica (Wolfram Research, Champaign, USA), as illustrated in Seidel (2018). The box-dimension can be regarded as a holistic gauge of a tree's architectural complexity (Seidel et al., 2019b). This method is based on the revolutionary works of Mandelbrot (1977) and a breakthrough investigation by Sarkar & Chaudhuri (1994). The  $D_b$  of each tree was computed by calculating the number of simulated boxes of a specific size required to contain all of the above-ground tree components in the point cloud. We performed along the steps outlined in Seidel et al. (2019a). In essence, we counted the number of simulated boxes of a specific size required to include all above-ground tree parts in the point cloud in order to estimate  $D_b$ . These numbers of boxes are calculated for various box sizes, commencing with the largest box, which is the smallest bounding box encompassing the whole tree. Then moving on to gradually smaller boxes, each of which is consistently 1/8<sup>th</sup> the volume of the prior box-size (or half the edge length). The demo showed in figure 1.4 below. The lower cut-off (smallest box) in this procedure was defined to be the last sub-box still larger than the point cloud resolution. Here we picked 10 cm as a careful option.

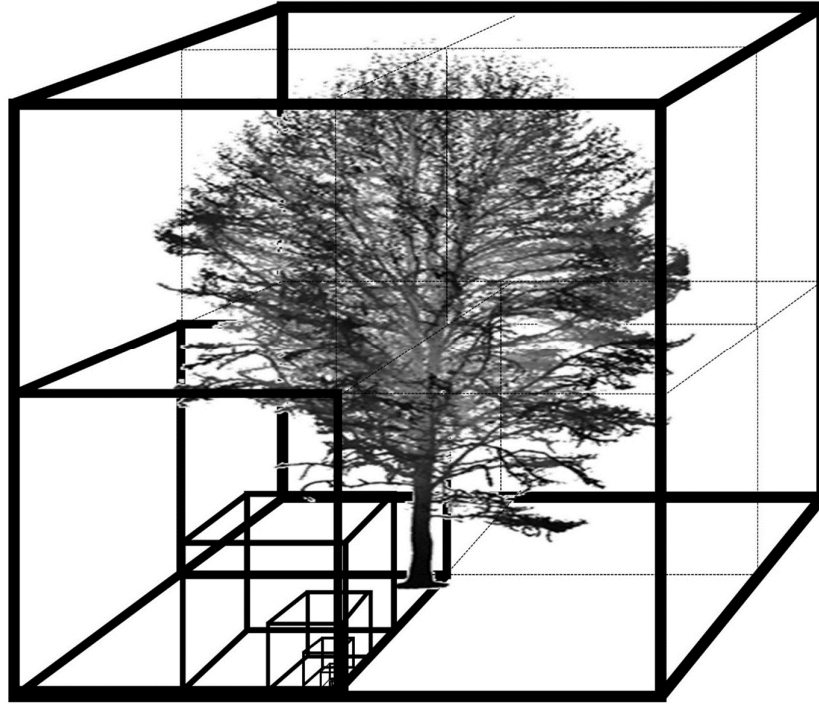


**Figure 1.3** Shows the various box sizes, commencing with the largest box, which is the smallest bounding box encompassing the whole tree, and moving on to gradually smaller boxes.

A least-squares line was then fitted across the scatterplot of the logarithm of required number of boxes (variable  $Y$ ) over the logarithm of the inverse of the actual box size (the  $X$  variable). The slope of the regression line is the box-dimension ( $D_b$ ). The coefficient of determination ( $R^2$ ) is a measure of the tree architecture's self-similarity across the various tested dimensions (box sizes), and the intercept of the regression line ( $D_b$ -intercept) with the  $y$ -axis is a representation of the tree size (Seidel et al., 2019a). See figure 2.4 of chapter 2 for visualization.

In theory, every 3D object's  $D_b$  could range from 1 to 3, with a cubic object's  $D_b$  being 3 and a pipe-like object's  $D_b$  being 1 (Seidel et al., 2019b; see also figure 3.4 of chapter 3). However, a  $D_b$  of 3 cannot be anticipated for trees (Mandelbrot, 1977). Therefore, a  $D_b$  of 2.72, corresponding to an object called Menger-sponge, is considered the highest  $D_b$  a tree could obtain (Seidel et al., 2019a). However, again, a  $D_b$  of 2.72 would rather be unfavourable for light utilization owing to the tree's enhanced self-shading (cf. Seidel et al., 2019a). As a result, in reality, trees ought to have a  $D_b$  between 1 and a value less than 2.72. (Seidel, 2018).

## 1.7 Xylem pressure as a unit for Hydraulic vulnerability

Xylem pressure leading to cavitation and embolism is often utilized as an index of resistance to xylem breakdown under drought conditions (Meinzer et al., 2009; Rowland et al., 2015). Drought causes greater xylem stress and an elevated risk of emboli spreading across the xylem network, resulting in systemic vascular deterioration (Brodribb & Cochard, 2009; Rodriguez et al., 2018). These characteristics determine how quickly plant tissue degrades during a dry spell and the threshold at which water deficit results in hydraulic collapse and death (Martin-StPaul et al., 2017; Blackman et al., 2016). During a water deficit, all drought-related deaths revolve around increased xylem tension (Choat et al., 2018). Therefore, to compare the hydraulic vulnerability of different tree species, xylem pressure at different levels of loss in conductivity (as an index of hydraulic vulnerability) was measured for all our study trees in this research. It was denoted by  $P_{12}$  (xylem pressure at 12% loss of conductance),  $P_{50}$  (xylem pressure at 50% loss of conductance), and  $P_{88}$  (xylem pressure at 88% loss of conductance). The detailed process of how the xylem pressure is obtained is outlined in the topic heading 4.2.5 of Chapter 4.

## 1.8 Research Study sites

For our first study (Chapter 2), the research data were obtained as part of the Biodiversity Exploratories project in Germany (Fischer et al., 2010), which covered a range of precipitation and temperature conditions across the country. The study sites were located in the Swabian Alb, Hainich-Dün, and Schorfheide-Chorin regions. The study's design can be found in more detail in the publication by Metz et al. (2019). The locations of the study sites and the study design are depicted in Figure 2.1 of Chapter 2.

The second and third studies were carried out in Stutel Arboretum. This research is part of the extensive Klimabäume Stutel project, which is overseen by the Bavarian State Institute for Viticulture and Horticulture (LWG). The study was conducted in Stutel-Arboretum, located on the right bank of the river Main, near Wuerzburg, Bavaria, Germany, at an elevation of 180 meters above sea level. The coordinates are 49° 51' 49" N and 9° 51' 8" E. The region's average annual temperature is 9.5 °C, with an average annual precipitation of 603 mm. The region has a continental climate, and as such, it endures periodic drought episodes, particularly during the hot summer months. The soil is mostly sandy anthrosol, with a pH of 7.3. The Stutel-Arboretum is home to over 400



different tree species, which were originally grown in various nurseries across Europe and Asia before being transferred to the arboretum as young seedlings, around two years old.

The LWG established plantations at the arboretum in 2010 to investigate the potential of different tree species as urban trees that can withstand droughts. The trees in the arboretum are observed for their growth and development under the same environmental conditions. However, they are not altered in any way, such as with fertilization or irrigation. They are left to grow in their natural state without any disturbances.

## 1.9 References:

- Akay, A. E., Oğuz, H., Karas, I. R., & Aruga, K. J. E. m., & assessment. (2009). *Using LiDAR technology in forestry activities*, 151(1-4), 117-125.
- Archibald, S., & Bond, W. J. (2003). Growing tall vs growing wide: tree architecture and allometry of *Acacia karroo* in forest, savanna, and arid environments. *Oikos*, 102(1), 3-14.
- Astrup, R., Ducey, M. J., Granhus, A., Ritter, T., & von Lüpke, N. (2014). Approaches for estimating stand-level volume using terrestrial laser scanning in a single-scan mode. *Canadian Journal of Forest Research*, 44(6), 666-676.
- Bauwens, S., Bartholomeus, H., Calders, K., & Lejeune, P. (2016). Forest inventory with terrestrial LiDAR: A comparison of static and hand-held mobile laser scanning. *Forests*, 7(6), 127.
- Bayer, D., Seifert, S., & Pretzsch, H. (2013). Structural crown properties of Norway spruce (*Picea abies* [L.] Karst.) and European beech (*Fagus sylvatica* [L.]) in mixed versus pure stands revealed by terrestrial laser scanning. *Trees*, 27(4), 1035-1047.
- Beech, E., Rivers, M., Oldfield, S., & Smith, P. P. (2017). GlobalTreeSearch: The first complete global database of tree species and country distributions. *Journal of Sustainable Forestry*, 36(5), 454-489.
- Bentley, L. P., Stegen, J. C., Savage, V. M., Smith, D. D., von Allmen, E. I., Sperry, J. S., ... & Enquist, B. J. (2013). An empirical assessment of tree branching networks and implications for plant allometric scaling models. *Ecology letters*, 16(8), 1069-1078.
- Blackman, C. J., Pfautsch, S., Choat, B., Delzon, S., Gleason, S. M., & Duursma, R. A. (2016). Toward an index of desiccation time to tree mortality under drought. *Plant, Cell & Environment*, 39(10), 2342-2345.
- Burkardt, K., Pettenkofer, T., Ammer, C., Gailing, O., Leinemann, L., Seidel, D., & Vor, T. (2021). Influence of heterozygosity and competition on morphological tree characteristics of *Quercus rubra* L.: a new single-tree based approach. *New Forests*, 52(4), 679-695.
- Cabo, C., Del Pozo, S., Rodríguez-González, P., Ordóñez, C., & González-Aguilera, D. (2018). Comparing terrestrial laser scanning (TLS) and wearable laser scanning (WLS) for individual tree modeling at plot level. *Remote Sensing*, 10(4), 540.
- Calders, K., Verbeeck, H., Burt, A., Origo, N., Nightingale, J., Malhi, Y., ... & Disney, M (2022). Laser scanning reveals potential underestimation of biomass carbon in temperate forest. *Ecological Solutions and Evidence*.
- Chen, S., Liu, H., Feng, Z., Shen, C., & Chen, P. (2019). Applicability of personal laser scanning in forestry inventory. *PLoS One*, 14(2), e0211392.
- Choat, B., Brodribb, T. J., Brodersen, C. R., Duursma, R. A., López, R., & Medlyn, B. E. (2018). Triggers of tree mortality under drought. *Nature*, 558(7711), 531-539.
- De Langre, E. (2008). Effects of wind on plants. *Annu. Rev. Fluid Mech.*, 40, 141-168.
- Demol, M., Verbeeck, H., Gielen, B., Armston, J., Burt, A., Disney, M., ... & Calders, K. (2022). Estimating forest above-ground biomass with terrestrial laser scanning: Current status and future directions. *Methods in Ecology and Evolution*, 13(8), 1628-1639.
- Dorji, R (2020). Genetical and environmental drivers of tree architecture: Assessment via fractal analysis. (Master Thesis, Georg-August-Universität Göttingen, Germany).
- Dorji, Y., Schuldt, B., Neudam, L., Dorji, R., Middleby, K., Isasa, E., ... & Seidel, D. (2021). Three-dimensional quantification of tree architecture from mobile laser scanning and geometry analysis. *Trees*, 35(4), 1385-1398.
- Dubayah, R. O., & Drake, J. B. (2000). Lidar remote sensing for forestry. *Journal of forestry*, 98(6), 44-46.
- Fischer, M., Bossdorf, O., Gockel, S., Hänsel, F., Hemp, A., Hessenmöller, D., ... & Weisser, W. W. (2010). Implementing large-scale and long-term functional biodiversity research: The Biodiversity Exploratories. *Basic and applied Ecology*, 11(6), 473-485.

- Gering, L. R., & May, D. M. (1995). The relationship of diameter at breast height and crown diameter for four species groups in Hardin County, Tennessee. *Southern Journal of Applied Forestry*, 19(4), 177-181.
- Gollob, C., Ritter, T., & Nothdurft, A. (2020). Comparison of 3D point clouds obtained by terrestrial laser scanning and personal laser scanning on forest inventory sample plots. *Data*, 5(4), 103.
- Gonzalez de Tanago, J., Lau, A., Bartholomeus, H., Herold, M., Avitabile, V., Raunonen, P., ... & Calders, K. (2018). Estimation of above-ground biomass of large tropical trees with terrestrial LiDAR. *Methods in Ecology and Evolution*, 9(2), 223-234.
- Hackenberg, J., Wassenberg, M., Spiecker, H., & Sun, D. (2015). Non destructive method for biomass prediction combining TLS derived tree volume and wood density. *Forests*, 6(4), 1274-1300.
- Hallé, F., & Oldeman, R. A. (1970). *Essai sur l'architecture et la dynamique de croissance des arbres tropicaux* (Vol. 6, pp. 1-178). Paris: Masson.
- Hallé, F., Oldeman, R. A., & Tomlinson, P. B. (1978). Opportunistic tree architecture. In *Tropical trees and forests* (pp. 269-331). Springer, Berlin, Heidelberg.
- Holopainen, M., Kankare, V., Vastaranta, M., Liang, X., Lin, Y., Vaaja, M., ... & Alho, P. (2013). Tree mapping using airborne, terrestrial and mobile laser scanning—A case study in a heterogeneous urban forest. *Urban forestry & urban greening*, 12(4), 546-553.
- Hopkinson, C., Chasmer, L., Young-Pow, C., & Treitz, P. (2004). Assessing forest metrics with a ground-based scanning lidar. *Canadian Journal of Forest Research*, 34(3), 573-583.
- Ishii, H. T., Tanabe, S. I., & Hiura, T. (2004). Exploring the relationships among canopy structure, stand productivity, and biodiversity of temperate forest ecosystems. *Forest Science*, 50(3), 342-355.
- Iwasa, Y. O. H., Cohen, D. A. N., & Leon, J. A. (1985). Tree height and crown shape, as results of competitive games. *Journal of theoretical Biology*, 112(2), 279-297.
- Janus, J., & Bozek, P. (2018). Using ALS data to estimate afforestation and secondary forest succession on agricultural areas: An approach to improve the understanding of land abandonment causes. *Applied Geography*, 97, 128-141.
- Johnson, P. S., Shifley, S. R., Rogers, R., Dey, D. C., & Kabrick, J. M. (2019). *The ecology and silviculture of oaks*. Cabi.
- Juchheim, J., Ammer, C., Schall, P., & Seidel, D. (2017). Canopy space filling rather than conventional measures of structural diversity explains productivity of beech stands. *Forest Ecology and Management*, 395, 19-26.
- Juchheim, J., Annighöfer, P., Ammer, C., Calders, K., Raunonen, P., & Seidel, D. (2017). How management intensity and neighborhood composition affect the structure of beech (*Fagus sylvatica* L.) trees. *Trees*, 31(5), 1723-1735.
- Kelly, N., & Di Tommaso, S. (2015). Mapping forests with Lidar provides flexible, accurate data with many uses. *California Agriculture*, 69(1), 14-20.
- Kuuluvainen, T. (1992). Tree architectures adapted to efficient light utilization: is there a basis for latitudinal gradients?. *Oikos*, 275-284.
- Lang, A. C., Härdtle, W., Bruelheide, H., Geißler, C., Nadrowski, K., Schuldt, A., ... & von Oheimb, G. (2010). Tree morphology responds to neighbourhood competition and slope in species-rich forests of subtropical China. *Forest Ecology and Management*, 260(10), 1708-1715.
- Liang, X., Hyyppä, J., Kaartinen, H., Lehtomäki, M., Pyörälä, J., Pfeifer, N., ... & Wang, Y. (2018). International benchmarking of terrestrial laser scanning approaches for forest inventories. *ISPRS journal of photogrammetry and remote sensing*, 144, 137-179.
- Liang, X., Hyyppä, J., Kukko, A., Kaartinen, H., Jaakkola, A., & Yu, X. (2014). The use of a mobile laser scanning system for mapping large forest plots. *IEEE Geoscience and Remote Sensing Letters*, 11(9), 1504-1508.
- Lin, Y., Jaakkola, A., Hyyppä, J., & Kaartinen, H. (2010). From TLS to VLS: Biomass estimation at individual tree level. *Remote Sensing*, 2(8), 1864-1879.

- Lindh, M., Falster, D. S., Zhang, L., Dieckmann, U., & Brännström, Å. (2018). Latitudinal effects on crown shape evolution. *Ecology and evolution*, *8*(16), 8149-8158.
- MacArthur, R. H., & MacArthur, J. W. (1961). On bird species diversity. *Ecology*, *42*(3), 594-598.
- Malhi, Y., Jackson, T., Patrick Bentley, L., Lau, A., Shenkin, A., Herold, M., ... & Disney, M. I. (2018). New perspectives on the ecology of tree structure and tree communities through terrestrial laser scanning. *Interface Focus*, *8*(2), 20170052.
- Mandelbrot, B. (1977). *Fractals*. San Francisco: Freeman.
- Martin-Garin, B., Lathuilière, B., Verrecchia, E. P., & Geister, J. (2007). Use of fractal dimensions to quantify coral shape. *Coral Reefs*, *26*(3), 541-550.
- McDowell, N. G., & Allen, C. D. (2015). Darcy's law predicts widespread forest mortality under climate warming. *Nature Climate Change*, *5*(7), 669-672.
- Méndez, V., Rosell-Polo, J. R., Pascual, M., & Escolà, A. (2016). Multi-tree woody structure reconstruction from mobile terrestrial laser scanner point clouds based on a dual neighbourhood connectivity graph algorithm. *Biosystems Engineering*, *148*, 34-47.
- Moles, A. T., Perkins, S. E., Laffan, S. W., Flores-Moreno, H., Awasthy, M., Tindall, M. L., ... & Bonser, S. P. (2014). Which is a better predictor of plant traits: temperature or precipitation?. *Journal of Vegetation Science*, *25*(5), 1167-1180.
- Muth, C. C., & Bazzaz, F. A. (2003). Tree canopy displacement and neighborhood interactions. *Canadian Journal of forest research*, *33*(7), 1323-1330.
- Neill, A. R., & Puettmann, K. J. (2013). Managing for adaptive capacity: thinning improves food availability for wildlife and insect pollinators under climate change conditions. *Canadian Journal of Forest Research*, *43*(5), 428-440.
- Neudam, L., Annighöfer, P., & Seidel, D. (2022). Exploring the Potential of Mobile Laser Scanning to Quantify Forest Structural Complexity. *Frontiers in Remote Sensing*, *3*.
- Newnham, G. J., Armston, J. D., Calders, K., Disney, M. I., Lovell, J. L., Schaaf, C. B., ... & Danson, F. M. (2015). Terrestrial laser scanning for plot-scale forest measurement. *Current Forestry Reports*, *1*(4), 239-251.
- Niinemets, Ü., & Kull, O. (1995). Effects of light availability and tree size on the architecture of assimilative surface in the canopy of *Picea abies*: variation in needle morphology. *Tree physiology*, *15*(5), 307-315.
- Nishimura, M., & Setoguchi, H. (2011). Homogeneous genetic structure and variation in tree architecture of *Larix kaempferi* along altitudinal gradients on Mt. Fuji. *Journal of plant research*, *124*(2), 253-263.
- Oker-Blom, P., & Kellomäki, S. (1982). Theoretical computations on the role of crown shape in the absorption of light by forest trees. *Mathematical Biosciences*, *59*(2), 291-311.
- Oveland, I., Hauglin, M., Giannetti, F., Schipper Kjørsvik, N., & Gobakken, T. (2018). Comparing three different ground based laser scanning methods for tree stem detection. *Remote Sensing*, *10*(4), 538.
- Potter, T. L. (2019). *Mobile laser scanning in forests: Mapping beneath the canopy* (Doctoral dissertation, University of Leicester).
- Price, C. A., Weitz, J. S., Savage, V. M., Stegen, J., Clarke, A., Coomes, D. A., ... & Swenson, N. G. (2012). Testing the metabolic theory of ecology. *Ecology letters*, *15*(12), 1465-1474.
- Qian, C., Liu, H., Tang, J., Chen, Y., Kaartinen, H., Kukko, A., ... & Hyypä, J. (2016). An integrated GNSS/INS/LiDAR-SLAM positioning method for highly accurate forest stem mapping. *Remote Sensing*, *9*(1), 3.
- Reichstein, M., Bahn, M., Ciais, P., Frank, D., Mahecha, M. D., Seneviratne, S. I., ... & Wattenbach, M. (2013). Climate extremes and the carbon cycle. *Nature*, *500*(7462), 287-295.

- Ribe, R. G. (2009). In-stand scenic beauty of variable retention harvests and mature forests in the US Pacific Northwest: The effects of basal area, density, retention pattern and down wood. *Journal of Environmental Management*, 91(1), 245-260.
- Richter, J. P. (1970). The notebooks of Leonardo da Vinci (Vol. 2). Courier Corporation.
- Da Vinci, L. (1967). The notebooks of Leonardo da Vinci (Vol. 1). Lulu. com. Rieg, L., Wichmann, V., Rutzinger, M., Sailer, R., Geist, T., & Stötter, J. (2014). Data infrastructure for multitemporal airborne LiDAR point cloud analysis—Examples from physical geography in high mountain environments. *Computers, Environment and Urban Systems*, 45, 137-146.
- Rowland, L., da Costa, A. C., Galbraith, D. R., Oliveira, R. S., Binks, O. J., Oliveira, A. A., ... & Meir, P. (2015). Death from drought in tropical forests is triggered by hydraulics not carbon starvation. *Nature*, 528(7580), 119-122.
- Sarkar, N., & Chaudhuri, B. B. (1994). An efficient differential box-counting approach to compute fractal dimension of image. *IEEE Transactions on systems, man, and cybernetics*, 24(1), 115-120.
- Schaberg, P. G., DeHayes, D. H., Hawley, G. J., & Nijensohn, S. E. (2008). Anthropogenic alterations of genetic diversity within tree populations: Implications for forest ecosystem resilience. *Forest ecology and management*, 256(5), 855-862.
- Scharnweber, T., Manthey, M., Criegee, C., Bauwe, A., Schröder, C., & Wilmking, M. (2011). Drought matters—Declining precipitation influences growth of *Fagus sylvatica* L. and *Quercus robur* L. in north-eastern Germany. *Forest Ecology and Management*, 262(6), 947-961.
- Seidel, D. (2018). A holistic approach to determine tree structural complexity based on laser scanning data and fractal analysis. *Ecology and evolution*, 8(1), 128-134.
- Seidel, D., Annighöfer, P., Stiers, M., Zemp, C. D., Burkardt, K., Ehbrecht, M., ... & Ammer, C. (2019). How a measure of tree structural complexity relates to architectural benefit-to-cost ratio, light availability, and growth of trees. *Ecology and evolution*, 9(12), 7134-7142.
- Seidel, D., Ehbrecht, M., Dorji, Y., Jambay, J., Ammer, C., & Annighöfer, P. (2019). Identifying architectural characteristics that determine tree structural complexity. *Trees*, 33(3), 911-919.
- Setiawan, N. N., Vanhellemont, M., Baeten, L., Dillen, M., & Verheyen, K. (2014). The effects of local neighbourhood diversity on pest and disease damage of trees in a young experimental forest. *Forest Ecology and Management*, 334, 1-9.
- Settele, J., Scholes, R., Betts, R. A., Bunn, S., Leadley, P., Nepstad, D., ... & Winter, M. (2015). Terrestrial and inland water systems. In *Climate change 2014 impacts, adaptation and vulnerability: Part A: Global and sectoral aspects* (pp. 271-360). Cambridge University Press.
- Simonse, M., Aschoff, T., Spiecker, H., & Thies, M. (2003, September). Automatic determination of forest inventory parameters using terrestrial laser scanning. In *Proceedings of the scandlaser scientific workshop on airborne laser scanning of forests* (Vol. 2003, pp. 252-258). Umeå: Sveriges Lantbruksuniversitet.
- Sprinz, P. T., & Burkhart, H. E. (1987). Relationships between tree crown, stem, and stand characteristics in unthinned loblolly pine plantations. *Canadian Journal of Forest Research*, 17(6), 534-538.
- Sterck, F. J., & Bongers, F. (2001). Crown development in tropical rain forest trees: patterns with tree height and light availability. *Journal of Ecology*, 89(1), 1-13.
- Tao, S., Wu, F., Guo, Q., Wang, Y., Li, W., Xue, B., ... & Fang, J. (2015). Segmenting tree crowns from terrestrial and mobile LiDAR data by exploring ecological theories. *ISPRS Journal of Photogrammetry and Remote Sensing*, 110, 66-76.
- Travelletti, J., Oppikofer, T., Delacourt, C., Malet, J. P., & Jaboyedoff, M. (2008). Monitoring landslide displacements during a controlled rain experiment using a long-range terrestrial laser scanning (TLS). *International Archives of Photogrammetry and Remote Sensing*, 37, 485-490.
- Trenberth, K. E., Dai, A., Van Der Schrier, G., Jones, P. D., Barichivich, J., Briffa, K. R., & Sheffield, J. (2014). Global warming and changes in drought. *Nature Climate Change*, 4(1), 17-22.
- Valladares, F., & Niinemets, Ü. (2007). The architecture of plant crowns: from design rules to light capture and performance. In *Functional plant ecology* (pp. 101-150). CRC Press.

- Vatandaşlar, C., & Zeybek, M. (2020). Application of handheld laser scanning technology for forest inventory purposes in the NE Turkey. *Turkish Journal of Agriculture and Forestry*, 44(3), 229-242.
- Went, F. W. (1953). The effect of temperature on plant growth. *Annual Review of Plant Physiology*, 4(1), 347-362.
- West, G. B., Enquist, B. J., & Brown, J. H. (2009). A general quantitative theory of forest structure and dynamics. *Proceedings of the National Academy of Sciences*, 106(17), 7040-7045.
- Williams, K., Olsen, M. J., Roe, G. V., & Glennie, C. (2013). Synthesis of transportation applications of mobile LiDAR. *Remote Sensing*, 5(9), 4652-4692.
- Wu, R., & Hinckley, T. M. (2001). Phenotypic plasticity of sylleptic branching: genetic design of tree architecture. *Critical Reviews in Plant Sciences*, 20(5), 467-485.
- Zande, D. V. D., Jonckheere, I., Stuckens, J., Verstraeten, W. W., & Coppin, P. (2008). Sampling design of ground-based lidar measurements of forest canopy structure and its effect on shadowing. *Canadian Journal of Remote Sensing*, 34(6), 526-538.
- Zeide, B., & Gresham, C. A. (1991). Fractal dimensions of tree crowns in three loblolly pine plantations of coastal South Carolina. *Canadian Journal of Forest Research*, 21(8), 1208-1212.

## **Presenting Three Manuscripts of this Cumulative Dissertation**

In the following three of four chapters, I will present three studies conducted in the framework of this PhD that are published manuscripts (1<sup>st</sup> and 2<sup>nd</sup>) and the last one in review (3<sup>rd</sup>). The first study is focused on the relationship between tree architectural complexity and competition (**Chapter 2**). Then, we focus on the relationship between tree architecture and sunlight angle, seed dispersal strategy, and growth performance (**Chapter 4**). Finally, **chapter 5** will elucidate the relationship between tree architecture and hydraulic safety and efficiency (drought vulnerability).

# CHAPTER 2

---

## **Response of Beech (*Fagus sylvatica* L.) Trees to Competition - New Insights from Using Fractal Analysis**

This chapter is published as a research article in *Remote Sensing*, Volume 11(22), 2656, 13 November 2019, MDPI.

DOI: <https://doi.org/10.3390/rs11222656>

Yonten Dorji<sup>1, \*</sup>, Peter Annighöfer<sup>1</sup>, Christian Ammer<sup>1</sup> and Dominik Seidel<sup>1</sup>

<sup>1</sup>Georg-August-Universität Göttingen, Silviculture and Forest Ecology of the Temperate Zones, Faculty of Forest Sciences, Büsgenweg 1, 37077 Göttingen, Germany

\*Correspondence: [Yonten.dorji@uni-goettingen.de](mailto:Yonten.dorji@uni-goettingen.de); Tel.: +49 551 3933680



## Abstract

Individual tree architecture and the composition of tree species play a vital role for many ecosystem functions and services provided by a forest, such as timber value, habitat diversity, and ecosystem resilience. However, knowledge is limited when it comes to understanding how tree architecture changes in response to competition. Using 3D-laser scanning data from the German Biodiversity Exploratories, we investigated the detailed three-dimensional architecture of 24 beech (*Fagus sylvatica* L.) trees that grew under different levels of competition pressure. We created detailed quantitative structure models (QSMs) for all study trees to describe their branching architecture. Furthermore, structural complexity and architectural self-similarity were measured using the box-dimension approach from fractal analysis. Relating these measures to the strength of competition, the trees are exposed to reveal strong responses for a wide range of tree architectural measures indicating that competition strongly changes the branching architecture of trees. The strongest response to competition ( $\rho = -0.78$ ) was observed for a new measure introduced here, the intercept of the regression used to determine the box-dimension. This measure was discovered as an integrating descriptor of the size of the complexity-bearing part of the tree, namely the crown, and proven to be even more sensitive to competition than the box-dimension itself. Future studies may use fractal analysis to investigate and quantify the response of tree individuals to competition.

**Keywords:** terrestrial laser scanning; QSM; structure; fractal analysis; branching pattern; tree architecture; competition

## 2.1 Introduction

In Europe, the conversion of pure stands into mixed stands is still ongoing (Von Lüpke et al., 2004; Filipescu et al., 2007; Ammer et al., 2008). The corresponding silvicultural interventions are made under the assumption that they result in ecologically and economically beneficial stands (Knoke et al., 2008; Juchheim et al., 2017). However, site conditions, competition processes and ontogenetic stage all affect the growth of an individual tree, be it in a mixed or pure stand (Shi et al., 2010; Ledermann, 2010). Among the mentioned factors, competition is the only one that can be cost-efficiently influenced through silviculture, and it is therefore of special importance (Ammer et al., 2008). In mixed stands, the growth response of the individual tree depends on the species identity of the surrounding neighbors (Canham et al., 2004; Zhao et al., 2006; Pretzsch et al., 2009). Accordingly, in order to understand and model the dynamics in mixed stands, it is necessary to look into the development of tree morphological characteristics and branching architecture under competition in mixed neighborhoods.

According to earlier research, (Munro et al., 1974; Biging & Dobbertin, 1995; Porté & Bartelink, 2002), there are two ways to quantify an individual tree's competition, namely distance independent and distance dependent approaches. In distant-independent approaches, stand density measures are used to estimate the competition pressure of an individual tree, whereas the distant-dependent approaches use the competitive effect determined by the size, position and number of the neighbors (Tomé & Burkhart, 1989). Distant-dependent indices are particularly popular and they are therefore known to offer a reliable prognosis of single-tree growth (Biging & Dobbertin, 1995; Bachmann, 1998). Lately, new, spatially explicit competition indices that are based on 3D stand models from terrestrial laser scanning (TLS) have also been introduced and showed large potential to explain tree growth and tree shape in response to competition (Metz et al., 2013; Seidel et al., 2015ab; Olivier et al., 2016; Seidel et al., 2018). TLS is being increasingly used to measure and record high quality tree individual parameters such as stem volume and crown structure with high accuracy (Yu et al., 2013; Astrup et al., 2014; Newnham et al., 2015).

Despite these advancements, there was limited research focusing on the effects of competition on distinct tree characteristics within a species. The main reason was that a comprehensive measurement of branching pattern and detailed tree architecture was almost impossible based on conventional methods of forest inventory (Seidel et al.,

2011). TLS, however, not only provides solid measures of competition (Seidel et al., 2015a; Olivier et al., 2016), as mentioned above but also millimeter-level detail on the tree structure and ultimately, a rapid assessment of each individual tree in a stand (Liang et al., 2018).

Thus far, only a few recent pioneering studies used the technology to investigate responses of the branching architecture to competition (Olivier et al., 2016; Bayer et al., 2013; Juchheim et al., 2017). Olivier et al. (2016) used TLS data to overcome the limits of traditional canopy studies, when it comes to quantifying differences in tree crowns. For sugar maple (*Acer saccharum*, Marsh.) stands with different compositions and developmental stages, they found TLS-based competition indices to be better predictors of crown metric variability than stand type, also highlighting the potential of TLS data to quantify tree competition and space occupancy.

Juchheim et al. (2017) used TLS data to calculate structural measures for European beech (*Fagus sylvatica* L.) trees that grew either in intra- or interspecific neighborhoods in unmanaged stands and their findings provide evidence of different phenotypic responses of European beech, as a consequence of different types of competition.

Again, through application of a TLS and a new point cloud skeletonization approach, Bayer et al. (2013) determined structural crown properties of European beech trees and Norway spruce growing in mixed and pure stands. The results yielded detailed information on the morphological traits of the trees and revealed that different competitor species results in significantly different crown structures of the study trees.

Recently, the toolset for the analysis of tree architecture was further extended by methods of fractal analysis, for example the box dimension (abbreviation  $D_b$ ; cf. [Seidel et al., 2018]). When fractal analysis became famous in the 1970s, the box-dimension was introduced by the mathematician Mandelbrot (Mandelbrot, 2012). It is a holistic approach to the architectural complexity of trees (Seidel et al., 2018) that is rested on observing the change in the number of virtual boxes one needs to enclose all parts of an object (its 3D model) in dependence of the size of the boxes one uses. Based on the relationship (regression line) between the number of boxes (y-axis) and their size (x-axis), fractal analysis allows conclusions to be drawn on the complexity of an object, its dimensions, and its geometrical self-similarity. Self-similarity can be understood as a measure of geometrical repetition across scales, meaning that similar architectural pattern, for example a y-shaped branch bifurcation occurs across several scales. Therefore, starting

with the first bifurcation of the stem, the two major branches would bifurcate again in the same way, each into two more branches and with the same y-shape. This process would repeat down to the smallest twigs. Such trees can easily be created from computer models such as the famous Lindenmayer l-system (Prusinkiewicz et al., 2012). Real plants however, deviate from perfect self-similarity to various degrees due to external or internal factors.

When it comes to the dimensional aspects of tree architecture, the intercept of the regression line for the relationship between number of boxes used to calculate the box-dimension and their size (see previous paragraph) was predicted to be a useful measure in an earlier study (Seidel et al., 2019a).

Using fractal analysis to address tree architecture bears great potential for the investigation of competition–architecture relationships. According to Seidel et al. (2019), the box-dimension approach addresses a large number of architectural characteristics at once, including the tree crown lengths, crown diameter, branch angles, and others. In the same study, it was also shown that the branching patterns of the trees, together with the crown dimension, are solid surrogates for a tree structural complexity.

Here, we used the box-dimension, self-similarity derived from fractal analysis, as well as conventional topological measures of tree architecture to analyze the effect of competition on the shape of beech (*Fagus sylvatica* L.) trees.

We hypothesized that competition strength affects the architecture of beech trees. More precisely, we hypothesized that competition affects (i) branching pattern, as well as (ii) measures of tree complexity derived from fractal analysis. We will explore the potential and meaning of measures from fractal analysis in the hope to gain new insights into competition–architecture relationships.

## **2.2 Materials and Methods**

### ***2.2.1 Study Sites and Objects***

Our data were taken in the framework of the Biodiversity Exploratories (Fischer et al., 2010). Covering a gradient in precipitation and temperature across Germany, the three Exploratories were located in the Swabian Alb (South-West Germany), the Hainich–Dün (Central Germany) and the Schorfheide-Chorin (North-East Germany). The location of the study sites and the study design are shown in Figure 2.1.

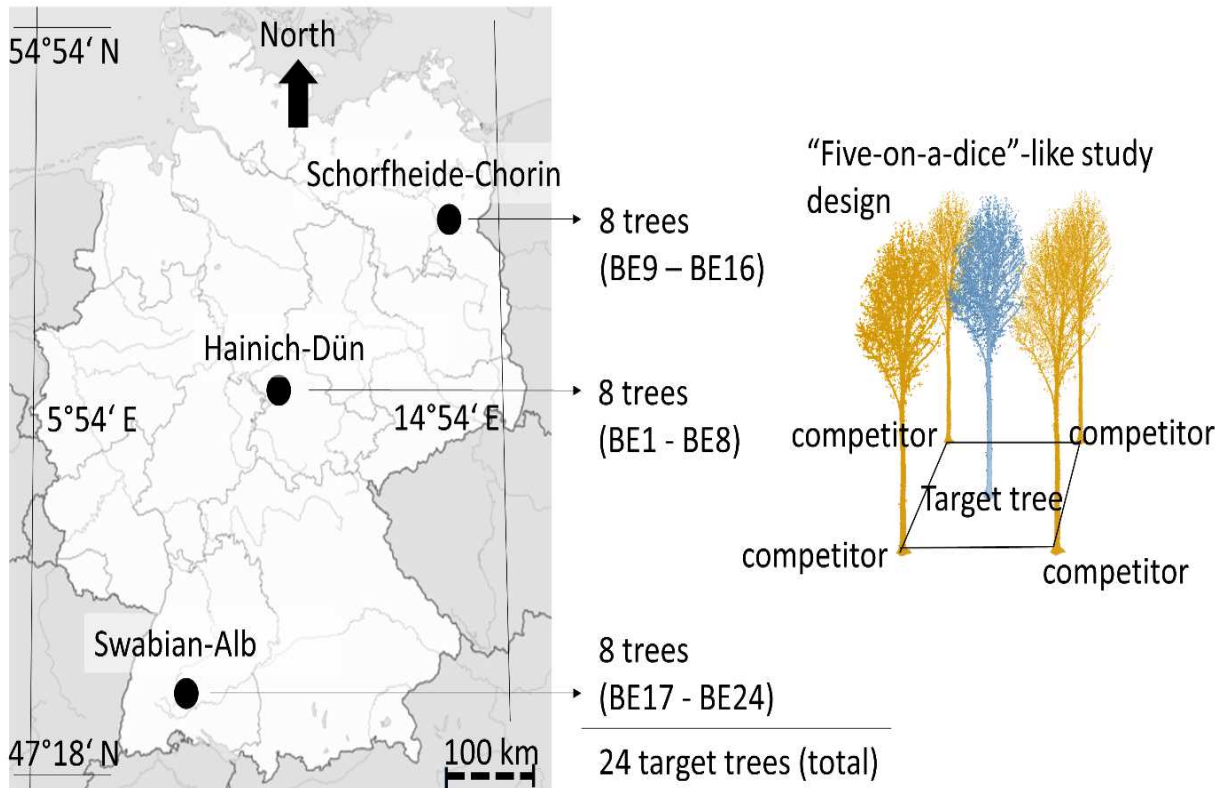


**Figure 2.1.** Study areas within Germany (left side) and sampling design (right side).

In each area, we investigated the architecture of eight adult beech (*Fagus sylvatica* L.) trees (total =  $3 \times 8 = 24$ ) that grow in the center of a quadrat. Each quadrat was defined by four competitor trees growing in the corners of the quadrat cornering the respective study tree in the center. In an earlier study, these tree quadrats were chosen, as they differed in species composition and hence competitive neighborhood of the subject beech trees (Metz et al., 2013). The quadrats were intended to resemble a five-on-a-dice-like layout with the four competitor trees growing in the corners. Competitor trees comprised Scots pine (*Pinus sylvestris* L.), Norway spruce (*Picea abies* L.), Sycamore maple (*Acer pseudoplatanus* L.), European ash (*Fraxinus excelsior* L.), oak (*Quercus* spp.), small-leaved lime (*Tilia cordata* Mill.), and hornbeam (*Carpinus betulus* L.). Due to some natural variation in distances, small deviations from the ideal spatial layout occurred. Details on the study sites can be found in Metz et al. (2013), including climatic and soil-related properties. A summary of the main characteristics of the study trees is provided in Table 2.1. While Metz et al. (2013) focused on the effect of competition on diameter growth, here we examine the effect of competition on crown structural characteristics.

**Table 2.1** Major characteristics of the 24 investigated beech trees (adapted from Metz et al. (2013). DBH = Diameter at breast height (1.3 m). HAI = Hainich Dün, SCH = Schorfheide Chorin, ALB = Swabian Alb.

Target Tree ID	Exploratory	Height (m)	DBH (cm)	Competing Species
BE 1	HAI	32.03	41.60	ash
BE 2	HAI	31.24	45.50	beech
BE 3	HAI	34.44	50.40	beech
BE 4	HAI	31.63	41.60	beech
BE 5	HAI	31.88	42.70	beech
BE 6	HAI	22.72	31.30	maple, ash
BE 7	HAI	29.30	51.50	maple, lime, oak, hornbeam
BE 8	HAI	23.72	30.30	ash
BE 9	SCH	27.92	37.20	pine
BE10	SCH	23.25	26.20	pine
BE11	SCH	25.18	42.30	pine
BE12	SCH	36.01	40.00	beech
BE13	SCH	34.11	50.10	beech
BE14	SCH	24.33	37.30	pine
BE15	SCH	26.47	43.30	beech
BE16	SCH	26.09	37.00	beech
BE17	ALB	27.21	30.00	beech
BE18	ALB	32.51	34.70	beech
BE19	ALB	30.29	42.00	beech
BE20	ALB	23.67	22.10	spruce
BE21	ALB	22.43	37.70	spruce
BE22	ALB	24.55	35.20	spruce
BE23	ALB	26.49	34.70	beech
BE24	ALB	24.00	27.30	spruce

### 2.2.2 Laser Scanning

Each study tree was scanned using a Zoller and Fröhlich Imager 5006 terrestrial laser scanner (Zoller and Fröhlich GmbH, Wangen i.A, Germany). The instrument was set to scan with a resolution of 0.036 degrees using a field of view of 310° (vertically) and 360° (horizontally). The maximum range of the instrument was 179 m and we conducted six or more scans (depending on stand density and visibility) surrounding the study trees and their immediate neighbors. All scans were conducted in March 2012, in leafless conditions to ensure free sight on the upper crowns (Metz et al., 2013). We used 24 artificial chessboard targets that were distributed in the scanned scene as tie points for spatial co-registration of the individual scans. Scans were merged using Zoller and Fröhlich Laser Control 8.2 software (Zoller and Froehlich GmbH). As a result of the laser scanning procedure, each study trees and the surrounding forest area were available as virtual three-dimensional high-resolution (3D) point cloud representations of the real world.

### ***2.2.3 Point Cloud Processing and Quantitative Structure Models***

Each point cloud of a study tree and its surroundings was used to manually separate the study trees from the remaining forest. This was conducted manually using Leica Cyclone Software (Leica Geosysteme, Heerbrugg, Switzerland). After the study trees were available as single-tree point clouds (see Figure 2.2, left), they were processed using the CompuTree software (Piboule et al., 2013) to create a quantitative structure model (abbreviation QSM; see Figure 2.2, right) for each individual. A QSM-model can be understood as a representation of the tree point cloud based on cylinders of various diameters and lengths (Piboule et al., 2013). We decided to use the same QSM-parameter settings for all trees in order to allow for a better reproducibility of our results. The parameters were 0.10 m for clustering tolerance, a maximum of 600-point clusters with at least 400 points each (automatically adjusted by the software if less clusters are found). Each cluster needed to contain at least 0.5% of all points in order to be created.

We decided for this set of parameters based on visual inspection of the resulting QSM models with the point clouds overlaid for quality assessment. We are not aware of any method that enables a less subjective quality control for QSM models. However, we argue, that a set of parameters used for all trees shall produce an objective and reproducible QSM model for our study trees.

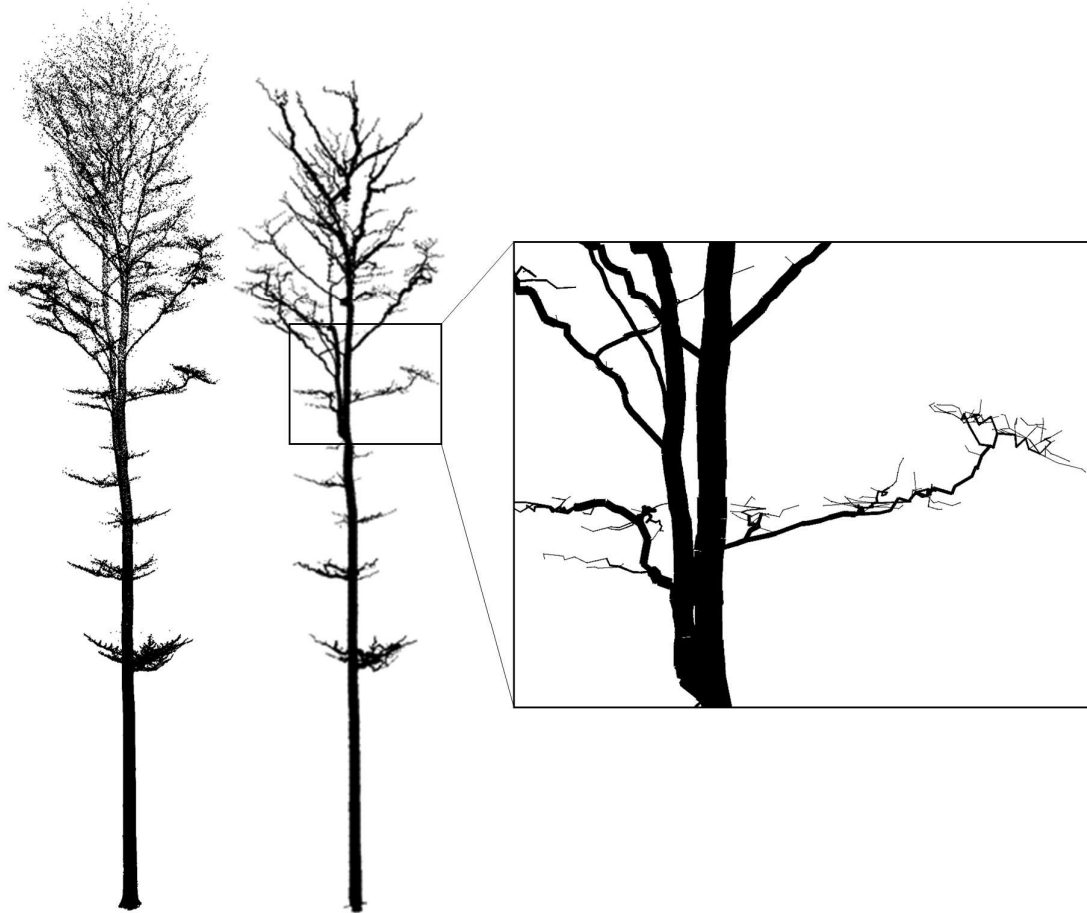


**Figure 2.2** Example of a study tree point cloud (**left**), the corresponding quantitative structure model (**middle**) and a close-up of the quantitative structure model (**right**).

Here, we applied QSM-models in order to obtain information on the branching pattern of the beech trees for branches up to the 3rd order. For all 24 study trees, the branching patterns were calculated using the same settings for the CompuTree software. These settings can theoretically be adapted to optimize the modeling for trees of different species, varying height, etc., but were kept the same to ensure repeatability in our study focusing on trees of only one species and of similar dimensions. We derived the mean branch volume of 1st, 2nd, and 3rd order branches, mean branch angle of 1<sup>st</sup>, 2<sup>nd</sup>, and 3<sup>rd</sup> order branches, range of branch angle of 1<sup>st</sup>, 2<sup>nd</sup>, and 3<sup>rd</sup> order branches, total branch length and mean branch length. In addition to these eleven measures, we also tested three measures obtained from fractal analysis. Those are explained in the following.



#### **2.2.4 Box-dimension, Intercept and Self-Similarity**

The box-dimension ( $D_b$ ) can be considered a measure of a tree's architectural complexity. It was calculated from the single-tree point clouds following the approach introduced in Seidel (2018). This approach rests on the ideas of Sarkar and Chaudhuri (Sarkar & Chaudhuri, 1994) and the ground-breaking work of Mandelbrot (Mandelbrot, 1977). In short, we determined  $D_b$  by counting the number of virtual boxes of a given size needed to enclose all aboveground tree organs in the point cloud. This number of boxes is determined for different box-sizes, starting with the largest box, which is the minimum bounding box enclosing the full tree, and continuing with successively smaller boxes always being  $1/8^{\text{th}}$  the volume of the previous box size (or  $1/2$  the edge length). Then, a least-square line was fit through the scatterplot of the number of boxes needed (dependent variable) over the inverse of the box-size used (given in relation to the largest box used; explanatory variable). The slope of this line is defined as the  $D_b$ , its coefficient of determination ( $R^2$ ) is defined as a measure of self-similarity of the tree architecture across the different tested scales (box-sizes), and the intercept of the regression line ( $D_b$ -intercept) with the y-axis is a surrogate for trees size (Seidel et al., 2019a) (Figures 2.3 and 2.4). Here, we will explore all three variables for their responsiveness to competition. First, we evaluated the intercept for correlation with established measures of tree size and correlation with competition strength. Since Mandelbrot (1977) stated that the intercept is a measure of object dimension (size), we tested whether  $D_b$ -intercept responded to competition strength and whether it was related more to conventional measures of tree size (total tree height [TTH]), diameter at breast height (DBH), or to crown-related measure of dimension (crown volume and crown radius). Then, in addition to  $D_b$  as a dimensionless measure of tree architectural complexity, we evaluated whether self-similarity ( $R^2$  of the regression) as a new architectural attribute may respond to competition.



**Figure 2.3.** Exemplary three-dimensional tree point clouds with a high box-dimension (**left:**  $D_b$ : 2.02) and a low box-dimension (**right:**  $D_b$ : 1.50). Box-dimension is considered a measure of structural complexity.

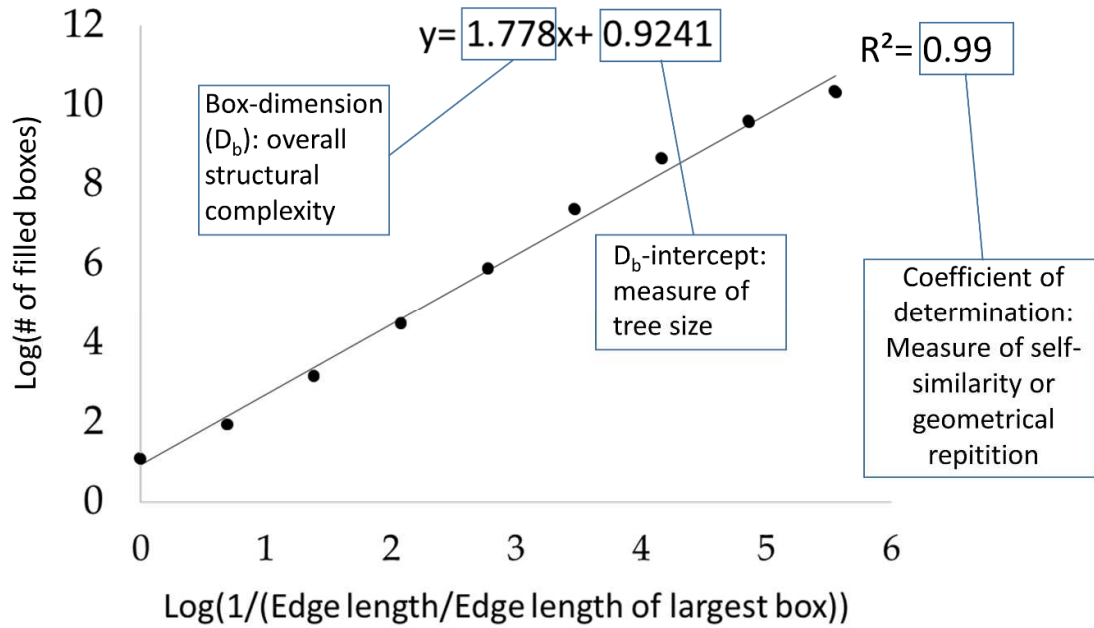


**Figure 2.4** Explanatory graph on the calculation of the three tested measures from fractal analysis, namely box-dimension ( $D_b$ ), intercept of the regression line ( $D_b$ -intercept) and the coefficient of determination of the regression line (self-similarity).

### 2.2.5 Calculation of Competitive Pressure

Competition strength enforced on the study trees was determined using the cumulative crown surface area (CCSA) of the competitor trees. For the trees investigated in our study, Metz et al. (2013) showed that CCSA is a good predictor of the competitive situation the trees were facing, thereby explaining tree growth ( $R^2 = 0.34$ ; cf. [Metz et al., 2013]). The crown surface area of each competitor tree was determined using the convex hull polygon approach and the total for the four competitors was calculated per study tree. Using an algorithm written in Mathematica (Wolfram Research, Champaign, USA), we determined the surface of the convex hull polygons from the triangle points building the convex hull by applying Heron's formula.

### 2.2.6 Statistical Analysis

Using the statistical software R (R Core Team, 2013), we tested for relationships between all structural attributes and competition strength using correlation analysis (Spearman's rank rho). Level of significance was  $< 0.05$  in all tests. The within data trend of selected significant correlations was further analyzed using non-linear Generalized Additive Modeling (GAM) techniques because assumptions for linear regressions were

not met. Also, to avoid over-fitting, the effective degrees of freedom (EDF) were set to 3 with smoothing then chosen automatically through cross-validation (Wood et al., 2017). Models' evaluation occurred through interpreting the EDF value as complexity of the smoothing function, p-values of the smoothing function, and the deviance explained by the GAM. The EDF values were all one, which means the within data trend suggests linearity (comp. results and discussion).

## 2.3 Results

Out of the 14 tested structural attributes, five were significantly correlated to competition strength (Table 2.2).

**Table 2.2** All tested attributes of tree architecture and their relationship with competition strength.

Architectural Attribute	rho	p-value
Branch volume 1st order	-0.26	0.227
Branch volume 2nd order	-0.20	0.355
Branch volume 3rd order	-0.25	0.237
Total branch length 1st order	-0.53	<b>0.007</b>
Mean branch length 1st order	-0.52	<b>0.009</b>
Mean branch angle 1st order	0.11	0.624
Mean branch angle 2nd order	-0.07	0.755
Mean branch angle 3rd order	-0.22	0.291
Range of branch angles 1st order	-0.21	0.323
Range of branch angles 2nd order	-0.62	<b>0.002</b>
Range of branch angles 3rd order	-0.28	0.179
$D_b$ (box dimension)	-0.65	<b>0.006</b>
Intercept of $D_b$ -regression	-0.78	<b>&lt;0.001</b>
Self-similarity	0.31	0.142

(p-values in bold indicate statistically significant relationships).

We found significant correlations between competition strength and the following measures; total branch length 1st order (rho: -0.53;  $p < 0.01$ ), mean branch length 1st order (rho: -0.52;  $p < 0.01$ ), and the range of branch angles 2nd order (rho: -0.62;  $p < 0.01$ ) (Table 2.2).

Competition not only reduced branch lengths, but it also reduced the variability in branching angles (Figure 2.5A, B) and it reduced the box-dimension of the trees (Figure 2.5C).

The intercept of the  $D_b$ -regression line was the attribute that was most sensitive to competition strength and the relationship was again negative ( $\rho: -0.78; p < 0.001$ ), with the GAM also resulting in the highest explained deviance of all tested measures (Figure 2.5D and Table 2.2).

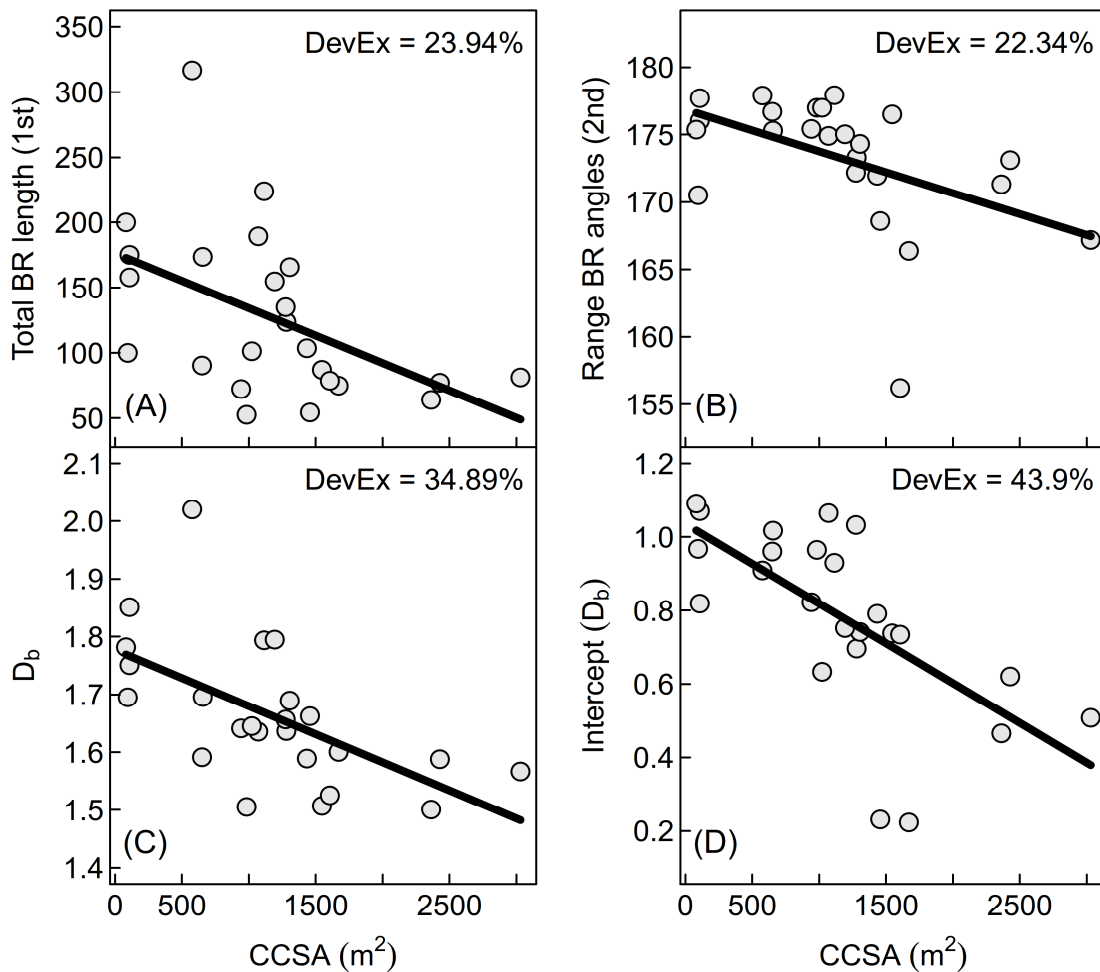


**Figure 2.5** Scatterplots of architectural features (A = total length of 1<sup>st</sup> order branches; B = range of 2<sup>nd</sup> order branch angles; C = box dimension ( $D_b$ ); D = intercept of box dimension) with GAM and explained deviance (DevEx), respectively, of beech trees in dependence of competition strength as cumulative crown surface area (CCSA [ $m^2$ ]). Black solid lines show significant GAM models, the effective degrees of freedom (EDF) for all models were 1, suggesting linear within-data relationships.

We also discovered positive correlations between the  $D_b$ -regression and crown morphological variables, like crown radius (rho: 0.42;  $p < 0.05$ ) and crown volume (rho: 0.50;  $p < 0.05$ ) (comp. Figure 2.6C, D). The two conventional measures of tree size, diameter at breast height (rho: -0.44;  $p < 0.05$ ) and total tree height (rho: -0.59;  $p < 0.05$ ) were, however, negatively correlated with  $D_b$ -intercept (Figure 2.6A, B).

The third measure derived from fractal analysis, namely self-similarity, showed no significant correlation with competition strength (rho: 0.31;  $p = 0.142$ ).

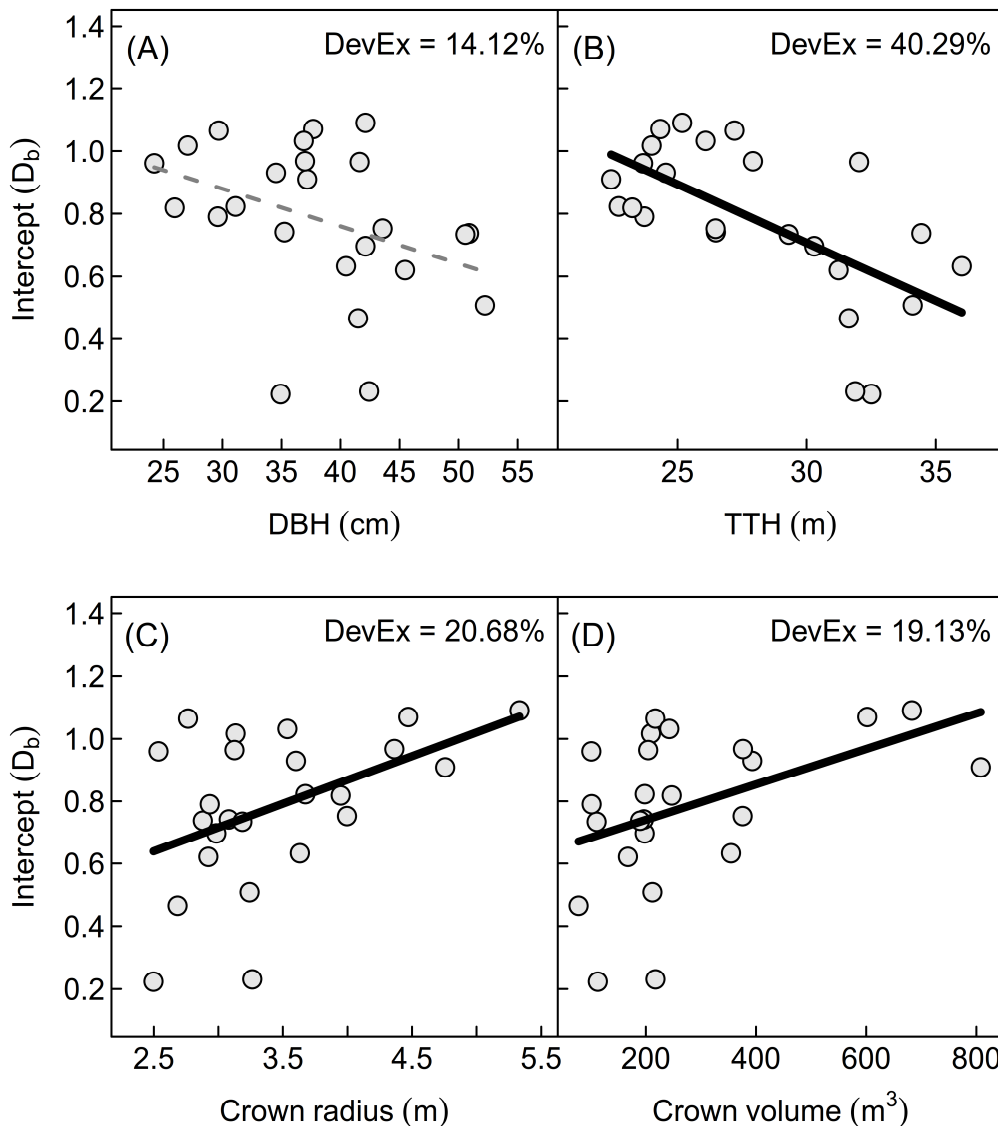


**Figure 2.6** Scatterplots of  $D_b$ -Intercept against conventional measures of tree size (A = diameter at breast height (DBH (cm))); B = total tree height (TTH (m)) and crown morphology (C = Crown radius (m); D = Crown volume (m<sup>3</sup>)) with GAM and explained

deviance (DevEx), respectively, of beech trees. Black solid lines show significant GAM models, dashed grey line shows insignificant model. The effective degrees of freedom (EDF) for all models were 1, suggesting linear within data relationships.

## 2.4 Discussion

We investigated whether the branching architecture of beech trees responds to competition strength, as was indicated in earlier studies on European beech (Bayer et al., 2013; Juchheim et al., 2017). We hypothesized that competition strength affects the architecture of beech trees in terms of branching pattern, as already indicated by Bayer et al. (2013), as well as measures of tree structural complexity derived from fractal analysis. Our results strongly support this assumption, as we identified a significant response of branch length, branch angles as well as the box-dimension and  $D_b$ -intercept of the target trees to competition enforced on them by the neighboring trees.

Not all tree species may be as responsive to competition strength as beech. Its high adaptive capacity is clearly expressed in its phenotypic plasticity and was reported repeatedly in the literature (Schröter et al., 2012; Valladares et al., 2017). For example, the study by Bayer et al. (2013) showed first results on changes in the branching angles of beech in dependence of the species of the neighboring trees. Similarly, Juchheim et al. (2017) showed that the structure of the crown of European beech, assessed using QSM-model like in our present study, significantly varied depending on competition type (intra vs. interspecific competition). Our research added knowledge on the general response of beech architecture to competition strength (irrespective of competition type), and most importantly, that the entire structural complexity of the trees is negatively affected by competition.

Together with the crown size, the distribution of the branches and leaves is an important aspect of productivity (Maguire et al., 1996; Jucker et al., 2015) and it is therefore not surprising that competition effects directly relate to the difference in a tree's productivity, as already shown for our study trees by Metz et al. (2013). Earlier studies using fractal analysis also confirmed that a reduction in architectural complexity comes at the cost of productivity (Seidel, 2018). It is also known that structural complexity, assessed as box-dimension, translates well to the growing efficiency of a tree (Seidel et al., 2019b). Summarizing, competition enforced on a tree's results in adaptations of the

tree's growth pattern (branching pattern), results in lower  $D_b$ -values and consequently in a lower growth efficiency.

Using only crown shapes and dimensions to evaluate the effects of competition strength may lead to false conclusions, as changes in the branching architecture may result in changes in the light transmissivity of tree crowns and consequently forest canopies (Oliver et al., 1996). Those are not accounted for when only the dimensional extent of a crown (e.g., crown radius) is considered. Here, fractal analysis provides summarizing measures that address the tree's architecture more comprehensively (branches and stem architecture together) and that should respond to competition as well. In fact, we found that the box-dimension and  $D_b$ -intercept showed a strong negative correlation with competition strength (see Table 2.2 and Figure 2.5C, D), indicating that competitive pressure indeed reduces the structural complexity of beech trees. This supports the findings of an earlier study focusing on European beech (Seidel et al., 2019b).

We argue that the intercept of the  $D_b$ -regression line is actually a proxy for the dimension of the complexity-bearing part of a tree, more precisely the tree crown (comp. Figure 2.6). This was confirmed by the positive correlations with crown morphological variables, like crown radius and crown volume (comp. Figure 2.6C, D). The two conventional measures of tree size, diameter at breast height and total tree height were, however, negatively correlated with  $D_b$ -intercept. Despite the significant correlation, the smoothing term of the GAM model for the regression between DBH and  $D_b$ -intercept was not significant (Figure 2.6A). This indicates that the DBH per se is not necessarily a complexity-bearing measure for a tree, meaning that trees with the same DBH can be of greatly varying complexity in architecture. Surprisingly, the  $D_b$ -intercept decreased with increasing total tree height (Figure 2.6B). Actually, a similar result as described for the DBH would have been expected, namely that height alone is not related to complexity, but if at all one would have expected a positive relationship between the two variables. The only explanation for the negative trend is that the higher intraspecific competition led to slightly higher TTH across the sites due to increased height growth. As increased height growth resulted in reduced canopy dimensions (horizontal extent), it also resulted in a lower complexity of the postulated complexity-bearing tree part (crown).

In the dataset used here, self-similarity could not be confirmed as a measure that responded to competition but one has to consider that this may be due to our small sample size. The rho-value of 0.31 (Table 2.2) points towards some correlation but it is too



weak to draw conclusions from it. In a future study, we will address this measure in more detail.

The advent of TLS provides the avenue to measure details of the tree architecture thereby giving new insight into the effects of competition on tree morphology and branching pattern (Henning et al., 2006). Such knowledge is crucial to understand structure–productivity relationships (Bayer et al., 2013; Seidel et al., 2019b), but also to get a better understanding of structure-biodiversity relationships (Bazzaz et al., 1975; Tews et al., 2004), as they all depend on the architecture of individual trees.

## **2.5 Conclusions**

Our study based on high-resolution terrestrial laser scanning, delved further into the response of branching architecture and fractal characteristics of crown structures to competition. The objective was to provide a deeper understanding on how tree architecture changes in response to competition.

Using terrestrial laser scanning data of individual trees, we determined quantitative structure models to derive branching pattern and applied fractal analysis to describe the tree architectural complexity. We showed that crowns of European beech are highly responsive to competition, changing not only dimensions and branching pattern, as shown in early work, but also the entire structural complexity.

We discovered the intercept of the regression line of the box-dimension to be strongly related to competition pressure. We argue that this is because it integrates several dimensional measures of the tree crown that respond strongly to competition.

Future studies may use fractal analysis to investigate and quantify the response of tree individuals to competition, as we discovered a strong architectural response of beech trees to competition pressure.

### **Author Contributions:**

Conceptualization: Y.D., P.A., C.A., D.S.; methodology: Y.D., D.S.; software: D.S.; formal analysis: Y.D., D.S., P.A.; resources: D.S., C.A.; writing-original draft preparation: Y.D., D.S.; writing- review and editing: Y.D., P.A., C.A., D.S.; visualization: Y.D., D.S., P.A.; supervision: D.S., C.A., P.A.; project administration: D.S.; funding acquisition: D.S., C.A.

**Funding:**

The German Research Foundation (DFG) is acknowledged for funding this research through grant SE2383/5-1 provided to Dominik Seidel. This work was also supported by funds from the German Government's Special Purpose Fund held at Landwirtschaftliche Rentenbank (844732).

**Acknowledgments:**

We are grateful to Jeromé Metz, who provided us with the scan data of the trees. We also thank the managers of the three Exploratories, Kirsten Reichel-Jung, Swen Renner, Katrin Hartwich, Sonja Gockel, Kerstin Wiesner, and Martin Gorke for their work in maintaining the plot and project infrastructure; Christiane Fischer and Simone Pfeiffer for giving support through the central office, Michael Owonibi for managing the central database, and Markus Fischer, Eduard Linsenmair, Dominik Hessenmöller, Jens Nieschulze, Daniel Prati, Ingo Schöning, François Buscot, Ernst-Detlef Schulze, Wolfgang W. Weisser and the late Elisabeth Kalko for their role in setting up the Biodiversity Exploratories project. We thank Falk Hänsel, Stephan Wöllauer, Frank Suschke, Mathias Groß, Martin Fellendorf and Thomas Nauss for the operation and maintenance of meteorological stations in the research plots.

**Conflicts of Interest:** The authors declare no conflict of interest

## 2.6 References:

- Ammer, C. (2008). Konkurrenzsteuerung–Anmerkungen zu einer Kernaufgabe des Waldbaus beim Aufbau vielfältiger Wälder. *Eberswalder Forstliche Schriftenreihe*, 36(April), 21-26.
- Ammer C, Bickel E, & Koelling C (2008). Converting Norway spruce stands with beech - a review of arguments and techniques. *Austrian Journal of Forest Science*, 125 (1), 3-26.
- Astrup, R., Ducey, M. J., Granhus, A., Ritter, T., & von Lüpke, N. (2014). Approaches for estimating stand-level volume using terrestrial laser scanning in a single-scan mode. *Canadian Journal of Forest Research*, 44(6), 666-676.
- Bachmann, M. (1998). Indizes zur Erfassung der Konkurrenz von Einzelbäumen.
- Bayer, D., Seifert, S., & Pretzsch, H. (2013). Structural crown properties of Norway spruce (*Picea abies* [L.] Karst.) and European beech (*Fagus sylvatica* [L.]) in mixed versus pure stands revealed by terrestrial laser scanning. *Trees*, 27(4), 1035-1047.
- Bazzaz, F. A. (1975). Plant species diversity in old-field successional ecosystems in southern Illinois. *Ecology*, 56(2), 485-488.
- Biging, G. S., & Dobbertin, M. (1995). Evaluation of competition indices in individual tree growth models. *Forest science*, 41(2), 360-377.
- Canham, C. D., LePage, P. T., & Coates, K. D. (2004). A neighborhood analysis of canopy tree competition: effects of shading versus crowding. *Canadian Journal of Forest Research*, 34(4), 778-787.
- Filipescu, C. N., & Comeau, P. G. (2007). Competitive interactions between aspen and white spruce vary with stand age in boreal mixedwoods. *Forest Ecology and Management*, 247(1-3), 175-184.
- Fischer, M., Bossdorf, O., Gockel, S., Hänsel, F., Hemp, A., Hessenmöller, D., ... & Weisser, W. W. (2010). Implementing large-scale and long-term functional biodiversity research: The Biodiversity Exploratories. *Basic and applied Ecology*, 11(6), 473-485.
- Henning, J. G., & Radtke, P. J. (2006). Ground-based laser imaging for assessing three-dimensional forest canopy structure. *Photogrammetric Engineering & Remote Sensing*, 72(12), 1349-1358.
- Juchheim, J., Ammer, C., Schall, P., & Seidel, D. (2017). Canopy space filling rather than conventional measures of structural diversity explains productivity of beech stands. *Forest Ecology and Management*, 395, 19-26.
- Juchheim, J., Annighöfer, P., Ammer, C., Calders, K., Raunonen, P., & Seidel, D. (2017). How management intensity and neighborhood composition affect the structure of beech (*Fagus sylvatica* L.) trees. *Trees*, 31(5), 1723-1735.
- Jucker, T., Bouriaud, O., & Coomes, D. A. (2015). Crown plasticity enables trees to optimize canopy packing in mixed-species forests. *Functional Ecology*, 29(8), 1078-1086.
- Knoke, T., Ammer, C., Stimm, B., & Mosandl, R. (2008). Admixing broadleaved to coniferous tree species: a review on yield, ecological stability and economics. *European journal of forest research*, 127(2), 89-101.
- Ledermann, T. (2010). Evaluating the performance of semi-distance-independent competition indices in predicting the basal area growth of individual trees. *Canadian journal of forest research*, 40(4), 796-805.
- Liang, X., Hyyppä, J., Kaartinen, H., Lehtomäki, M., Pyörälä, J., Pfeifer, N., ... & Wang, Y. (2018). International benchmarking of terrestrial laser scanning approaches for forest inventories. *ISPRS journal of photogrammetry and remote sensing*, 144, 137-179.
- Maguire, D. A., & Bennett, W. S. (1996). Patterns in vertical distribution of foliage in young coastal Douglas-fir. *Canadian Journal of Forest Research*, 26(11), 1991-2005.
- Mandelbrot, B. (1977). *Fractals*. San Francisco: Freeman.
- Metz, J., Seidel, D., Schall, P., Scheffer, D., Schulze, E. D., & Ammer, C. (2013). Crown modeling by terrestrial laser scanning as an approach to assess the effect of aboveground intra-and interspecific competition on tree growth. *Forest Ecology and Management*, 310, 275-288.

- Munro, D. D. (1974). Forest growth models—a prognosis. In *Growth models for tree and stand simulation* (Vol. 30, pp. 7-21). Research Note 30. Department of Forest Yield Research, Royal College of Forestry, Stockholm.
- Newnham, G. J., Armston, J. D., Calders, K., Disney, M. I., Lovell, J. L., Schaaf, C. B., ... & Danson, F. M. (2015). Terrestrial laser scanning for plot-scale forest measurement. *Current Forestry Reports*, 1(4), 239-251.
- Oliver, C. D., & Larson, B. C. (1996). *Forest stand dynamics: Updated edition*. John Wiley and sons.
- Olivier, M. D., Robert, S., & Fournier, R. A. (2016). Response of sugar maple (*Acer saccharum*, Marsh.) tree crown structure to competition in pure versus mixed stands. *Forest Ecology and Management*, 374, 20-32.
- Piboule, A., M. Krebs, L. Esclatine, and J. C. Hervé. "Computree: a collaborative platform for use of terrestrial lidar in dendrometry." In *Proceedings of the International IUFRO Conference MeMoWood, Nancy, France*, pp. 1-4. 2013.
- Porte, A., & Bartelink, H. H. (2002). Modelling mixed forest growth: a review of models for forest management. *Ecological modelling*, 150(1-2), 141-188.
- Pretzsch, H., & Schütze, G. (2009). Transgressive overyielding in mixed compared with pure stands of Norway spruce and European beech in Central Europe: evidence on stand level and explanation on individual tree level. *European Journal of Forest Research*, 128(2), 183-204.
- Prusinkiewicz, P., & Runions, A. (2012). Computational models of plant development and form. *New Phytologist*, 193(3), 549-569.
- Team, R. C. (2013). R: A language and environment for statistical computing.
- Sarkar, N., & Chaudhuri, B. B. (1994). An efficient differential box-counting approach to compute fractal dimension of image. *IEEE Transactions on systems, man, and cybernetics*, 24(1), 115-120.
- Schröter, M., Härdtle, W., & von Oheimb, G. (2012). Crown plasticity and neighborhood interactions of European beech (*Fagus sylvatica* L.) in an old-growth forest. *European Journal of Forest Research*, 131(3), 787-798.
- Seidel, D. (2018). A holistic approach to determine tree structural complexity based on laser scanning data and fractal analysis. *Ecology and evolution*, 8(1), 128-134.
- Seidel, D., Annighöfer, P., Stiers, M., Zemp, C. D., Burkardt, K., Ehbrecht, M., ... & Ammer, C. (2019). How a measure of tree structural complexity relates to architectural benefit-to-cost ratio, light availability, and growth of trees. *Ecology and evolution*, 9(12), 7134-7142.
- Seidel, D., Ehbrecht, M., Dorji, Y., Jambay, J., Ammer, C., & Annighöfer, P. (2019). Identifying architectural characteristics that determine tree structural complexity. *Trees*, 33(3), 911-919.
- Seidel, D., Hoffmann, N., Ehbrecht, M., Juchheim, J., & Ammer, C. (2015). How neighborhood affects tree diameter increment—new insights from terrestrial laser scanning and some methodical considerations. *Forest Ecology and Management*, 336, 119-128.
- Seidel, D., Leuschner, C., Müller, A., & Krause, B. (2011). Crown plasticity in mixed forests—quantifying asymmetry as a measure of competition using terrestrial laser scanning. *Forest Ecology and Management*, 261(11), 2123-2132.
- Seidel, D., Schall, P., Gille, M., & Ammer, C. (2015). Relationship between tree growth and physical dimensions of *Fagus sylvatica* crowns assessed from terrestrial laser scanning. *iForest-Biogeosciences and Forestry*, 8(6), 735.
- Shi, H., & Zhang, L. (2003). Local analysis of tree competition and growth. *Forest Science*, 49(6), 938-955.
- Tews, J., Brose, U., Grimm, V., Tielbörger, K., Wichmann, M. C., Schwager, M., & Jeltsch, F. (2004). Animal species diversity driven by habitat heterogeneity/diversity: the importance of keystone structures. *Journal of biogeography*, 31(1), 79-92.
- Tomé, M., & Burkhart, H. E. (1989). Distance-dependent competition measures for predicting growth of individual trees. *Forest Science*, 35(3), 816-831.

- Valladares, F., Gianoli, E., & Gómez, J. M. (2007). Ecological limits to plant phenotypic plasticity. *New phytologist*, *176*(4), 749-763.
- von Lüpke, B., Ammer, C., Bruciamacchie, M., Brunner, A., Ceitel, J., Collet, C., ... & Zientarski, J. (2004). Silvicultural strategies for conversion. In *Norway Spruce Conversion* (pp. 121-164). Brill.
- Wood, S. N., Li, Z., Shaddick, G., & Augustin, N. H. (2017). Generalized additive models for gigadata: modeling the UK black smoke network daily data. *Journal of the American Statistical Association*, *112*(519), 1199-1210.
- Yu, X., Liang, X., Hyyppä, J., Kankare, V., Vastaranta, M., & Holopainen, M. (2013). Stem biomass estimation based on stem reconstruction from terrestrial laser scanning point clouds. *Remote Sensing Letters*, *4*(4), 344-353.
- Zhao, D., Borders, B., Wilson, M., & Rathbun, S. L. (2006). Modeling neighborhood effects on the growth and survival of individual trees in a natural temperate

# CHAPTER 3

---

## **Three-dimensional Quantification of Tree Architecture from Mobile Laser Scanning and Geometry Analysis**

This chapter is published as a research article in *Trees – Structure and Function*, Volume 35, 1385–1398, 12 April 2021, Springer Nature.

DOI: <https://doi.org/10.1007/s00468-021-02124-9>

Yonten Dorji<sup>\*1,6</sup>, Bernhard Schuldt<sup>2</sup>, Liane Neudam<sup>1</sup>, Rinzin Dorji<sup>1</sup>, Kali Middleby<sup>3</sup>, Emilie Isasa<sup>2</sup>, Klaus Körber<sup>4</sup>, Christian Ammer<sup>1</sup>, Peter Annighöfer<sup>5</sup>, Dominik Seidel<sup>1</sup>

<sup>1</sup> Georg-August-Universität Göttingen, Silviculture and Forest Ecology of the Temperate Zones, Faculty of Forest Sciences, Büsgenweg 1, 37077 Göttingen, Germany

<sup>2</sup> Ecophysiology and Vegetation Ecology, Julius-Maximilian University of Würzburg, Julius- von-Sachs-Platz 3, 97082 Würzburg

<sup>3</sup> College of Science and Engineering, James Cook University, Cairns, 4870 Queensland, Australia

<sup>4</sup> Institute for Commercial and Recreational Horticulture, Bavarian State Institute for Viticulture and Horticulture, An der Steige 15, 97209 Veitshochheim, Germany

<sup>5</sup> Forest and Agroforest Systems, Technical University of Munich, Hans-Carl-v.-Carlowitz-Platz 2, 85354 Freising, Germany

<sup>6</sup> College of Natural Resources, Royal University of Bhutan, 1264 Punakha, Bhutan

\* Correspondence: [Yonten.dorji@uni-goettingen.de](mailto:Yonten.dorji@uni-goettingen.de); Tel.: +49 551 3933680

ORCID ID: <https://orcid.org/0000-0002-6508-9582>

## Abstract

The structure and dynamics of a forest are defined by the architecture and growth patterns of its individual trees. In turn, tree architecture and growth result from the interplay between the genetic building plans and environmental factors. We set out to investigate whether (i) latitudinal adaptations of the crown shape occur due to characteristic solar elevation angles at a species' origin, (ii) architectural differences in trees are related to seed dispersal strategies, and (iii) tree architecture relates to tree growth performance. We used Mobile Laser Scanning (MLS) to scan 473 trees and generated three-dimensional data for each tree. Tree architectural complexity was then characterized by fractal analysis using the box-dimension approach along with a topological measure of the top-heaviness of a tree. The tree species studied originated from various latitudinal ranges but were grown in the same environmental settings in the arboretum. We found that trees originating from higher latitudes had significantly less top-heavy geometries than those from lower latitudes. Therefore, to a certain degree, the crown shape of tree species seems to be determined by their original habitat. We also found that tree species with wind-dispersed seeds had a higher structural complexity than those with animal-dispersed seeds ( $p < 0.001$ ). Furthermore, tree architectural complexity was positively related to the growth performance of the trees ( $p < 0.001$ ). We conclude that the use of 3D data from MLS in combination with geometrical analysis, including fractal analysis, is a promising tool for investigating tree architecture.

**Keywords:** Tree architecture, LiDAR, Fractal analysis, Seed dispersal strategy, Latitude, Tree growth

**Key Message:** Mobile laser scanning and geometrical analysis revealed relationships between tree geometry and seed dispersal mechanism, latitude of origin as well as growth.

### 3.1 Introduction

The science of tree structure and form dates back to Leonardo da Vinci, who investigated the cross-sectional area of branches and found it to be maintained across branching orders (Da Vinci, 1967; Richter, 1970). Later, the ‘concept of tree architecture’ and its effect on the ecology and adaptive strategy of trees was comprehensively presented by Hallé & Oldeman (1970). Further, 23 different tree architectural models or ‘genetic blueprints’ were developed to describe tree growth and form, which were considered universal descriptions of tree growth for various species (Hallé et al. 1978). The structure and dynamics of a forest stand are ultimately related to the architecture of the individual trees (West et al., 2009; Price et al., 2012; Seidel et al., 2019a). Therefore, the study of tree structure and form is highly relevant to diverse research fields, such as phylogeny and taxonomy, ecosystem modeling, tree physiology, and crucial for remote sensing of canopy landscapes, tree wind damage studies, carbon stock calculation for climate change mitigation schemes, as well as metabolic scaling theory (Malhi et al., 2018).

Tree architecture ranges from slender, pole-like forms to large, sprawling, multilayered canopies (Beech et al., 2017), and there is likely no identically shaped pair of trees amongst all, even within a species (Seidel et al., 2019b). It is already known that tree architecture is not entirely random (Valadares & Niinemets, 2007) and that it is determined by the dynamic response of tree growth to its abiotic and biotic environment in the context of its genetic code (Hallé et al., 1978; Scorza et al., 2002; Busov et al., 2008; Burkardt et al., 2020). Tree shape has been shown to be influenced by environmental factors such as wind (Noguchi, 1979; Watt et al., 2005; De Langre, 2008), water availability (Archibald & Bond, 2003), light availability (Kuuluvainen, 1992; Niinemets & Kull, 1995), terrain slope (Barij et al., 2007), and competition (Bayer et al. 2013; Juchheim et al., 2017). This adaptive geometry of trees (Horn, 1971; Borchert & Slade, 1981) is likely the result of an individual’s need to optimize fitness in a given location, which would include the need for structural stability, light interception, and reproductive success (Valladares & Niinemets, 2007; Honda & Fisher, 1978; Hollender et al., 2015). Over time, many studies have observed an effect of genetic predisposition on tree growth and branching patterns (Bradshaw & Stettler, 1995; Scotti-Saintagne et al., 2004; Wu & Stettler, 1998; Kenis & Keulemans, 2007; Segura et al., 2006). Depending on the environ-



mental conditions at the growing site, many trees have a particular form that is distinguishable (Lindh et al., 2018; Malhi et al., 2018).

For trees, branching geometry and the resulting crown shape have a great influence on radiation utilization (Niklas, 1986). Several studies showed the major role of crown architecture in the light interception process (Hallé et al., 1978; Iwasa et al., 1985; Guisasaola et al., 2015; Forrester et al., 2018; Lindh et al., 2018). Therefore, crown architecture is also decisive for carbon and water fluxes between the trees and the atmosphere (Enquist et al., 2009). Kuuluvainen (1992) observed that depending on the solar angle of the sun determined by the latitude, there are different crown shapes of trees. It was argued that the variation in sun elevation angle in a given location is so systematic that “it seems reasonable to expect that tree architectures show traits that allow them to efficiently utilize light” (Kuuluvainen, 1992).

Solar interception is not the only factor determining species fitness. For example, seed dispersal impacts the success of propagation and is also influenced by tree architecture (Malhi et al., 2018). Although seed dispersal strategies have been studied extensively (Darwin, 1859; Schmidt, 1918; Hamrick et al., 1993; Wagner et al., 2004; Tiebel et al., 2019), studies on the relationship between seed dispersal strategy and tree architecture are less common (Malhi et al., 2018). To date, we are aware of no study that has investigated the relationship between tree crown complexity and seed dispersal strategy. This is because tree architecture and structural complexity are difficult to quantify (Su et al., 2020; Guzmán et al., 2020). While Xu & colleagues (2019) did find a relationship between tree parameters of height-stem diameter relationships and seed dispersal type in a subtropical montane moist forest (with wind-dispersed strategies common in large-statured tree species and animal-mediated dispersal more common in understory species), their study did not consider crown complexity. In addition, individuals were measured in the field, where confounding variables such as competition by neighboring trees could not be controlled.

Until recently, highly labor-intensive and time-consuming methods were used to address tree structure in detail (Bentley et al., 2013) whenever the rather qualitative architectural models of the past did not satisfy the needs of modern science. Approaches to quantitatively assess tree structure and form were based on measures of specific tree features, such as height (e.g., Sterck & Bongers, 2001), diameter of the stem (e.g., Gering & May, 1995) or crown base height (e.g., Sprinz & Burkhardt, 1987) among many others.

Lately, three-dimensional data from laser scanning approaches (LiDAR) are also used to derive tree characteristics such as tree crown volume (Moorthy et al., 2011), crown surface area (Metz et al., 2013), crown radius (Seidel et al., 2015), or even detailed branching pattern like branch angles, branch lengths and branch volumes (Tao et al., 2015; Disney, 2018; Li et al., 2018; Dorji et al., 2019). In fact, LiDAR is revolutionizing the way we look at trees (Gonzalez de Tanago et al., 2018). By allowing changes in tree architecture to be observed, the 3D data of the actual tree form can help improve our understanding of why trees are shaped a certain way.

Recently, with the new means of 3D characterization of tree structures based on laser scanning, the use of fractal analysis has become possible for further analysis of tree architecture (Seidel et al., 2018). Fractal geometry has been utilized as a tool for analyzing nonlinear, fragmented, and irregularly structured objects, such as corals (Martin-Garin et al., 2007), organs (Losa et al., 2012), and plants (Hasting & Sugihara, 1993). It was introduced by the mathematician Benoit Mandelbrot in the 1970s to describe the complexity of a broad range of objects based on the degree to which the object can fill the available space (Mandelbrot, 1977). In fractal analysis, the box-dimension ( $D_b$ ) is a measure that can be used to assess the architectural complexity of trees holistically (Seidel et al., 2019a). By observing the change in the number of virtual boxes one needs to fill the entire space occupied by an object in dependence of the size of the boxes one uses, the box-dimension is quantified in 3D model space.  $D_b$  was shown to be sensitive to characteristics of tree shape as well as the internal structure of the tree crowns (Seidel, 2018). It was also shown to be positively related to the growth of several temperate and tropical species (Seidel, 2018; Seidel et al., 2019b). The approach integrates the whole tree architecture in a single number, the box-dimension, which was also successfully related to the functional aspects of trees (Seidel et al., 2019b).

In this study, we use  $D_b$  with the aim to observe the relationship between seed dispersal strategy and tree architecture, as well as to investigate the effect of  $D_b$  on tree growth. Additionally, we used a topological measure of a tree's top-heaviness, namely the relative height of maximum horizontal crown area (Rel.Hmaxarea), to address Kuuluvainen's theory of tree shapes depending on the latitude of a species' home range due to the prevalent solar elevation angles.

We aimed to address the question of whether the adaptation of tree species to the solar elevation at their place of origin is still visible in the tree architecture of individuals of

the same species at their place of growth. In theory, there is a gradient from wider and flatter or domed tree crowns in the tropics to more vertically shaped and elongated crowns at high latitudes (Oker-Blom & Kellomaki, 1982; Kuuluvainen, 1992). Therefore, from our 3D point cloud data of the trees, we hypothesize that 1) trees originating from different latitudes show crown shapes reflecting adaptations to the condition at their home range latitude, 2) the genetic building plan of a tree is optimized for the seed dispersal strategy which may reflect in the box-dimension and 3) the radial increment of a tree is related to the box-dimension of the tree.

## **3.2 Materials and Method**

### **3.2.1 Study site**

This study was conducted in the Stutel-Arboretum near Würzburg, Bavaria, Germany (49°51'49"N, 9°51'8"E). It is located at an elevation of 180 m above sea level at the right bank of the river Main. The climate of the study area is characterized by a mean annual temperature of 9.5 °C and a mean annual precipitation of 603 mm. It falls under the humid continental climate type as per the Köppen climate classification. However, drought events occur frequently on the site during summer months. The study site is characterized by a sandy anthrosol (according to the world reference base for soil resources) with a pH value of around 7.3.

The arboretum harbors more than 400 tree species from different origins around the world, with latitudinal midpoints spanning approximately from 25° to 75°. The trees were first raised in different nurseries in Europe and Asia, then brought to the arboretum as seedlings (maximum age of 2 years). The trees were then planted and raised in the arboretum since 2010 under the extensive project called 'Klimabäume Stutel' by the Bavarian State Institute for Viticulture and Horticulture (LWG), which aims to assess the suitability of various tree species as future urban trees. The trees are monitored periodically by recording their growth but are maintained without disturbance to their growth form, with the exception of some minor pruning in the first year after planting. We investigated 473 trees of 41 genera and 105 species and varieties. The trees were planted in 42 rows with a spacing of at least 3 x 3 m. The location of the study site is provided in Figure 3.1.

In the arboretum, trees were grown in a fashion suitable for the interpretation of tree architectures resulting from their genetic makeup. Specifically, trees shared a common

soil, geographical setting (southwest facing aspect and mild slope), climatic condition and were grown without interference from neighboring trees or any major disturbance to their growth form.

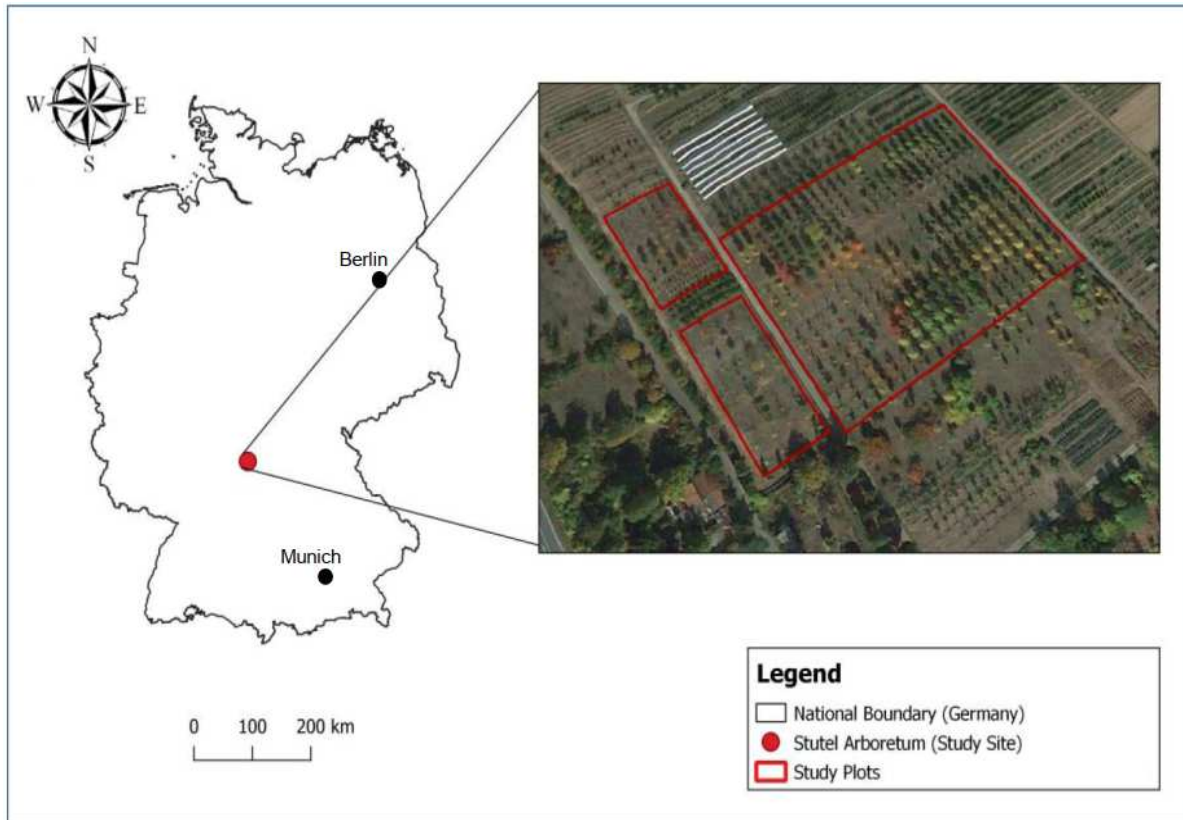


**Figure 3.1.** Map of Germany with the location of the research site at Stutel arboretum, Würzburg, Germany, and an aerial view of the arboretum (Google Earth, 2013) with the three study plots chosen for our scanning campaign.

### **3.2.2 Mobile Laser scanning**

A ground-based mobile laser scanning (MLS) system was used (Geoslam ZEB-HORIZON, Geoslam Ltd., UK, 2019) to obtain 3D point cloud data for accurate measurement and mapping of the environment. The MLS device has the advantage of being easy to use without preparations on site. It saves the time required to set up a tripod or reference points (as common practice in terrestrial laser scanning) and also provides automatic data registration (coregistration of the different scan perspectives). The maximum range of the ZEB-HORIZON is 100 m under ideal conditions and about 50 m in real-life outdoor conditions. It uses a laser with a wavelength of 903 nm and scans at a rate of 300,000 points per second. The scan range noise is  $\pm 30$  mm. Based on the SLAM-

Algorithm (Simultaneous Locating and Mapping), the scanner constantly captures the environment while walking around.

### **3.2.3 Data Collection**

The scanning was carried out in February 2020, when the trees were leafless, to ensure free sight on the tree crowns. All 473 trees were scanned carrying the scanner in hand at around breast height with the arm outstretched while moving at a slow walking pace. In MLS, the selection of the walking path is important for a good tree representation from all sides. We walked in a zig-zag route around the trees and covered two planting rows at a time in each scan by following the direction of the row and finally ending at the exact point where the scan started (up and down the row). We made sure to close the loop every time. By zig-zagging every other tree on the way back, we covered all trees from both sites (see Figure 2.2).

We obtained records of the periodical circumference measurements for 391 of the individual trees since the time of plantation from the Bavarian State Institute for Viticulture and Horticulture (LWG). Tree circumference was measured using calipers. We calculated the difference between the initial plantation radial measurement and the present radius of the tree individuals as a measure of tree growth and expressed it as an annual radial increment.

### **3.2.4 Species information (origin, latitudinal range, and seed dispersal strategy)**

The secondary data for the places of species origin and latitudinal range were obtained from the database of the European Forest Genetic Resources Program (EUFORGEN, 1994) and Van Den Berk Nurseries (Vdberk, 2020). To compare the top-heaviness (Rel.Hmaxarea, see Chapter 3.2.8) with the latitudinal range of the species, the mid-point of their maximum and minimum latitudinal distribution was calculated. We are aware that this mid-point latitude is of limited accuracy since highly detailed geographical information on every species' natural distribution would be needed for an exact mid-point determination. This is, however, unavailable for many species. We used the absolute values of the latitudes in order to analyze both hemispheres together since we do not assume an effect on tree architecture based on the hemisphere (average solar elevation angles are the same). This analysis was performed for 431 trees from 83 species since we could not find exact origins for some cultivars.

Information regarding seed dispersal strategy was obtained from the Royal Botanic Gardens Kew Seed Information Database (SID, 2020) as well as from additional literature (Howe & Smallwood, 1982; Clark et al., 1999; Loewer, 2005; Oyama et al., 2018). Tree species were excluded from analysis if their primary seed dispersal strategy could not be clearly identified from literature, or if there were insufficient individuals for statistical analysis (i.e., species with water-dispersed or unassisted dispersal strategies). For analysis of the relationship between seed dispersal strategy and the tree architectural complexity, we considered tree species for which the major seed dispersal strategy was animal-based or wind-based. Out of the 473 trees measured, 320 were used for the analysis of seed dispersal strategy, wherein 130 of these were animal dispersed, and 191 were wind-dispersed.

### ***3.2.5 Scan data post-processing***

The raw data collected by the MLS was processed using the 3D SLAM algorithm in the GeoSLAM Hub 6.0 processing software (Geoslam Ltd. UK) to create a .txt-file for each scan and a trajectory-file containing the 3D trajectory of the walking path. Open source CloudCompare software (CloudCompare v2.10.1, <https://www.danielgm.net/cc/>) was then used for post-processing the point clouds. First, we subsampled each scan point cloud to a 1 cm - resolution (downsampling for homogenous point cloud density). Then, we extracted each tree's point cloud in subsequent steps. We cut the rows of trees (Figure 3.2), and then we cut each tree from the rows and subsequently cleaned outlier points around the individual trees (Figure 3.3).

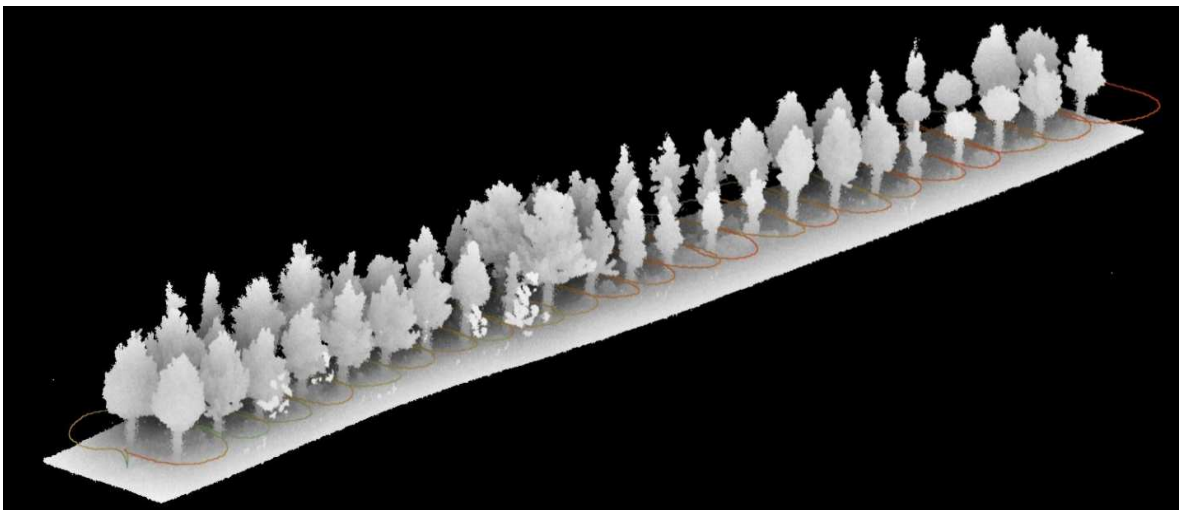


**Figure 3.2** Exemplary picture of trees of two rows after processing a mobile scan in GeoSlam Hub. The red line indicates the trajectory of the device during scanning, with the loop being closed for each scan at the front left (start and end at the beginning of the row). Two tree rows were always scanned at a time by a zig-zagging walking path trajectory surrounding each tree in the two rows



**Figure 3.3** Exemplary cleaned and filtered 3D point cloud of an Elm tree (*Ulmus*) obtained from mobile laser scanning

### **3.2.6 Statistical analysis**

We used the free statistical software R (Vers.3.4, R Development Core Team) for the statistical analysis. We carried out Welch's t-test (assuming unequal variance) to test for significant differences between the mean of the box-dimension of tree species of the two seed dispersal strategies. Linear regression analysis was used to investigate the relationship between the Rel.Hmaxarea (top-heaviness) and the latitude of origin. Due to missing linearity, the relationship between the box-dimension and tree growth, presented here as annual radial increment, was analyzed using non-linear Generalized Additive Modeling (GAM) techniques. The effective degrees of freedom (EDF) were limited to a maximum of 4 (number of knots = 5), whereas the amount of smoothing was then chosen automatically through generalized cross-validation (Wood, 2017). The data fam-

ily was set to Gaussian type with an identity-link function. The level of significance was  $p < 0.05$  for all tests.

### **3.2.7 Fractal analysis with box-dimension**

We used an algorithm written in Mathematica (Wolfram Research, Champaign, USA) to determine the structural complexity of each individual tree, as shown in Seidel (2018). The box-dimension can be considered a measure of a tree structural complexity (Seidel et al., 2019b). This approach is based on the groundbreaking works of Mandelbrot (1977) and a pioneering study by Sarkar & Chaudhuri (1994). The  $D_b$  of each tree was determined by counting the number of virtual boxes of a given size needed to enclose all the above-ground tree parts in the point cloud. We followed the procedure described in Seidel et al. (2019a). In short, we started with an initial box defined by the minimum bounding cube encapsulating the entire tree point cloud and subsequently used smaller boxes by cutting in half the edge length until the lower cut-off of 10 cm in edge length was reached. The  $D_b$  is considered as the slope of the fitted straight line (least square fit) through the scatterplot of the number of boxes in the y-axis represented by  $\log(N)$  and their size in the x-axis represented by  $\log(1/r)$ . The  $\log()$  here is the natural logarithm. 'N' is the number of boxes of the size 'r' required to enclose the entire tree's 3D point cloud. In short, the slope of the regression line through the log-log-graph is defined as  $D_b$  (Mandelbrot, 1977).

Conceptually, any 3D object's  $D_b$  could range from one to three, with a cylindrical object having a  $D_b$  of one and a cubical object having a  $D_b$  of three (Seidel et al., 2019b, see also Figure 3.4). However, in natural objects, especially trees, a  $D_b$  of three cannot be expected (Mandelbrot, 1977). Theoretically, the maximum  $D_b$  that the tree could achieve is assumed to be 2.72 (Seidel et al., 2019a). However, a  $D_b$  of 2.72 would be highly disadvantageous for light utilization due to maximized self-shading of the tree (cf. Seidel et al., 2019a). Therefore, for trees, a  $D_b$  between one and some number lower than 2.72 is to be expected (Seidel, 2018).



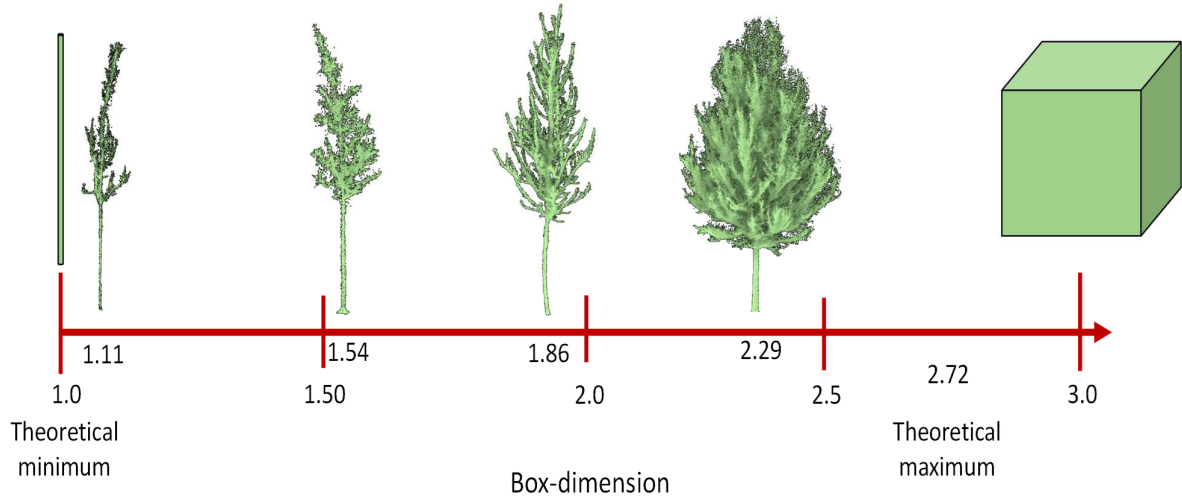


**Figure 3.4** Example objects for box-dimension minimum (box-dimension: 1.0 = pole, topological dimension is also 1) and maximum (box-dimension: 3.0 = cube, topological dimension is also 3). For trees, examples are shown for 1.11 (lowest value observed in our study), 1.54, 1.86, and 2.29 (highest value observed in our study)

### 3.2.8 Topological measure of geometry

We used the relative height of the maximum horizontal crown area (Rel.Hmaxarea) to describe the top-heaviness of a tree's geometry. It was calculated based on the height of the maximum horizontal crown area in relation to the total tree height. Therefore, it is a relative measure corrected for tree height and given in percent. The underlying parameter "height of maximum crown area" was calculated as described in Seidel et al. (2011). In short, the tree point clouds were split into horizontal layers of 10 cm in thickness, and the area of the convex hull polygon enclosing all points in each horizontal layer was calculated. The height of the layer with the largest area is considered Hmaxarea (or 'HCPA' (height of maximum crown projection area) in earlier studies). The relative Hmaxarea was then given in percent of the total tree height. Tree height was derived from the point cloud as the difference between highest point and lowest point in the point cloud of a tree ( $z_{\max} - z_{\min}$ ).

## 3.3 Results

Table 3.1 provides an overview of the studied trees and some general characteristics that were used in our study.

**Table 3.1** Summary of all investigated trees, the number of samples per species/cultivar, mean box-dimension (Db), mean height, mean latitude of origin, respec-

tive seed dispersal strategy, and mean annual radial increment as a measure of growth. The abbreviation 'n.a.' refers to missing data. "Not included" indicates the species' seed dispersal strategy was not relying on a single mechanism or the mechanism could not be identified

Species/Cultivar	Number of trees	Mean $D_b$	Mean Height (m)	Mean Latitude (°)	Seed dispersal strategy	Mean annual radial increment (cm)
<i>Acer buergerianum</i>	2	2.14	6.44	36.99	Wind	0.27
<i>Acer campestre</i>	16	1.99	6.88	42.92	Wind	0.37
<i>Acer cappadocicum</i>	2	1.97	6.07	40.24	Wind	0.32
<i>Acer davidii</i>	1	1.64	5.59	31.80	Wind	n.a.
<i>Acer freemanii</i>	4	1.95	7.64	48.67	Wind	0.19
<i>Acer griseum</i>	1	2.00	4.89	46.14	Wind	0.22
<i>Acer monspessulanum</i>	2	2.21	6.87	40.09	Wind	0.41
<i>Acer opalus</i>	4	1.94	6.00	37.32	Wind	0.42
<i>Acer platanoides</i>	18	2.01	7.10	50.47	Wind	0.38
<i>Acer pseudoplatanus</i>	2	2.03	6.83	41.86	Wind	0.41
<i>Acer rubrum</i>	11	2.01	5.99	48.65	Wind	0.33
<i>Acer truncatum</i>	4	1.90	7.26	36.99	Wind	0.27
<i>Acer x neglectum</i>	2	2.13	6.92	n.a.	Not included	0.44
<i>Aesculus arnoldia</i>	1	1.36	4.22	48.88	Animals	n.a.
<i>Aesculus glabra</i>	2	1.49	4.58	48.88	Not included	n.a.
<i>Ailanthus altissima</i>	2	2.00	6.78	31.15	Wind	0.67
<i>Alnus cordata</i>	2	2.11	6.59	40.47	Wind	0.32
<i>Alnus spaethii</i>	8	2.12	7.53	51.11	Not included	0.35
<i>Amelanchier arborea</i>	2	2.08	7.32	36.35	Animals	0.25
<i>Betula albosinensis</i>	2	2.09	7.02	36.99	Not included	0.13
<i>Betula pendula</i>	4	2.14	8.58	53.57	Not included	0.34
<i>Betula utilis</i>	4	2.11	6.67	30.91	Wind	0.17
<i>Carpinus betulus</i>	12	1.93	5.88	50.69	Not included	0.30
<i>Celtis australis</i>	2	2.07	6.75	54.23	Animals	0.40
<i>Celtis julianae</i>	4	2.08	8.29	31.00	Not included	0.61
<i>Celtis occidentalis</i>	4	2.10	7.23	43.80	Animals	0.43
<i>Cladrastis kentukea</i>	3	2.00	5.90	40.21	Animals	0.43

<i>Corylus colurna</i>	4	2.01	6.29	36.75	Animals	0.26
<i>Crataegus lavalleyi</i>	4	1.77	6.11	46.71	Animals	0.23
<i>Crataegus persimilis</i>	4	1.82	5.99	48.88	Animals	0.12
<i>Diospyros virginiana</i>	1	1.84	4.29	48.25	Animals	n.a.
<i>Eucommia ulmoides</i>	4	2.01	6.46	36.99	Wind	0.31
<i>Euonymus europaeus</i>	2	1.77	4.19	53.57	Animals	0.14
<i>Euonymus plainipes</i>	2	1.69	3.55	50.16	Animals	0.09
<i>Fraxinus americana</i>	4	1.77	5.61	48.88	Wind	0.12
<i>Fraxinus angustifolia</i>	4	2.06	7.50	24.92	Not included	0.34
<i>Fraxinus cuspidata</i>	4	1.33	5.74	29.63	Wind	n.a.
<i>Fraxinus ornus</i>	20	1.88	5.99	38.28	Not included	n.a.
<i>Fraxinus penn</i>	4	1.56	5.46	62.95	Wind	0.10
<i>Ginkgo biloba</i>	4	1.71	5.15	45.62	Not included	n.a.
<i>Gleditsia triacanthos</i>	7	2.02	6.84	36.35	Animals	n.a.
<i>Gymnocladus dioicus</i>	2	1.57	5.45	48.25	Not included	0.15
<i>Koelreuteria paniculata</i>	1	2.04	5.37	36.99	Not included	0.37
<i>Liquidambar styraciflua</i>	7	1.77	5.70	51.16	Wind	0.16
<i>Magnolia denudata</i>	3	1.65	5.52	30.65	Animals	n.a.
<i>Malus tschonoskii</i>	3	1.82	5.74	32.98	Animals	0.15
<i>Morus alba</i>	2	2.08	5.87	36.99	Animals	0.41
<i>Ostrya japonica</i>	2	1.66	5.73	32.98	Wind	0.10
<i>Ostrya carpinifolia</i>	8	2.05	6.04	40.09	Wind	0.19
<i>Parrotia persica</i>	3	1.62	4.38	36.05	Not included	0.16
<i>Platanus acerifolia</i>	4	2.10	4.78	n.a.	Wind	0.31
<i>Platanus hispanica</i>	4	1.98	7.70	52.12	Wind	0.31
<i>Platanus orientalis</i>	8	2.03	7.82	45.30	Wind	0.45
<i>Populus trichocarpa</i>	2	1.88	6.73	50.49	Wind	n.a.
<i>Prunus n.a.</i>	2	1.57	5.10	35.62	Animals	0.09
<i>Prunus padus</i>	3	1.99	6.38	51.06	Animals	0.29
<i>Prunus serrulata</i>	4	1.78	5.84	38.27	Animals	0.37
<i>Prunus x yedonensis</i>	2	1.96	5.38	32.98	Not included	0.22
<i>Ptelea trifoliata</i>	3	1.90	4.38	43.26	Wind	n.a.
<i>Pyrus calleryana</i>	8	1.93	7.55	47.05	Animals	0.29
<i>Quercus bicolor</i>	6	1.79	5.79	48.25	Not included	0.33
<i>Quercus castaneifolia</i>	8	1.64	5.52	35.41	Animals	n.a.
<i>Quercus cerris</i>	8	1.87	6.98	41.92	Animals	n.a.

<i>Quercus ellipsoidalis</i>	1	2.09	6.55	54.18	Animals	0.31
<i>Quercus frainetto</i>	7	1.69	5.99	46.60	Not included	n.a
<i>Quercus hispanica</i>	2	1.94	6.89	52.12	Not included	0.29
<i>Quercus imbricaria</i>	2	1.83	5.03	48.25	Animals	n.a
<i>Quercus macrocarpa</i>	3	1.69	5.91	52.41	Animals	0.30
<i>Quercus n.a.</i>	2	1.44	4.92	48.56	Not included	n.a
<i>Quercus palustris</i>	2	1.37	4.88	48.88	Animals	0.18
<i>Quercus phellos</i>	2	1.80	5.28	48.25	Not included	n.a.
<i>Quercus pubescens</i>	5	1.94	6.07	41.23	Animals	n.a.
<i>Quercus rhysophylla</i>	2	1.73	5.17	26.43	Animals	n.a
<i>Quercus sargentii</i>	1	1.53	5.08	38.91	Not included	0.16
<i>Quercus serrata</i>	1	1.43	5.05	36.99	Animals	0.25
<i>Quercus Shumardii</i>	4	1.74	5.51	25.53	Not included	0.23
<i>Quercus texana</i>	6	1.64	5.51	32.47	Animals	n.a.
<i>Quercus velutina</i>	1	1.68	5.59	36.35	Animals	n.a.
<i>Sophora japonica</i>	6	2.19	7.41	40.74	Animals	0.56
<i>Sorbus incana</i>	2	1.86	5.53	55.68	Animals	0.35
<i>Sorbus latifolia</i>	8	1.98	6.09	51.11	Animals	0.31
<i>Sorbus thuringiaca</i>	6	1.90	6.02	n.a.	Animals	0.26
<i>Sycoparrotia semidecidua</i>	1	1.72	3.37	36.99	Not included	n.a.
<i>Taxodium distichum</i>	1	2.01	6.23	26.78	Not included	0.18
<i>Tetradium daniellii</i>	2	2.00	5.83	44.80	Not included	0.36
<i>Thuja plicata</i>	1	2.02	6.17	48.88	Wind	0.30
<i>Tilia tomentosa</i>	1	1.52	4.93	41.69	Not included	0.36
<i>Tilia americana</i>	2	2.12	6.95	48.88	Not included	0.35
<i>Tilia cordata</i>	12	2.07	6.63	52.74	Not included	n.a.
<i>Tilia euchlora</i>	2	1.88	6.14	n.a.	Not included	0.36
<i>Tilia euchlora x mongolica</i>	2	1.58	5.53	n.a.	Not included	0.21
<i>Tilia europaea</i>	4	2.12	7.52	53.57	Not included	0.39
<i>Tilia henryana</i>	2	1.69	4.54	31.00	Wind	0.19
<i>Tilia japonica x mongolica</i>	2	1.54	4.99	39.16	Not included	0.24
<i>Tilia mandshurica</i>	2	1.56	4.27	45.24	Not included	n.a.
<i>Tilia mongolica</i>	6	1.94	5.20	43.99	Wind	n.a.
<i>Tilia monticola</i>	2	1.24	5.31	48.88	Not included	0.19
<i>Tilia platyphyllos</i>	8	2.05	7.33	47.84	Not included	0.37
<i>Tilia tomentosa</i>	20	2.06	6.51	48.23	Animals	n.a.

<i>Tilia x moltkei</i>	1	1.54	4.90	n.a.	Not included	0.25
<i>Ulmus laevis</i>	2	2.00	8.35	57.76	Wind	0.62
<i>Ulmus spp.</i>	47	1.99	7.84	52.74	Wind	n.a.
<i>Viburnum lentago</i>	2	1.94	3.92	43.80	Animals	0.07
<i>Zelkova serrata</i>	6	2.02	6.37	32.98	Wind	0.33
Total	473					

We discovered a significant but weak correlation between the latitudinal mid-point of a species' origin and the trees' top-heaviness (Rel.Hmaxarea) (Figure 3.5). The most top-heavy tree geometries were found for species originating from Japan and Korea (*Prunus serulata* Lindl.) with a latitudinal mid-point of around 38°N. Individuals of this species had a Rel.Hmaxarea of 76 % on average. Lowest Rel.Hmaxarea of 35 % was identified for individuals of *Betula pendula*. R originating from higher latitudes (mid-point > 53°)

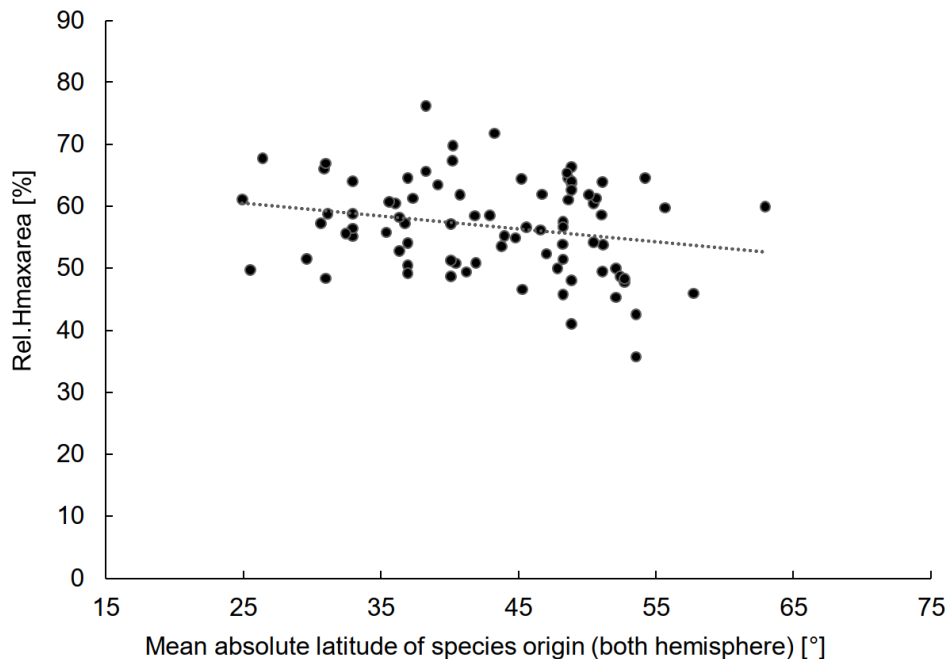


**Figure 3.5** Scatterplot of relative height of maximum horizontal crown area (Rel.Hmaxarea) over mean absolute latitude (latitudinal mid-point) of each species origin. The coefficient of determination ( $R^2$ ) was 0.052 but significant with  $p < 0.05$ ;  $n = 83$  species (mean values per species)

We also found a significant difference in tree architecture between different seed dispersal strategies. Despite a similar range of values, trees with wind-dispersed seeds

showed, on average, a higher structural complexity ( $D_b$ ) than trees with seeds dispersed by animals (Figure 3.6).

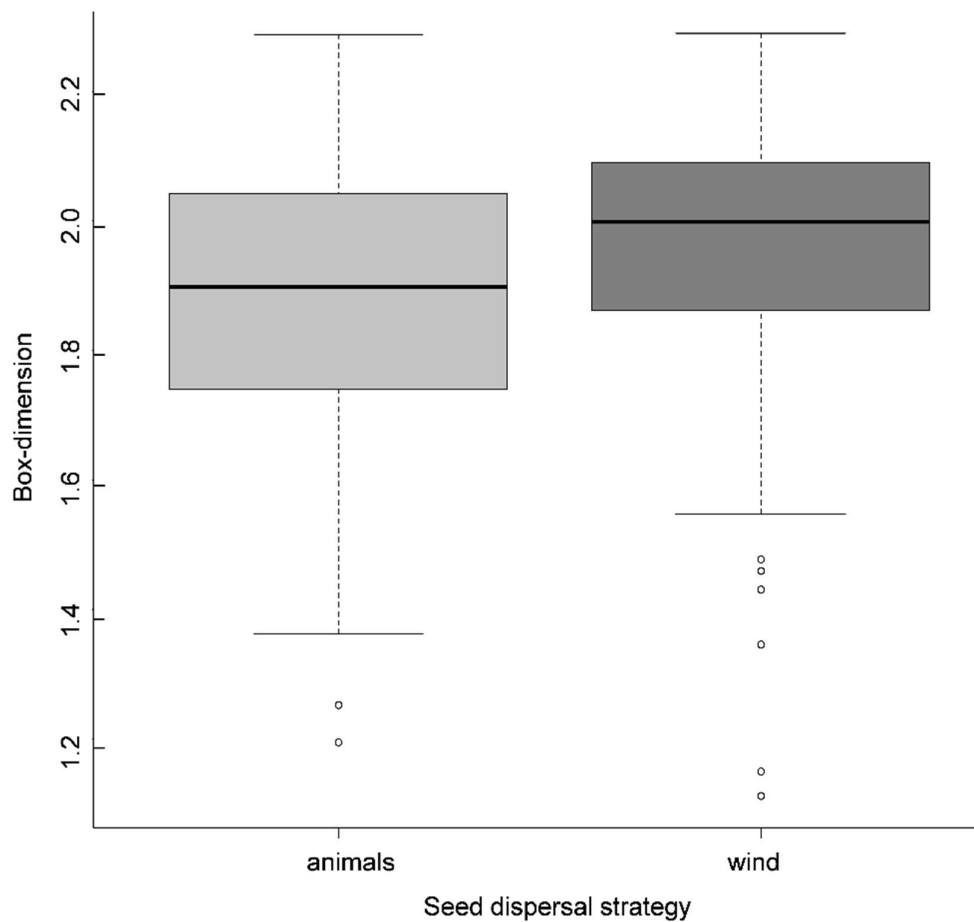


**Figure 3.6** Box-and-Whisker plot of trees of different seed dispersal strategies, namely, wind ( $n = 192$ ) and animal ( $n = 130$ ) dispersed. The difference in means was significant at  $p < 0.001$  (animal-dispersed mean: 1.87; wind-dispersed mean: 1.95)

We also discovered a significant non-linear relationship (represented by the EDF value of 2.58) between the box-dimension and the corresponding annual radial increment of the trees (Figure 3.7). While trees with a high  $D_b$  showed large variability in growth, trees with a low  $D_b$  seemed to asymptotically approach a value around  $2 \text{ mm yr}^{-1}$  and were hence unable to reach high growth rates. Even though the scatter of the data is high, the GAM model explained more than 35 % of the deviance.

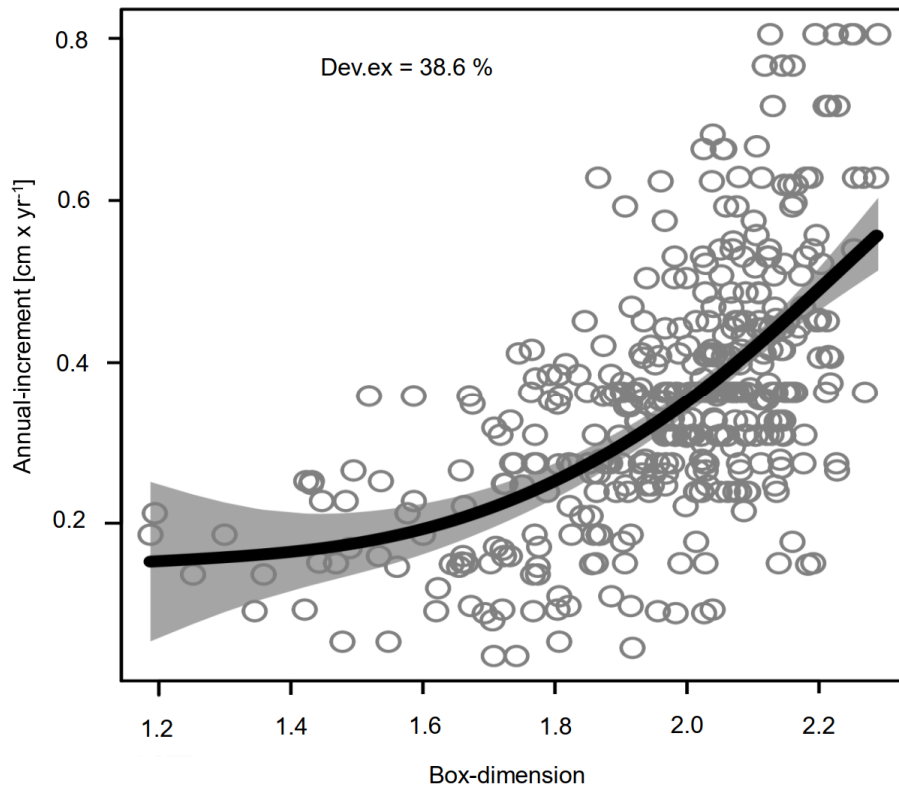


**Figure 3.7** Scatterplot of annual radial increment as a measure of growth over the box-dimension and GAM regression. The relationship is significant at  $p < 0.001$ ; adjusted  $R^2 = 0.364$ ; effective degrees of freedom (EDF) = 2.58. Growth data were available for  $n = 391$  tree individuals. Dev.ex = deviation explained.

### 3.4 Discussion

We hypothesized that trees growing in the Stutel-Arboretum originating from different latitudes would show crown shapes indicating adaptations to the solar elevation angles at the latitude of their species' home range. Our results derived from 3D point cloud data obtained through MLS support this hypothesis (See Figure 3.5). Trees from species of different origins tended to have a more top-heavy geometry when the latitude of their species origin was lower, despite the fact that the individuals investigated here were growing in the same geographical and environmental settings. Even though the relationship was weak ( $R^2 = 0.052$ ), it was significant, indicating the existence of a genetic determination. Trees originating from high latitudes with prevailing low solar elevation angles developed deeper crowns with lower Rel.Hmaxarea to efficiently intercept light when compared to trees of lower latitudes exposed to higher solar elevation angles. The latter develop more top-heavy crowns resulting in a higher Rel.Hmaxarea. This empiri-

cal data supports previous studies that suggested there should be a measurable role of the solar incident angle on the shape of trees (Hallé et al., 1978; Whitmore, 1975; Terborgh, 1985; Hiura, 1998; King, 2005; Tateishi et al., 2010; Bomfleur et al., 2013). However, on our experimental site, with comparable growing conditions for all study trees, we found only a small strength of the effect of crown shape adaption to the latitude of origin. It is important to consider that the mid-point latitude of a species' origin could only be estimated since exact information on the natural distribution of the species is often unavailable. This may partly explain the rather lower explanatory power of latitude for Rel.Hmaxarea (Figure 3.5). Furthermore, we argue that the relationship is not very strong because tree architecture is not just determined by the solar angle. According to the optimized resource utilization strategy, the trees need to balance various biotic and abiotic factors in order to result in an optimized tree shape (Archibald & Bond, 2003; Minamino & Tateno, 2014). Therefore, during the last years, the trees also responded plastically to the conditions at the study site, strongly reducing the observable "legacy" in geometry.

According to literature, there is reason to expect a relationship between the solar geometry at a particular latitude and the shape of the trees that grow there (Kuuluvainen, 1992). Our approach to analyzing this relationship was limited to measuring a genetic legacy effect of solar geometry by relating a tree's shape to the latitude of the tree species' natural distribution. We suspect that the reason for the small effect size of the relationship described in Figure 3.5 is that the capability of a tree to adapt its shape to prevailing biotic and abiotic factors may strongly outweigh the genetic predisposition of a tree to grow a particular shape. However, if we want to gain a better understanding of exactly how strong the influence of solar geometry on tree morphology is, it is necessary to directly relate a tree's latitude (or solar zenith angle at that latitude) to the shape of the tree. This would require extensive point cloud data of many trees from a wide range of latitudes. Pooling together a large number of georeferenced tree point clouds would enable the establishment of a more direct relationship between solar geometry and tree morphology, moving beyond the limitation of only being able to look at genetic legacy effects. Future research in this field should focus on international collaborations and data sharing, for that matter.

Since many crucial factors were the same for all our trees (e.g., water availability, temperature, nutrient availability, competition), we were able to investigate the relation-



ship between tree architectural complexity ( $D_b$ ) and seed dispersal strategy.  $D_b$  is a measure of tree architecture that integrates many other conventional topological measures, like tree height, crown volume, crown radius, branch angle variability, and others (Seidel et al., 2019a, c). Hence, we hypothesized that  $D_b$  should be related to a species' seed dispersal strategy since seed dispersal and reproduction are the key functional roles of tree architecture (Malhi et al., 2018). Indeed, we found that mean structural complexity, as summarized by the  $D_b$ -values, differed significantly between tree species with wind-dispersed and animal-dispersed seeds. Hence, our second hypothesis is supported by our results (Figure 3.6). Malhi et al. (2018) proposed that there are differences in the tree architecture, for example, between Southeast Asian forests, in which species predominantly rely on wind dispersal, and trees of the forest in central Africa and central Amazonia, which are predominantly animal-dispersed. Our data indicate that anemochorus tree species are more structurally complex in shape than zoochorus tree species. We hypothesize that less-complex tree crowns provide easier access and visual attraction for animals while highly complex tree crowns with many branches and greater overall surface, as indicated by the high  $D_b$  value, maybe a greater barrier to wind and hence increase wind speeds wherever wind funnels through the crown. Final conclusions on this matter require more research since our study trees were of rather young age.

Our third hypothesis was that a higher  $D_b$  is related to a higher radial increment, which was supported by our results (Figure 3.7). Earlier studies already identified this relationship for some selected tree species, including some temperate and tropical species (Seidel, 2018; Seidel et al., 2019b). While previous studies observed linear relationships, the observed relationship in our current study appeared to be non-linear according to the GAM-model with more than 35% explained deviation. In fact, when modelled linearly, the deviance explained is still 32% in our data. So far, the functional explanation of the relationship between the box-dimension and tree growth has been that an increased  $D_b$  is often a result of reduced competition (e.g., Dorji et al., 2019) that leads to unrestricted growth and hence better growth performance. Additionally, it was shown that a greater  $D_b$  was directly linked to a more efficient ratio of the photosynthetic surface area to wooden tree volume, or in other words, a better ratio between “producing” and “consuming” organs (Seidel et al., 2019b). We hypothesize that a greater positive effect on productivity at higher rates of complexity than at lower rates of complexity may be

explained by the fractal nature of the tree crown, with increased levels of branching (higher branch order being built) resulting in disproportional benefit to the tree. Since additional higher-order twigs are present in trees with greater complexity, there may often be smaller 'investments' (in terms of wooden structures) needed to produce additional light-capturing tissue surface in those canopies, when compared to rather pole-like tree crowns, where additional branches must first reach the light-exposed outer area of the crown (= larger investment) before light-capturing tissue can be exposed to sunlight. While this remains a hypothesis until further research addresses the issue, we could show that there seems to be a general positive relationship between structural complexity and productivity. Particularly for temperate climates, a large  $D_b$  is related to a more efficient tree architecture (cf. Seidel et al., 2019a). However, if genetically disposed towards more domed, umbrella-like crowns, as required for efficient growth in the subtropics, trees can only adapt to a certain extent towards the conditions in the arboretum and hence carry the legacy of their original habitat. Together with potential other effects (adaptation to soil, climate, genetic predisposition, etc.), this results in lower growth rates compared to well-adapted tree species with optimized crown shapes. In subtropical or tropical climates, a high  $D_b$  would only be beneficial to trees that either grow in the understory (capturing indirect light), like those investigated in Seidel et al. (2019a), or trees that are predominantly facing overcast conditions with a large amount of indirect light. High solar angles in the tropics and subtropics would otherwise result in intense self-shading, resulting in a questionable benefit from a large, multilayered, and complex tree crown as indicated by a high  $D_b$ .

In all the above findings, the use of 3D data in combination with topological and particularly fractal geometry proved to be vital in translating the tree's architectural complexity into numbers that enable relating it to functional traits. In earlier times, characterizing the tree architecture mathematically was hardly possible due to the unavailability of 3D data (Borchert & Slade, 1981), which severely limited our advancement in understanding of drivers and passengers of tree structural complexity. As outlined by recent studies, laser scanning provides a new and unprecedented way of looking at the relationship between tree structure and functions (Malhi et al., 2018; Calders et al., 2020). Thus, it may be the perfect method for further developing functional-structural plant models that are needed to better explain the growth performance of mixed stands (Bongers, 2020).

### **3.5 Conclusion**

Here we used ground-based mobile laser scanning to scan 473 trees and generate three-dimensional data of each tree. We used fractal analysis and a topological measure of geometry to characterize the tree's architectural complexity and geometry. We detected a positive relationship between tree structural complexity and tree growth, as well as a difference in the tree architectural complexity based on different seed dispersal strategies. Furthermore, we detected an effect of the latitude of a species' origin on the geometry of trees growing at our study site. Tree species from lower latitudes were more top-heavy in shape than tree species originating from higher latitudes. We argue that 3D data from mobile laser scanning, particularly in combination with novel tools to assess geometry, like the box-dimension approach, is an efficient and holistic means to characterize tree architecture. Simplifying structural complexity and geometrical characteristics into single numbers can be applied to trees or entire forest stands, providing a means for quantifying complexity and relating it to a diverse functional pattern of trees and forests. This enables new insights into the relationship between the structure and function of terrestrial ecosystems.

### **Acknowledgment**

We are grateful to the anonymous reviewers for their valuable comments. We thank the Bavarian State Institute for Viticulture and Horticulture, Veitshochheim, Germany, for granting us access to the Stutel-Arboretum facility, as well as Andreas Lösch and all others involved in the 'Klimabäume Stutel' Project.

(<http://www.lwg.bayern.de/gartenbau/baumschule/101342/index.php/>).

### **Funding**

This research was funded through DFG grant SE2383/5-1 provided to Dominik Seidel and was further supported by funds of the German government's Special Purpose Fund held at Landwirtschaftliche Rentenbank (FKZ: 844732) provided to Dominik Seidel.

**Conflicts of interest/Competing interests:** The authors declare no conflict of interest.

**Availability of data and material:** The data is available at Dryad under the DOI <https://doi.org/10.5061/dryad.2fqz612n6>.

**Code availability:** The code will be made available upon request (please contact the corresponding author).

**Authors' contributions:** YD, BS, CA and DS developed the concept of the study. YD, LN, RD, KM, EI, KK and DS collected the data. YD, PA and DS analyzed the data. YD and DS wrote the manuscript and BS, RD, LN, EI, KK, KM, CA, and PA performed critical revision. All authors gave final approval.

### 3.6 References

- Guzmán Q, J. A., Sharp, I., Alencastro, F., & Sánchez-Azofeifa, G. A. (2020). On the relationship of fractal geometry and tree-stand metrics on point clouds derived from terrestrial laser scanning. *Methods in Ecology and Evolution*, 11(10), 1309-1318.
- Archibald, S., & Bond, W. J. (2003). Growing tall vs growing wide: tree architecture and allometry of *Acacia karroo* in forest, savanna, and arid environments. *Oikos*, 102(1), 3-14.
- Barij, N., Stokes, A., Bogaard, T., & Beek, R. V. (2007). Does growing on a slope affect tree xylem structure and water relations? *Tree Physiology*, 27(5), 757-764.
- Bayer, D., Seifert, S., & Pretzsch, H. (2013). Structural crown properties of Norway spruce (*Picea abies* [L.] Karst.) and European beech (*Fagus sylvatica* [L.]) in mixed versus pure stands revealed by terrestrial laser scanning. *Trees*, 27(4), 1035-1047.
- Beech, E., Rivers, M., Oldfield, S., & Smith, P. P. (2017). GlobalTreeSearch: The first complete global database of tree species and country distributions. *Journal of Sustainable Forestry*, 36(5), 454-489.
- Bentley, L. P., Stegen, J. C., Savage, V. M., Smith, D. D., von Allmen, E. I., Sperry, J. S., ... & Enquist, B. J. (2013). An empirical assessment of tree branching networks and implications for plant allometric scaling models. *Ecology letters*, 16(8), 1069-1078.
- Bomfleur, B., Decombeix, A. L., Escapa, I. H., Schwendemann, A. B., & Axsmith, B. (2013). Whole-plant concept and environment reconstruction of a *Telemachus conifer* (Voltziales) from the Triassic of Antarctica. *International Journal of Plant Sciences*, 174(3), 425-444.
- Bongers, F. J. (2020). Functional-structural plant models to boost understanding of complementarity in light capture and use in mixed-species forests. *Basic and Applied Ecology*, 48, 92-101.
- Borchert, R., & Slade, N. A. (1981). Bifurcation ratios and the adaptive geometry of trees. *Botanical gazette*, 142(3), 394-401.
- Bradshaw Jr, H. D., & Stettler, R. F. (1995). Molecular genetics of growth and development in populus. IV. Mapping QTLs with large effects on growth, form, and phenology traits in a forest tree. *Genetics*, 139(2), 963-973.
- Burkardt, K., Pettenkofer, T., Ammer, C., Gailing, O., Leinemann, L., Seidel, D., & Vor, T. (2021). Influence of heterozygosity and competition on morphological tree characteristics of *Quercus rubra* L.: a new single-tree based approach. *New Forests*, 52(4), 679-695.
- Busov, V. B., Brunner, A. M., & Strauss, S. H. (2008). Genes for control of plant stature and form. *New Phytologist*, 177(3), 589-607.
- Calders, K., Phinn, S., Ferrari, R., Leon, J., Armston, J., Asner, G. P., & Disney, M. (2020). 3D imaging insights into forests and coral reefs. *Trends in ecology & evolution*, 35(1), 6-9.
- Clark, J. S., Silman, M., Kern, R., Macklin, E., & HilleRisLambers, J. (1999). Seed dispersal near and far: patterns across temperate and tropical forests. *Ecology*, 80(5), 1475-1494.
- Darwin, C. R. (1859). *The Origin of Species*. Vol. XI. The Harvard Classics. New York: PF Collier & Son, 1909-14; Bartleby.com, 2001.
- De Langre, E. (2008). Effects of wind on plants. *Annu. Rev. Fluid Mech.*, 40, 141-168.
- EUFORGEN (1994). European forest genetic resources program. <http://www.euforgen.org/species/> Accessed 15 June 2020
- West, G. B., Enquist, B. J., & Brown, J. H. (2009). A general quantitative theory of forest structure and dynamics. *Proceedings of the National Academy of Sciences*, 106(17), 7040-7045.
- Forrester, D. I., Ammer, C., Annighöfer, P. J., Barbeito, I., Bielak, K., Bravo-Oviedo, A., ... & Pretzsch, H. (2018). Effects of crown architecture and stand structure on light absorption in mixed and monospecific *Fagus sylvatica* and *Pinus sylvestris* forests along a productivity and climate gradient through Europe. *Journal of Ecology*, 106(2), 746-760.
- GeoSLAM (2019) ZEB-HORIZON User's Manual v1.2 GeoSLAM. <https://geoslam.com/solutions/zeb-horizon/> Accessed 19 June 2020

- Gering, L. R., & May, D. M. (1995). The relationship of diameter at breast height and crown diameter for four species groups in Hardin County, Tennessee. *Southern Journal of Applied Forestry*, 19(4), 177-181.
- Gonzalez de Tanago, J., Lau, A., Bartholomeus, H., Herold, M., Avitabile, V., Raunonen, P., ... & Calders, K. (2018). Estimation of above-ground biomass of large tropical trees with terrestrial LiDAR. *Methods in Ecology and Evolution*, 9(2), 223-234.
- Google Earth (2013) Version: Google earth pro (7.1.2.2041). <https://www.google.com/earth/versions/>. Accessed 19 June 2020
- Guisasola, R., Tang, X., Bauhus, J., & Forrester, D. I. (2015). Intra-and inter-specific differences in crown architecture in Chinese subtropical mixed-species forests. *Forest Ecology and Management*, 353, 164-172.
- Hamrick, J. L., Murawski, D. A., & Nason, J. D. (1993). The influence of seed dispersal mechanisms on the genetic structure of tropical tree populations. *Vegetatio*, 107(1), 281-297.
- Hastings, H. M., & Sugihara, G. (1993). Fractals. A user's guide for the natural sciences. *Oxford Science Publications*.
- Hallé, F., & Oldeman, R. A. (1970). *Essai sur l'architecture et la dynamique de croissance des arbres tropicaux* (Vol. 6, pp. 1-178). Paris: Masson.
- Hallé, F., Oldeman, R. A., & Tomlinson, P. B. (1978). Opportunistic tree architecture. In *Tropical trees and forests* (pp. 269-331). Springer, Berlin, Heidelberg.
- Hiura, T. (1998). Shoot dynamics and architecture of saplings in *Fagus crenata* across its geographical range. *Trees*, 12(5), 274-280.
- Hollender, C. A., & Dardick, C. (2015). Molecular basis of angiosperm tree architecture. *New Phytologist*, 206(2), 541-556.
- Horn, H. S. (1971). *The adaptive geometry of trees*. Princeton University Press.
- Honda, H., & Fisher, J. B. (1978). Tree branch angle: maximizing effective leaf area. *Science*, 199(4331), 888-890.
- Howe, H. F., & Smallwood, J. (1982). Ecology of seed dispersal. *Annual review of ecology and systematics*, 13, 201-228.
- Iwasa, Y. O. H., Cohen, D. A. N., & Leon, J. A. (1985). Tree height and crown shape, as results of competitive games. *Journal of theoretical Biology*, 112(2), 279-297.
- Juchheim, J., Annighöfer, P., Ammer, C., Calders, K., Raunonen, P., & Seidel, D. (2017). How management intensity and neighborhood composition affect the structure of beech (*Fagus sylvatica* L.) trees. *Trees*, 31(5), 1723-1735.
- Kenis, K., & Keulemans, J. (2007). Study of tree architecture of apple (*Malus domestica* Borkh.) by QTL analysis of growth traits. *Molecular Breeding*, 19(3), 193-208.
- King, D. A. (2005). Architectural differences in saplings of temperate versus tropical angiosperms; consequences of the deciduous habit? *Botany*, 83(11), 1391-1401.
- Kuuluvainen, T. (1992). Tree architectures adapted to efficient light utilization: is there a basis for latitudinal gradients? *Oikos*, 275-284.
- Li, Y., Su, Y., Hu, T., Xu, G., & Guo, Q. (2018). Retrieving 2-D leaf angle distributions for deciduous trees from terrestrial laser scanner data. *IEEE Transactions on Geoscience and Remote Sensing*, 56(8), 4945-4955.
- Lindh, M., Falster, D. S., Zhang, L., Dieckmann, U., & Brännström, Å. (2018). Latitudinal effects on crown shape evolution. *Ecology and evolution*, 8(16), 8149-8158.
- Loewer, P. (2005). *Seeds: the definitive guide to growing, history and lore*. Timber Press.
- Losa, G. A. (2012). Fractals and their contribution to biology and medicine. *Medicographia*, 34(3), 364-374.

- Mandelbrot, B. B., & Mandelbrot, B. B. (1982). *The fractal geometry of nature* (Vol. 1). New York: WH freeman.
- Malhi, Y., Jackson, T., Patrick Bentley, L., Lau, A., Shenkin, A., Herold, M., ... & Disney, M. I. (2018). New perspectives on the ecology of tree structure and tree communities through terrestrial laser scanning. *Interface Focus*, *8*(2), 20170052.
- Metz, J., Seidel, D., Schall, P., Scheffer, D., Schulze, E. D., & Ammer, C. (2013). Crown modeling by terrestrial laser scanning as an approach to assess the effect of aboveground intra-and interspecific competition on tree growth. *Forest Ecology and Management*, *310*, 275-288.
- Minamino, R., & Tatenno, M. (2014). Tree branching: Leonardo da Vinci's rule versus biomechanical models. *PLoS one*, *9*(4), e93535.
- Moorthy, I., Miller, J. R., Berni, J. A. J., Zarco-Tejada, P., Hu, B., & Chen, J. (2011). Field characterization of olive (*Olea europaea* L.) tree crown architecture using terrestrial laser scanning data. *Agricultural and Forest Meteorology*, *151*(2), 204-214.
- Niinemets, Ü., & Kull, O. (1995). Effects of light availability and tree size on the architecture of assimilative surface in the canopy of *Picea abies*: variation in needle morphology. *Tree physiology*, *15*(5), 307-315.
- Noguchi, Y. (1979). Deformation of trees in Hawaii and its relation to wind. *The Journal of Ecology*, 611-628.
- Niklas, K. J. (1986). Computer simulations of branching-patterns and their implications on the evolution of plants. *Lectures on mathematics in the life sciences*, *18*, 1-50.
- Martin-Garin, B., Lathuilière, B., Verrecchia, E. P., & Geister, J. (2007). Use of fractal dimensions to quantify coral shape. *Coral Reefs*, *26*(3), 541-550.
- Oker-Blom, P., & Kellomäki, S. (1982). Theoretical computations on the role of crown shape in the absorption of light by forest trees. *Mathematical Biosciences*, *59*(2), 291-311.
- Oyama, H., Fuse, O., Tomimatsu, H., & Seiwa, K. (2018). Ecological properties of shoot-and single seeds in a hardwood, *Zelkova serrata*. *Data in brief*, *18*, 1734-1739.
- Price, C. A., Weitz, J. S., Savage, V. M., Stegen, J., Clarke, A., Coomes, D. A., ... & Swenson, N. G. (2012). Testing the metabolic theory of ecology. *Ecology letters*, *15*(12), 1465-1474.
- R Core Team (2018). R: A language and environment for statistical computing. R Foundation for Statistical Computing, Vienna, Austria.
- Richter, J. P. (1970). *The notebooks of Leonardo da Vinci* (Vol. 2). Courier Corporation.
- SID (2020) Royal Botanic Gardens Kew Seed Information Database. Version 7.1. <http://data.kew.org/sid/>. Accessed 15 July 2020.
- Sarkar, N., & Chaudhuri, B. B. (1994). An efficient differential box-counting approach to compute fractal dimension of image. *IEEE Transactions on systems, man, and cybernetics*, *24*(1), 115-120.
- Schmidt, W. (1918). Die Verbreitung von Samen und Blütenstaub durch die Luftbewegung. *Oesterr Bot Z*, *67*(10), 313-328.
- Segura, V., Cilas, C., Laurens, F., & Costes, E. (2006). Phenotyping progenies for complex architectural traits: a strategy for 1-year-old apple trees (*Malus x domestica* Borkh.). *Tree Genetics & Genomes*, *2*(3), 140-151.
- Seidel, D. (2018). A holistic approach to determine tree structural complexity based on laser scanning data and fractal analysis. *Ecology and evolution*, *8*(1), 128-134.
- Seidel, D., Annighöfer, P., Stiers, M., Zemp, C. D., Burkardt, K., Ehbrecht, M., ... & Ammer, C. (2019). How a measure of tree structural complexity relates to architectural benefit-to-cost ratio, light availability, and growth of trees. *Ecology and evolution*, *9*(12), 7134-7142.
- Seidel, D., Ehbrecht, M., Annighöfer, P., & Ammer, C. (2019). From tree to stand-level structural complexity—Which properties make a forest stand complex? *Agricultural and Forest Meteorology*, *278*, 107699.

- Seidel, D., Ehbrecht, M., Dorji, Y., Jambay, J., Ammer, C., & Annighöfer, P. (2019). Identifying architectural characteristics that determine tree structural complexity. *Trees*, 33(3), 911-919.
- Seidel, D., Leuschner, C., Müller, A., & Krause, B. (2011). Crown plasticity in mixed forests—quantifying asymmetry as a measure of competition using terrestrial laser scanning. *Forest Ecology and Management*, 261(11), 2123-2132.
- Seidel, D., Schall, P., Gille, M., & Ammer, C. (2015). Relationship between tree growth and physical dimensions of *Fagus sylvatica* crowns assessed from terrestrial laser scanning. *iForest-Biogeosciences and Forestry*, 8(6), 735.
- Scorza R, Bassi D, Liverani A (2002) Genetic interactions of pillar (columnar), compact, and dwarf peach tree genotypes.
- Scotti-Saintagne, C., Bodénès, C., Barreneche, T., Bertocchi, E., Plomion, C., & Kremer, A. (2004). Detection of quantitative trait loci controlling bud burst and height growth in *Quercus robur* L. *Theoretical and Applied Genetics*, 109(8), 1648-1659.
- Sprinz, P. T., & Burkhart, H. E. (1987). Relationships between tree crown, stem, and stand characteristics in unthinned loblolly pine plantations. *Canadian Journal of Forest Research*, 17(6), 534-538.
- Sterck, F. J., & Bongers, F. (2001). Crown development in tropical rain forest trees: patterns with tree height and light availability. *Journal of Ecology*, 89(1), 1-13.
- Su, Y., Hu, T., Wang, Y., Li, Y., Dai, J., Liu, H., ... & Guo, Q. (2020). Large-Scale Geographical Variations and Climatic Controls on Crown Architecture Traits. *Journal of Geophysical Research: Biogeosciences*, 125(2), e2019JG005306.
- Tao, S., Wu, F., Guo, Q., Wang, Y., Li, W., Xue, B., ... & Fang, J. (2015). Segmenting tree crowns from terrestrial and mobile LiDAR data by exploring ecological theories. *ISPRS Journal of Photogrammetry and Remote Sensing*, 110, 66-76.
- Tateishi, M., Kumagai, T. O., Suyama, Y., & Hiura, T. (2010). Differences in transpiration characteristics of Japanese beech trees, *Fagus crenata*, in Japan. *Tree Physiology*, 30(6), 748-760.
- Terborgh, J. (1985). The vertical component of plant species diversity in temperate and tropical forests. *The American Naturalist*, 126(6), 760-776.
- Tiebel, K., Leinemann, L., Hosius, B., Schlicht, R., Frischbier, N., & Wagner, S. (2019). Seed dispersal capacity of *Salix caprea* L. assessed by seed trapping and parentage analysis. *European Journal of Forest Research*, 138(3), 495-511.
- Valladares, F., & Niinemets, Ü. (2007). The architecture of plant crowns: from design rules to light capture and performance. In *Functional plant ecology* (pp. 101-150). CRC Press.
- Vdberk (2020). Van der Berk Nurseries. 1600 species of trees and shrubs <https://www.vdberk.com/trees/> Accessed 16 June 2020
- Wagner, S., Wälder, K., Ribbens, E., & Zeibig, A. (2004). Directionality in fruit dispersal models for anemochorous forest trees. *Ecological Modelling*, 179(4), 487-498.
- West, G. B., Enquist, B. J., & Brown, J. H. (2009). A general quantitative theory of forest structure and dynamics. *Proceedings of the National Academy of Sciences*, 106(17), 7040-7045.
- Watt, M. S., Moore, J. R., & McKinlay, B. (2005). The influence of wind on branch characteristics of *Pinus radiata*. *Trees*, 19(1), 58-65.
- Whitmore, T. C. (1984). *Tropical rain forests of the Par East*. Oxford. Clarendon Press.
- Wood, S. N., Li, Z., Shaddick, G., & Augustin, N. H. (2017). Generalized additive models for gigadata: modeling the UK black smoke network daily data. *Journal of the American Statistical Association*, 112(519), 1199-1210.
- Wu, R., & Stettler, R. F. (1998). Quantitative genetics of growth and development in *Populus*. III. Phenotypic plasticity of crown structure and function. *Heredity*, 81(3), 299-310.
- Xu, Y., Iida, Y., Huang, H., Shi, Z., Franklin, S. B., Luo, Y., ... & Jiang, M. (2019). Linkages between tree architectural designs and life-history strategies in a subtropical montane moist forest. *Forest Ecology and Management*, 438, 1-9.



# CHAPTER 4

---

## **Insights into the Relationship Between Hydraulic Safety, Hydraulic Efficiency and Tree Structural Complexity from Terrestrial Laser Scanning and Fractal Analysis**

This chapter is available as a preprint research article in the Research Square preprint server with the DOI link as:

DOI: <https://doi.org/10.21203/rs.3.rs-2744981/v1>

Authors: Yonten Dorji<sup>\*1,2</sup>, Emilie Isasa<sup>3</sup>, Juliano Sarmiento Cabral<sup>4,5</sup>, Tashi Tobgay<sup>2</sup>, Peter Annighöfer<sup>6</sup>, Bernhard Schuldt<sup>3,7</sup>, Dominik Seidel<sup>1</sup>

<sup>1</sup> Department for Spatial Structures and Digitization of Forests, Faculty of Forest Sciences, Georg-August-Universität Göttingen, Büsgenweg 1, 37077 Göttingen, Germany

<sup>2</sup> Department of Forest Science, College of Natural Resources, Royal University of Bhutan, 1264 Punakha, Bhutan

<sup>3</sup> Ecophysiology and Vegetation Ecology, Julius-von-Sachs-Institute of Biological Sciences, University of Würzburg, Julius-von-Sachs-Platz, 97082 Würzburg, Germany

<sup>4</sup> Ecosystem Modeling Group, Center for Computational and Theoretical Biology, University of Würzburg, Klara-Oppenheimer-Weg 32, 97074 Würzburg, Germany

<sup>5</sup> Biodiversity Modelling and Environmental Change, School of Biosciences, College of Life and Environmental Sciences, University of Birmingham, Birmingham B15 2TT, United Kingdom

<sup>6</sup> Forest and Agroforest Systems, Technical University of Munich, Hans-Carl-v.-Carlowitz-Platz 2, 85354 Freising, Germany

<sup>7</sup> Chair of Forest Botany, Institute of Forest Botany and Forest Zoology, Technical University of Dresden, Piennner Str. 7, 01737 Tharandt, Germany

\* Corresponding author: [Yonten.dorji@uni-goettingen.de](mailto:Yonten.dorji@uni-goettingen.de); Tel.: +49 551 3923680

ORCID ID: <https://orcid.org/0000-0002-6508-9582>

## Abstract

The potential of trees to adapt to drier and hotter climates will determine the future state of forests in the wake of a changing climate. Attributes connected to trees' hydraulic network are likely to determine their ability to endure drought. However, how a tree's architectural attributes relate to its drought tolerance remains understudied. We set out to quantify the relationship between tree structural complexity and drought tolerance, represented by xylem safety measures. We used terrestrial laser scanning (TLS) to scan 71 trees of 18 species and generated 3D attributes of each tree. We constructed quantitative structure models (QSMs) to characterize the branching patterns of all study trees.

Additionally, the box-dimension approach from fractal analysis was used to assess overall structural complexity of the trees. Three measures of xylem safety, i.e., the water potential at 12%, 50%, and 88% loss of hydraulic conductance ( $P_{12}$ ,  $P_{50}$ ,  $P_{88}$ ), were measured to characterize drought tolerance of the trees' hydraulic systems, completed by data on specific hydraulic conductivity ( $K_s$ ). Our findings revealed a significant relationship between the structural complexity ( $D_b$ ) and the three measures of xylem safety and  $K_s$ . Tree species with low structural complexity developed embolism-resistant xylem at the cost of hydraulic efficiency. The branching geometry of 2<sup>nd</sup> and 3<sup>rd</sup> order branches was also related to xylem safety. Our findings also revealed that the  $D_b$  had a more pronounced and significant relationship with branch hydraulic safety and efficiency than all other tested structural attributes. Our findings indicate that the box-dimension is a helpful and easy-to-measure descriptor of tree architecture that also relates to important branch hydraulic properties of a tree.

**Keywords:** tree architecture, Terrestrial Laser Scanning, drought tolerance, fractal analysis, xylem safety, climate change.

## 4.1 Introduction

As a consequence of climate change, the occurrence of severe droughts is increasing in several parts of the world (Trenberth et al., 2014; Settele et al., 2015). While forest systems are susceptible to a variety of severe climatic conditions, drought and its concomitant disruptions have the largest impact worldwide (Reichstein et al., 2013). It is the most common stressor impacting the forest carbon balance globally, potentially generating a sharp decline in net primary productivity at regional and global levels (Ciais et al., 2005; Lewis et al., 2011). There has been increasing concern that warmer temperatures may cause more extended and intense droughts, highlighting the need for accurate projections of drought impacts on forest ecosystems (Rousi et al., 2022). In addition, studies reveal that drought-related mass tree death is not limited to drier locations (Anderegg et al., 2012; Hammond et al., 2022). It has been reported in a range of forest biomes, including cold temperate (Nardini et al., 2013; Schuldt et al., 2020) and tropical forests (Rowland et al., 2018). As droughts severely impact tree structure and function (Nepstad et al., 2007; Phillips et al., 2010), the potential of trees to adapt to dry climates will determine the future state of forests in the face of climate change (Bittencourt et al., 2020). Therefore, it is of paramount importance to understand the relationship between tree architecture, forest structure and drought tolerance.

The structure and function of a forest ecosystem are ultimately tied to the species composition and the structures of the individual trees (West et al., 2009; Seidel et al., 2019a). Various ecological functions and services offered by a forest, such as wood value (Ishii et al., 2004), recreational value (Ribe et al., 2009), or ecosystem resilience (Neill & Puettmann, 2013) depend on the structural characteristics and species composition in the stand.

Tree structure and form are not the results of stochastic growth (Valladares & Niinemets, 2007). They are, in fact, the result of the interaction between the genetic growth plan and the biotic and abiotic environment (Scorza et al., 2002; Busov et al., 2008). Environmental factors like the wind (Watt et al., 2005), sunlight angle (Kuuluvainen, 1992), seed dispersal strategy (Dorji et al., 2021), water availability (Niinemets & Kull, 1995), and competition (Dorji et al., 2019) determine the final shape of a tree. The plasticity of tree geometry in response to environmental agents was considered to be the outcome of an individual's

drive to maximize strength in a certain area (Borchert & Slade 1981), such as reproductive potential or sunlight absorption (Hollender & Dardick, 2015).

The study of 3D tree structure and form was shown to be of importance for a variety of disciplines, such as tree phylogenetics, remote sensing of forest landscapes, ecosystem modeling, and carbon stock computation (Chave et al., 2005; Arseniou et al., 2021ab). Despite this great importance, the three-dimensional quantification of tree architecture was a challenging task in the past (destructive, laborious, and time-consuming). So far, the assessment was limited to only small trees (Moore et al., 2008; Bentley et al., 2013). Therefore, a lack of sufficient data has hampered the development and testing of theory, specifically linking tree structures with their physiological role and mechanism (Malhi et al., 2018).

The arrival of Laser scanning technology has transformed the way we perceive trees and quantify their structures (Gonzalez de Tanago et al., 2018). Apart from conventional tree size attributes, TLS is also being used to derive tree branching patterns (branch angles, lengths, volumes) with precision levels exceeding those of leading international allometric models (Liang et al., 2018; Demol et al., 2022). Thus, this has provided an avenue to analyze and understand how tree architecture and forest structure change in response to various factors like competition, drought, light availability, and utilization (e.g., Dassot et al., 2011).

Our grasp of how plants adapt to dry spells and how drought-induced tree mortality occurs depends on understanding tree hydraulic traits (Choat et al., 2018). As one of the most commonly reported metrics of xylem vulnerability to hydraulic failure (Anderegg et al., 2016), hydraulic safety is often quantified by the water potential at which 12%, 50% and 88% loss of hydraulic conductivity occur. Embolisms form when water potentials in conduits drop to levels that promote embolism formation (Tyree & Zimmermann, 2002). As a result, tree dieback seems predictable by hydraulic thresholds related to xylem dysfunction (Britton et al., 2022; Hajek et al., 2022). Therefore, plant hydraulic characteristics play an important role in drought survivability and carbon fluxes (Chen et al., 2021; McDowell et al., 2022).

Since water is conducted throughout the whole architectural system of the tree, fractal analysis offers a unique approach to addressing it. Benoit Mandelbrot, in the 1970s, developed the concept of fractal geometry to characterize and explain the complexity of a wide variety of objects based on how they fill space (Mandelbrot, 1977). With the advances

in 3D modeling of tree architecture, the application of fractal geometry has become possible in a comprehensive analysis of tree architecture (Seidel, 2018; Dorji et al., 2021). Several “fractal”-based theories have been propounded to comprehend tree structure and function, e.g., pipe-model theory (Valentine 1985) and metabolic scaling theory (West et al., 1997; Martin-Ducup et al., 2020). The fractal-like geometry of trees, according to these concepts, is a direct representation of both intrinsic and malleable morphological features that influence tree development and survival. Furthermore, fractal approaches are increasingly used to analyze nonlinear, unevenly structured elements, including landscape-level ecological phenomena (Hasting & Sugihara, 1993; Halley et al., 2004). Today, the box-dimension ( $D_b$ ) is a fractal analysis metric readily available to quantify the structural complexity of trees (e.g., Arseniou et al., 2021a; Saarinen et al., 2021).

We employed the box-dimension paradigm in this research to quantify the overall tree architectural complexity. We assessed how this complexity relates to the hydraulic thresholds of xylem safety across a range of temperate tree species. Specifically, we used detailed tree architectural measures related to branching patterns (up to the 3<sup>rd</sup> order branching orders) to address the following hypotheses: **1)** The box-dimension ( $D_b$ ), as a proxy for the overall tree structural complexity, directly relates to the drought tolerance represented by xylem pressure at a loss of hydraulic conductivity. **2)** Branch angles and lengths of the tree species have a significant relationship with xylem safety since the branching pattern directly relates to the hydraulic network. **3)** Tree structural complexity ( $D_b$ ) is more closely related to xylem safety than height and DBH since  $D_b$  is a holistic measure that incorporates overall tree architectural patterns and networks rather than selected single characteristics.

## **4.2 Materials and Methods**

### **4.2.1 Study site**

This research study is part of the extensive Klimabäume Stutel project managed under the Bavarian State Institute for Viticulture and Horticulture (LWG). The research was carried out at Stutel-Arboretum, located on the right bank of the river Main, near Wuerzburg, Bavaria, Germany, at an altitude of 180 meters above sea level. The geographical coordinates are at 49° 51' 49" N, 9° 51' 8" E. The mean annual temperature of the area is 9.5 °C, receiving average annual precipitation of 603 mm. A continental climate type characterizes the

region, and the area, as such, experiences frequent drought events, especially in hot summer months. The soil is primarily sandy anthrosol with a pH value of 7.3. The arboretum is home to over 400 tree species. All trees were initially grown in various nurseries across Europe and Asia before being transplanted as seedlings (two years of age) to the Stutel-Arboretum.

The plantations at the arboretum were established since 2010 by the LWG with the aim to examine the feasibility of trees of various species as future urban trees that are resilient to droughts. The trees in the arboretum are monitored for their growth development while experiencing the same climate conditions. However, they are kept in their natural state without disturbing their growth form and with no fertilization or irrigation applied.

Our research investigated 71 different tree individuals belonging to 18 species (see Table 4.1 for basic information on 18 species pooled together and the data repository for detailed 71 individual tree information).

**Table 4.1** Summary of all investigated tree species: the number of individual trees in each species, mean box-dimension (**D<sub>b</sub>**), mean height (**TTH**), mean diameter at breast height (**DBH**), mean crown volume (**CV**), mean crown surface area (**CSA**), and total mean number of branches (1<sup>st</sup>, 2<sup>nd</sup>, and 3<sup>rd</sup> order branches). Measurement units are given within parentheses.

Tree Species	Total Nos.	Mean $P_{12}$ (MPa)	Mean $P_{50}$ (MPa)	Mean $P_{88}$ (MPa)	Mean $D_b$	Mean TTH (m)	Mean DBH (cm)	Mean CV (m <sup>3</sup> )	Mean CSA (m <sup>2</sup> )	Mean No. of branches
<i>Acer campestre</i>	4	-4.721	-5.406	-6.0923	1.831	7.00	10.53	13.33	36.60	31
<i>Acer platanoides</i>	4	-3.5434	-4.2756	-5.0079	1.747	7.20	12.47	13.54	37.75	24
<i>Acer rubrum</i>	4	-2.4991	-2.8803	-3.2616	1.892	6.18	8.86	12.98	36.23	33
<i>Betula pendula</i>	4	-2.0034	-2.3839	-2.7645	1.893	8.42	11.18	19.31	54.74	37
<i>Betula utilis</i>	4	-1.8456	-2.0628	-2.2800	1.882	6.56	9.01	13.39	36.30	24
<i>Carpinus betulus</i>	4	-3.3497	-4.6168	-5.8840	1.927	7.45	10.78	9.63	30.39	33
<i>Crataegus persimilis</i>	4	-4.6567	-5.9116	-7.1666	1.674	5.92	7.46	5.22	24.89	21
<i>Ostrya carpinifolia</i>	4	-3.8300	-4.5611	-5.2923	1.874	6.02	8.97	11.51	34.06	26
<i>Platanus acerifolia</i>	4	-1.5450	-1.8528	-2.1606	1.987	4.73	9.93	8.59	26.48	31
<i>Platanus orientalis</i>	4	-1.2779	-1.8010	-2.3241	1.926	7.67	13.24	25.86	56.71	45

<i>Prunus padus</i>	3	-2.2919	-3.1274	-3.9628	1.800	6.36	10.88	15.77	41.24	24
<i>Prunus serrulata</i>	4	-2.8387	-4.0144	-5.1901	1.652	5.82	11.88	5.92	21.90	18
<i>Pyrus calleryana</i>	4	-4.4818	-5.7064	-6.9311	1.870	7.56	10.84	9.37	32.62	25
<i>Sorbus latifolia</i>	4	-3.8923	-5.7420	-7.5917	1.766	5.57	9.34	6.99	25.79	26
<i>Tilia cordata</i>	4	-2.2878	-3.1628	-4.0379	1.909	6.50	11.51	11.34	33.46	28
<i>Tilia mongolia</i>	4	-2.1461	-2.9245	-3.7029	1.803	5.10	8.75	2.38	15.87	27
<i>Tilia platyphyllus</i>	4	-2.8096	-3.3936	-3.9776	1.946	7.57	12.25	14.51	38.91	30
<i>Tilia tormentosa</i>	4	-2.6327	-3.2876	-3.9424	1.854	7.52	17.12	35.85	71.09	30

The trees were grown at a minimum spacing of 3 x 3 meters, as shown in figure 3.1. The study trees grew in the same soil, climate, and geographical positioning, i.e., the southwest-facing aspect with a gentle slope.

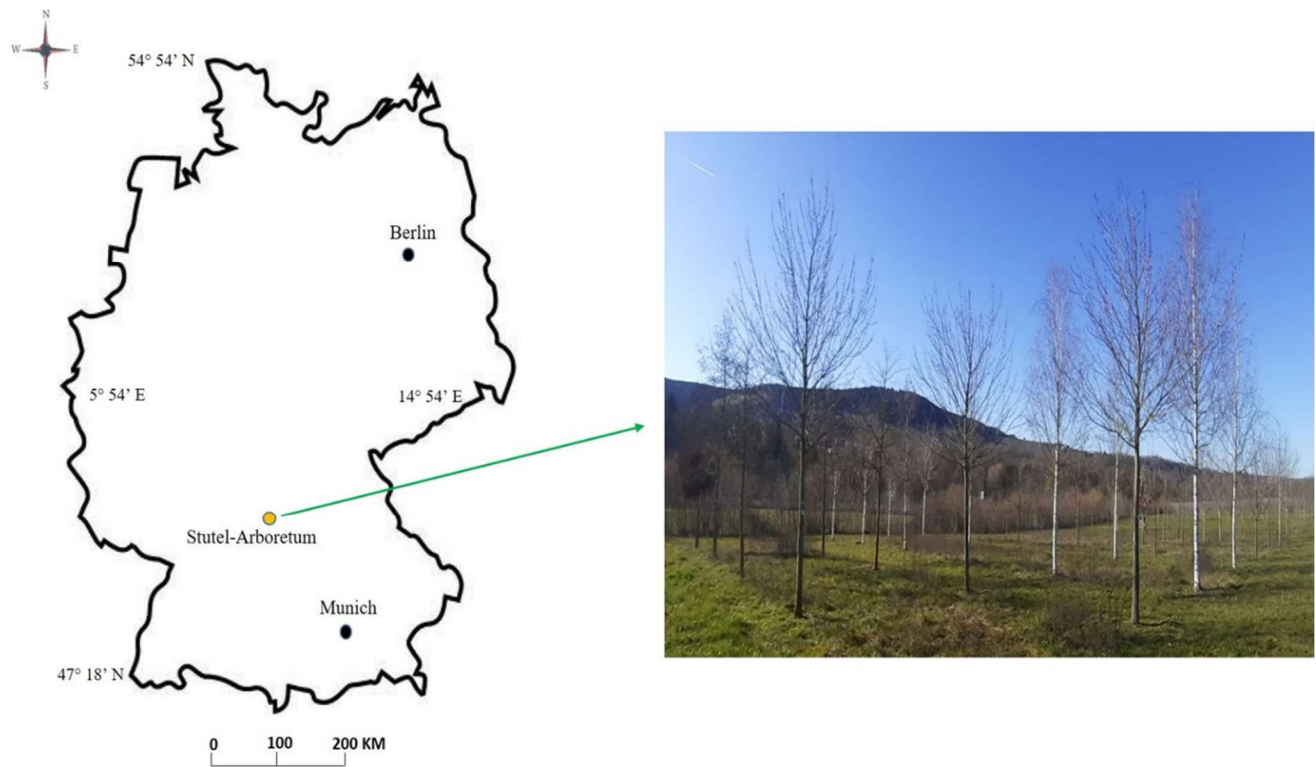


**Figure 4.1** Shows the map and location of the research site at Stutel, Wuerzburg, Germany, and a photograph depicting a section of the Stutel-Arboretum.

#### **4.2.2 Terrestrial LiDAR**

We used the Faro Focus M70 Terrestrial Laser Scanner (Faro Technologies Inc., Lake Mary, FL, USA) to obtain detailed three-dimensional point cloud data of all study trees. The instrument uses laser light with 650-690 nm wavelength for scanning the environment up to a distance of 70 m and covers a field of view of  $300^{\circ} \times 360^{\circ}$  with a precision of 0.03 degrees yielding 10,240 points per  $360^{\circ}$ . The scanner was set up on a tripod at breast height (1.3 meters) and levelled horizontally, employing a bubble level.

Scanning was carried out during a dry period with no wind (March 26, 2020) when the trees were in leafless condition (all study tree species were deciduous) to guarantee best visibility of the entire wooden tree crown. We performed a multi-scan procedure of all 71 trees, with four scans each, amounting to a total of 284 scans. We scanned each tree from four corner points with the tree always in the center, also referred to as ‘corner setup’ in the literature (Zande et al., 2008). We applied the instrument’s standard filters (clear con-



tour and clear sky) during scanning. The scan data was then automatically registered, filtered, and exported as single xyz.-files using Faro Scene (Faro Technologies Inc., Lake Mary, FL, USA). The generated 3D image of each tree is a composite of millions of three-dimensional measuring points, producing a precise and detailed replica of our study trees in the field.

### ***4.2.3 Point Cloud Processing and Quantitative Structure Models (QSM)***

Each tree was manually segmented from the surrounding scenery in the scan using open-source CloudCompare software (CloudCompare v2.10.1, <https://www.danielgm.net/cc/>). CompuTree software (Vers. 5.0, CompuTree Group; [http://computree.onf.fr/?page\\_id=42](http://computree.onf.fr/?page_id=42)) was then used to generate QSMs (Quantitative Structure Models) for all 71 trees. A QSM model is a depiction of the tree point cloud constructed out of cylinders of diverse diameters and lengths. We applied the same QSM-parameter configurations for all trees to ensure the reproducibility of our observations. Clustering tolerance was set at 1 cm, with a maximum of 600-point clusters containing at least 400 points each. If fewer clusters are found, the software will automatically modify them.

For all 71 trees, we used QSM models to acquire detailed information on the branching architecture of the trees. We obtained the i) total branch volume, ii) total branch length, iii) mean branch angle up to 3<sup>rd</sup> order of branches, iv) mean branch length up to 3<sup>rd</sup> order of branches, and v) mean branch volume up to 3<sup>rd</sup> order of branches. An exemplary tree QSM with a cylindrical demonstration of branching patterns is depicted in Figure 4.2.

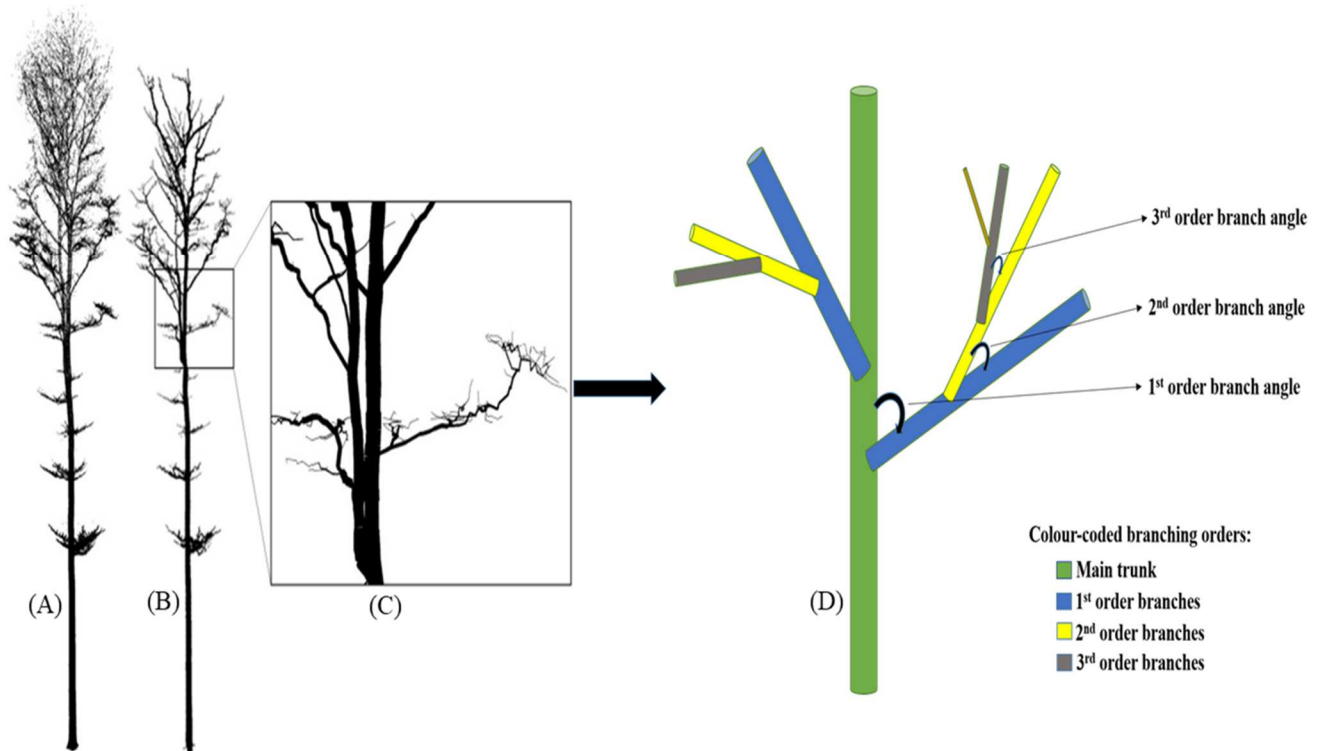


**Figure 4.2** Shows a two-dimensional depiction of a 3D point cloud of a tree in Fig. 4.2A and the corresponding Quantitative Structure Model in Figure 4.2B. A close-up of QSM in Figure 4.2C and a cylindrical demonstration of color-coded branching patterns on the right end in Figure 4.2D. Adapted and modified from Dorji et al. (2019).

#### 4.2.4 Box-dimension ( $D_b$ )

The box-dimension ( $D_b$ ) is a metric of structural complexity (Mandelbrot, 1977). For a tree, it integrates all structural attributes, including crown dimensions and branching patterns (Seidel et al., 2019b). The Box-dimension here was derived from single-tree point clouds using the methods outlined by Seidel (Seidel, 2018) and described in detail (including code) in Arseniou et al., (2021b), (supplementary material: <https://www.mdpi.com/article/10.3390/rs13142773/s1>). This technique is based on the concepts of Sarkar and Chaudhuri (Sarkar & Chaudhuri, 1994) and Mandelbrot's breakthrough contribution (Mandelbrot, 1977). In a nutshell, box-dimension was calculated by counting the number of boxes of a particular size required to encapsulate all aboveground tree structures in the 3D point cloud. The box-dimension is then determined as the slope of the regression line derived from a scatterplot of the number of boxes denoted by  $\log(N)$

over the inverse of the logarithm of the respective box size, with the box size expressed in relation to the initial box size. The theoretical range of  $D_b$  of a single tree spans between 1 and 3 (Mandelbrot, 1977). Figure 4.3 shows an exemplary point cloud of our study trees with the highest and lowest structural complexity, respectively.

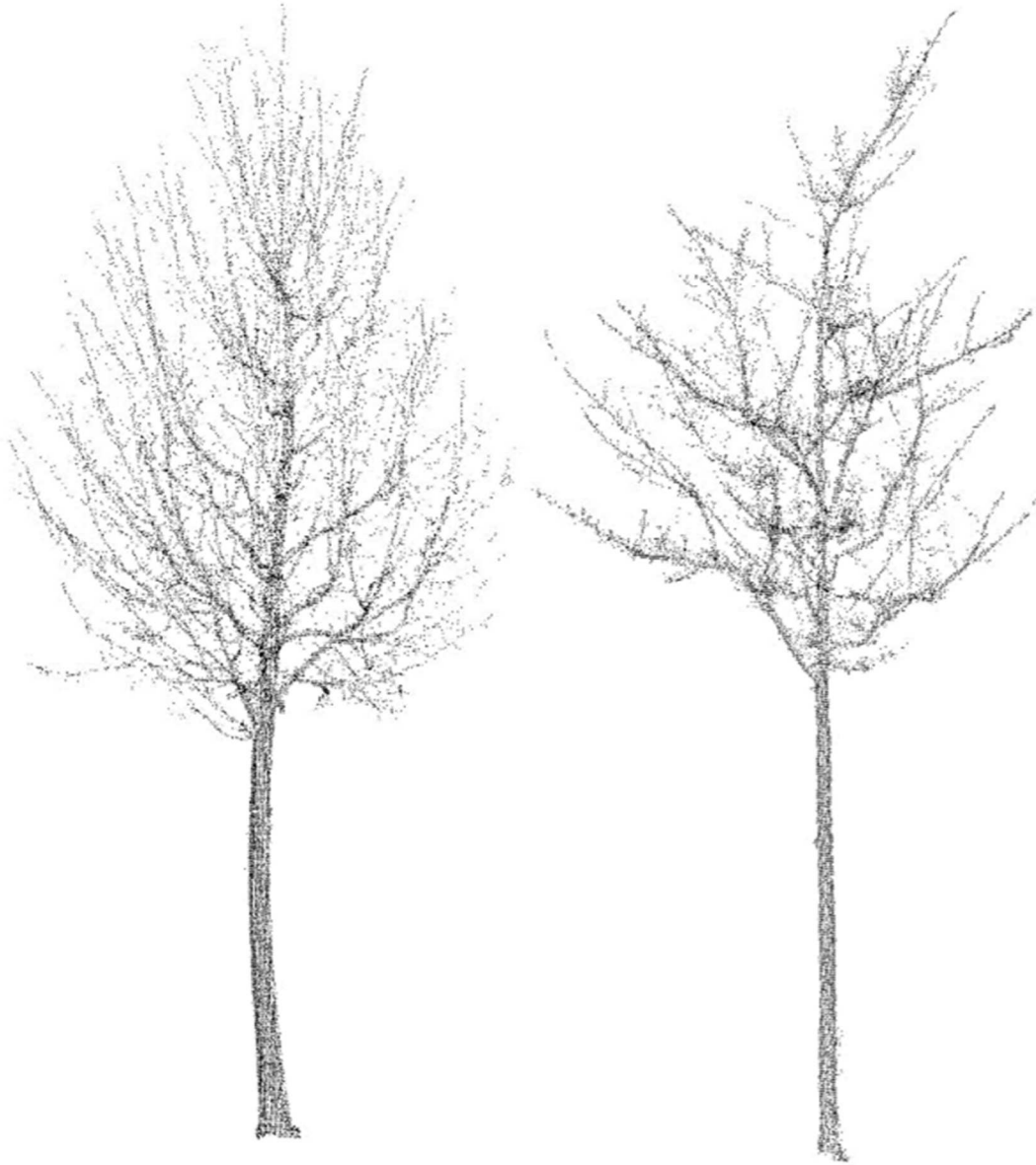


**Figure 4.3** Two exemplary three-dimensional tree point clouds with the highest (left) and lowest (right) box-dimension ( $D_b$ ) values observed in our research study. On the left is a *Tilia cordata* tree ( $D_b = 2.04$ ); on the right is an individual of *Crataegus persimilis* ( $D_b = 1.55$ ).

#### **4.2.5 Xylem pressure measurement ( $P_{12}$ , $P_{50}$ , $P_{88}$ )**

Leveraging the Cavitron instrument, vulnerability curves were measured using the flow-centrifuge technique (Cochard, 2002; Cochard et al., 2005; Cochard et al., 2013), constructed from a Sorval RC 5 series centrifuge with manual rotation speed control and using Cavisoft software (Cavisoft v.5.2.1, University of Bordeaux, Bordeaux, France). Flow centrifuges increase water tension in xylem segments and measure the loss of hydraulic conductance simultaneously using a centrifugal force. The sample's susceptibility to cavitation is shown by the relationship between the percentage loss of xylem conductance (PLC) and xylem water tension.

A subset of the vulnerability curve measurements discussed in this paper was used for addressing controversies in safety-vessel diameter relationships and for a methodological comparison with the pneumatic method (Paligi et al., 2021).

In total, 71 branches from the Stutel arboretum (mean diameter at basipetal end  $\pm$  SE:  $8.87 \pm 0.10$  mm;  $n = 71$ ) were sampled, immediately submerged in demineralized water and recut several times using pruning shears to a final length of 27.5 cm to release the tension in the xylem (Torres-Ruiz et al., 2015). Lateral leaves and twigs were removed, and lateral branches were evened with a razor blade to fit the sample into the Cavitron.

Before measurement in the Cavitron, the bark of the branch samples was removed at both sample ends for 4 cm. Both basipetal and acropetal end diameters were measured two times before insertion into the rotor with cuvettes on both sample ends. Vulnerability curves were measured in the Cavitron without prior flushing at high pressure and using ultrapure deionized and degassed water containing 10 mmol KCl and 1 mmol CaCl<sub>2</sub>. Conductance measurement started at a water potential of -0.834 MPa (equivalent to 3000 rotations per minute, rpm). Then, by raising the rotating speed and the conductivity ( $K$ ) gauged at each pressure level, the xylem pressure was gradually lowered.

Measurements were ended after the samples lost at least 90% of their initial conductance was recorded with Cavisoft software (Table 4.1). A 2-minute waiting time was maintained before measuring at each pressure step to ensure stable conductance values.

Vulnerability curves were then fitted in R (v. 4.1.0, R Core Team, 2021) with nonlinear least squares using the logistic model by Pammenter & Van der Willigen (1998) in a modified version based on raw conductivity measurements (Ogle et al., 2009):

$$k_i \sim \text{Normal} \left( k_{\text{sat}} \cdot \left( 1 - \frac{1}{1 + \exp \left( -\frac{S_{50}}{25} (P_i - P_{50}) \right)} \right), \sigma \right) \quad (1)$$

Where for each observation  $i$ , the conductivity  $k_i$  is assumed to be normally distributed around a logistic function of the water potential  $P_i$  with the parameters  $P_{50}$  (water potential at 50% loss of conductivity),  $S_{50}$  (corresponding slope of the vulnerability curve on the percent loss of conductivity scale),  $k_{\text{sat}}$  (initial conductivity at full saturation) and residual standard deviation  $\sigma$ . The calculation was repeated for  $P_{12}$  and  $P_{88}$ .

#### 4.2.6 Wood anatomy and hydraulic efficiency

Semi-thin transverse sections for wood anatomical analyses were cut from the same branch samples used for hydraulic measurements with a sliding microtome (G.S.L.1, Schenkung Dapples, Zürich, Switzerland), stained with safranin-alcian blue, rinsed with distilled water and ethanol (95%), and permanently mounted on glass slides using Euparal (Carl Roth, Karlsruhe, Germany). A light microscope equipped with an automated table and a digital camera (Observer.Z1, Carl Zeiss MicroImaging GmbH, Jena, Germany; Software: AxioVision c4.8.2, Carl Zeiss MicroImaging GmbH) was used for digitizing the complete cross-section at 100-times magnification. Image processing was done with GIMP v2.10.6 (GIMP Development Team 2018, <https://www.gimp.org/>) and the particle analysis function from ImageJ v1.52p (Schneider et al., 2012). We calculated vessel diameters ( $D$ ,  $\mu\text{m}$ ) from minor (a) and major vessel radii (b) as

$$D = ((32 \times (a \times b)^3) / (a^2 + b^2))^{1/4}, \quad (2)$$

according to White (1991) and used  $D$  to calculate the hydraulically-weighted average vessel diameter ( $D_h$ ,  $\mu\text{m}$ ) according to Sperry et al., (1994) as

$$D_h = \Sigma D^5 / \Sigma D^4. \quad (3)$$

For measuring branch sapwood area-specific hydraulic conductivity ( $K_s$ ,  $\text{kg m s}^{-1} \text{MPa}^{-1}$ ) with degassed, demineralized water containing 10 mM KCl and 1 mM  $\text{CaCl}_2$  using a Xylem Plus embolism meter (Bronkhorst, Montigny-Les-Cormeilles, France), fresh samples were

rehydrated in water for 20 minutes and recut to 35 cm length underwater. To prevent leakage, lateral twigs were removed, and the cuts were immediately sealed with a quick-drying adhesive (Loctite 431 with activator 7452; Henkel, Düsseldorf, Germany). After measuring initial hydraulic conductivity at a low-pressure head of 6 kPa for 5 minutes, samples were repeatedly flushed at high pressure of 120 kPa for 10 minutes to remove potential emboli to measure maximum hydraulic conductivity ( $K_h$ ,  $\text{kg m}^{-1} \text{MPa}^{-1} \text{s}^{-1}$ ) once the conductivity values were stable.  $K_s$  was calculated by dividing  $K_h$  by the basipetal cross-sectional area excluding the bark.

#### 4.2.7 Statistical Analysis

All statistical analyses were performed in software R (v. 4.1.0, R Core Team, 2021). We used linear regression to analyze the correlation between the xylem safety (represented by pressures inducing 12%, 50%, and 88% losses of stem hydraulic conductance) and different tree architectural attributes. To begin, we looked at the relationship between the overall tree structural complexity ( $D_b$ ) and the xylem pressures at  $P_{12}$ ,  $P_{50}$ ,  $P_{88}$ . We also performed species-level linear regression of the box-dimension ( $D_b$ ) in relation to the specific conductivity ( $K_s$ ) and the hydraulically-weighted vessel diameter ( $D_h$ ) of the corresponding tree species. Furthermore, we tested the relationship between all the tree architectural attributes like; CSA (Crown Surface Area), CV (Crown Volume), branch angles, branch lengths, branch numbers, branch volume, DBH, and height with the xylem pressures at  $P_{12}$ ,  $P_{50}$ ,  $P_{88}$  using correlation analysis (Spearman's rank). The significance level was kept at  $p < 0.05$  for all the above tests, and data were averaged per species. This was done to identify whether the relationships between the structural variables and hydraulic risk are detectable despite differences in wood anatomy between species.

### 4.3 Results

Overall, we observed a large range in structural complexity for the investigated trees, given that all individuals were growing under identical conditions. The values ranged from 1.55 to 2.04 units of  $D_b$  (see Figure 4.3 for visualization), with a mean value of 1.85 and a standard deviation of 0.11 units of  $D_b$ . Within single species, box-dimension showed some natural variation, as one would expect, ranging only 0.05 units of  $D_b$  within *Platanus Acerifolia* and up to 0.25 units for *Crataegus persimilis*.

The box-dimension for all trees, pooled by species, showed a significant positive correlation with the three measured of xylem safety, i.e., the water potentials at 12%, 50% and 88% loss of hydraulic conductance ( $P_{12}$ ,  $P_{50}$ ,  $P_{88}$ ) (Figure 4.4). The strongest correlation was found with the  $P_{12}$  value and the lowest with  $P_{88}$ , although all three correlation coefficients were very close ( $r = 0.51$  to  $r = 0.53$ ; Figure 4.4).

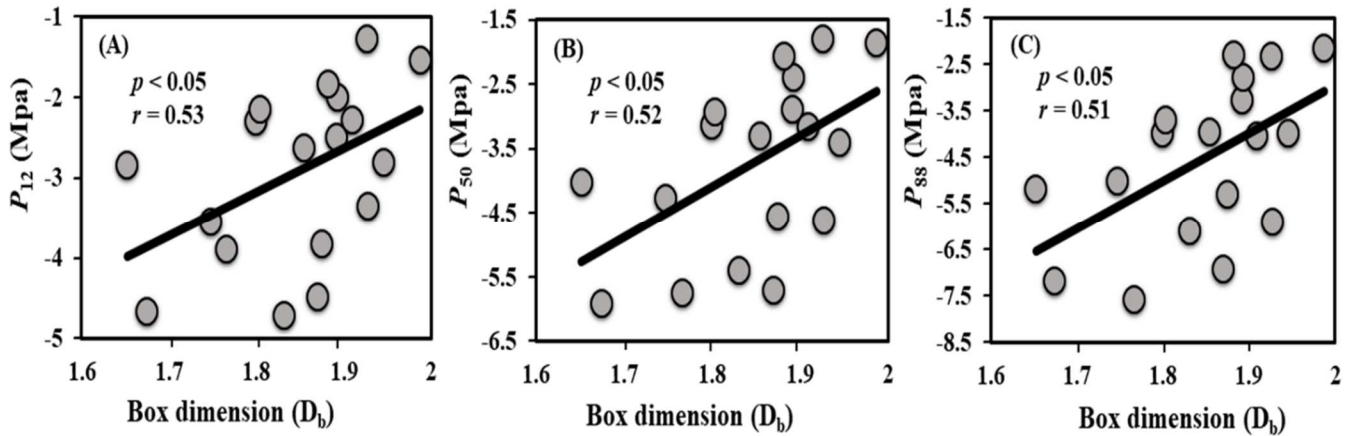


**Figure 4.4** Scatter plots showing the correlation between the mean structural complexity of the tree species represented by the box-dimension ( $D_b$ ) and **(A)**  $P_{12}$  (MPa), **(B)**  $P_{50}$  (MPa), and **(C)**  $P_{88}$  (MPa). The data were available and analyzed for  $n = 18$  tree species (with a mean of 3-4 individuals per species). Regression lines are shown as solid black lines indicating significant relationships for all at  $p < 0.05$ , with Spearman's rank correlation ranging from  $r = 0.51$  to  $0.53$ .

We further observed a close relationship between specific hydraulic conductivity ( $K_s$ ,  $\text{kg m}^{-1} \text{MPa}^{-1} \text{s}^{-1}$ ) of the branches and  $D_b$  (Figure 4.5A), while the hydraulically-weighted vessel diameter was only related to  $D_b$  at marginal significance (Figure 4.5B).

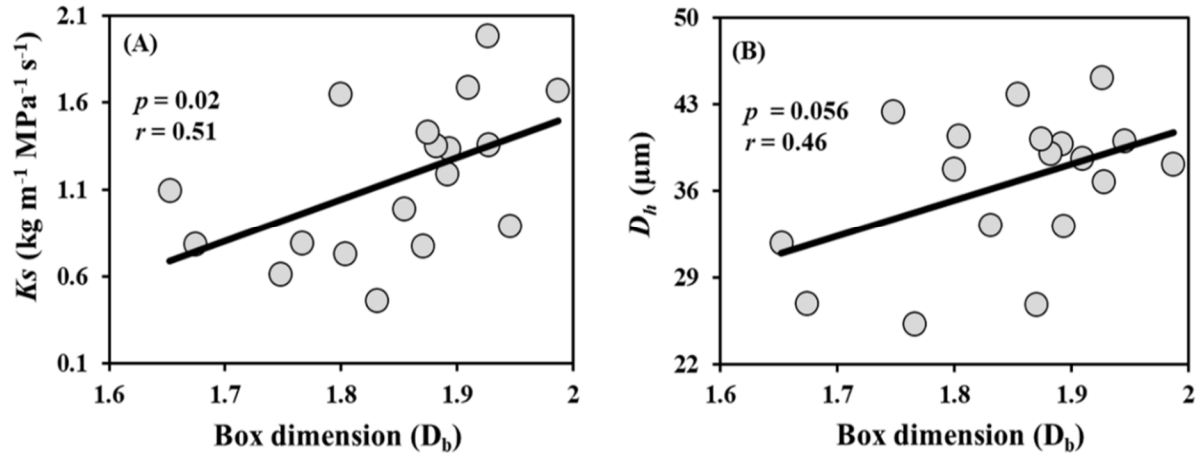


**Figure 4.5** Results of simple species-level linear regressions of box-dimension ( $D_b$ ) in relation to **A**) Specific conductivity ( $K_s$ ,  $\text{kg m}^{-1} \text{MPa}^{-1} \text{s}^{-1}$ ) and **B**) Hydraulically-weighted vessel diameter ( $D_h$ ,  $\mu\text{m}$ ). Shown are the species level averages with the model predictions  $\pm$  95% confidence bands.

Furthermore, the relationships between mean branch angles and xylem safety ( $P_{12}$ ,  $P_{50}$ ,  $P_{88}$ ) showed a positive trend for all branch orders. Despite quite some scatter, the relationship was statistically significant for 2<sup>nd</sup> and 3<sup>rd</sup> order branches but not for the first-order branches (See Figure 4.6).



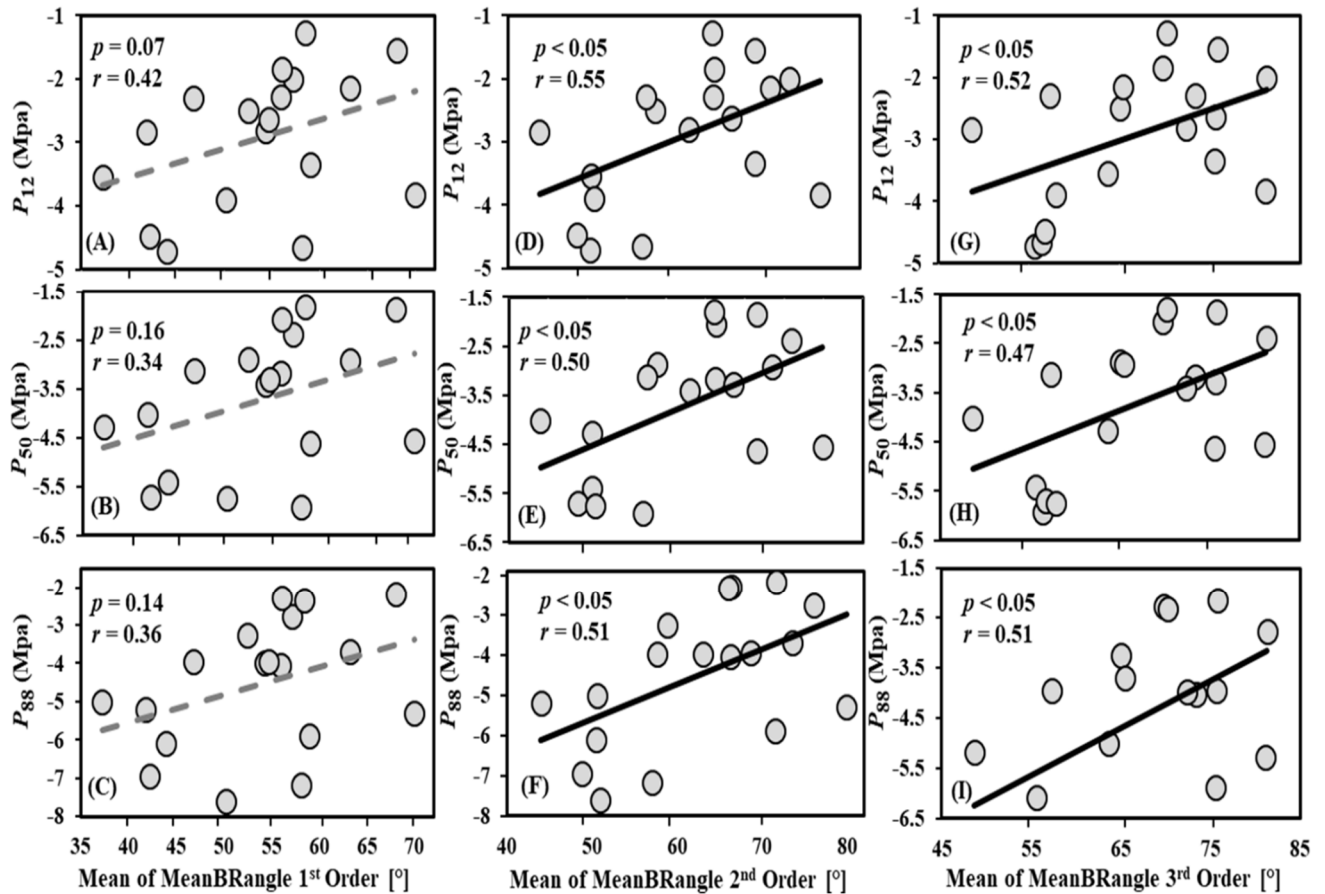


**Figure 4.6** Scatter plot for the three measures of xylem safety ( $P_{12}$ ,  $P_{50}$ ,  $P_{88}$ ; MPa) over mean of mean branch angle (MeanBRangle [ $^{\circ}$ ]) of 1<sup>st</sup> order branches (**A**, **B**, **C**); MeanBRangle [ $^{\circ}$ ] of 2<sup>nd</sup> order branches (**D**, **E**, **F**) and 3<sup>rd</sup> order branches (**G**, **H**, **I**) of all species (shown as mean values). Black solid lines indicate significant relationships and dashed grey lines indicate non-significant relationships (**A**, **B**, **C**). Spearman's rank correlations ranged from  $r = 0.34$  to 0.55;  $n = 18$  Species.

The xylem safety showed no significant relationship with the CSA (crown surface area) nor the CV (crown volume) (Figure 4.7).

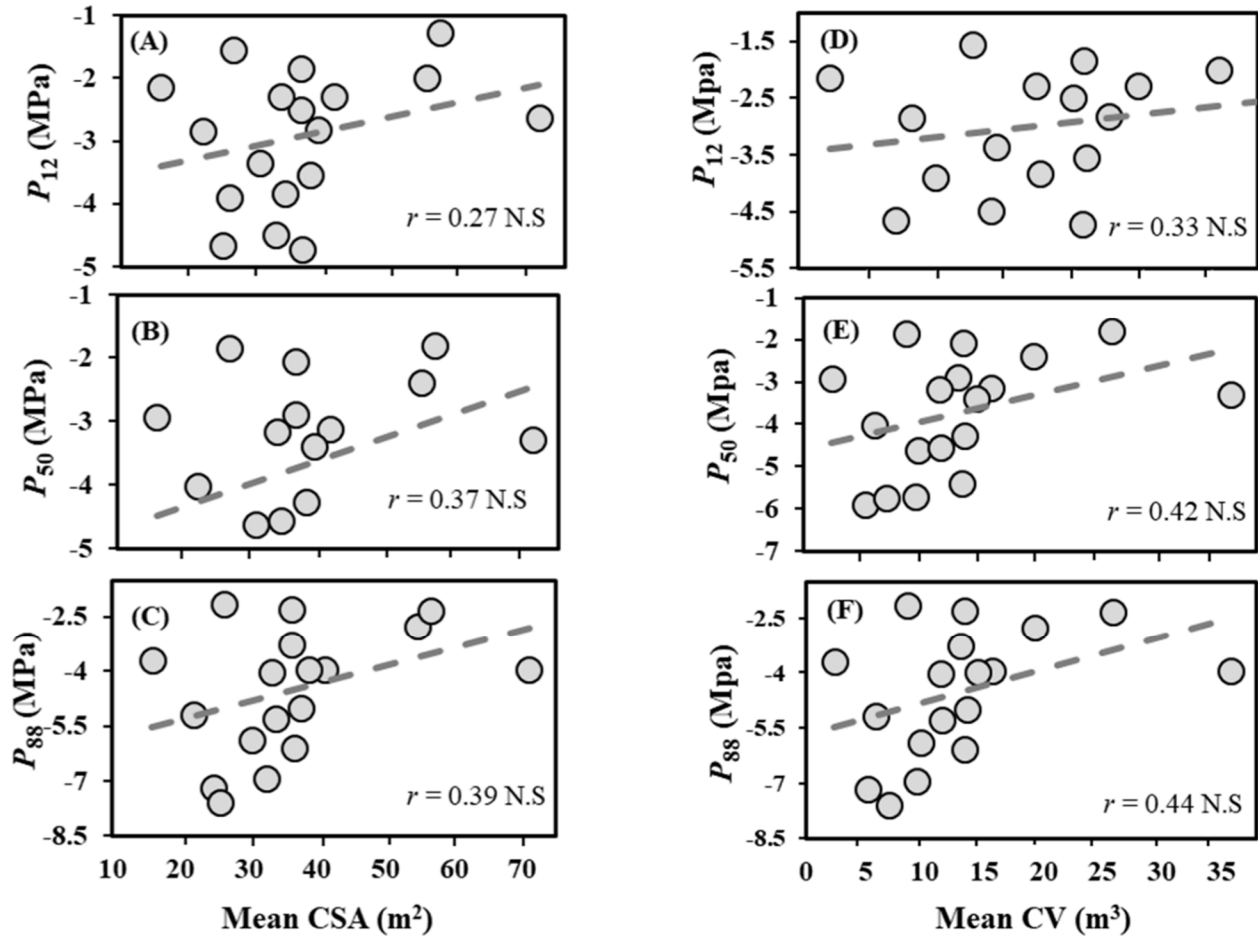


**Figure 4.7** Scatter plots of the three measures of xylem safety (**A**:  $P_{12}$ , **B**:  $P_{50}$ , **C**:  $P_{88}$ ; MPa) against the Crown Surface Area (CSA, [m<sup>2</sup>]) of all the studied trees (mean per species). Similarly, the scatterplots **(D)**, **(E)** and **(F)** show a correlation between different mean xylem pressure,  $P_{12}$ ,  $P_{50}$ , and  $P_{88}$ , with the Crown Volume (CV), respectively. Regression lines are shown as dashed lines indicating non-significant (N.S.). The data were available and analyzed for  $n = 18$  species. Spearman's rank correlations ranged from  $r = 0.27$  to 0.44.

The same pattern was observed for xylem safety ( $P_{12}$ ,  $P_{50}$  and  $P_{88}$ ) over the mean total branch length (Figure 4.8D, E, F) and mean total number of branches (Figure 4.8D, E, F), with positive trends but no significant relationships.

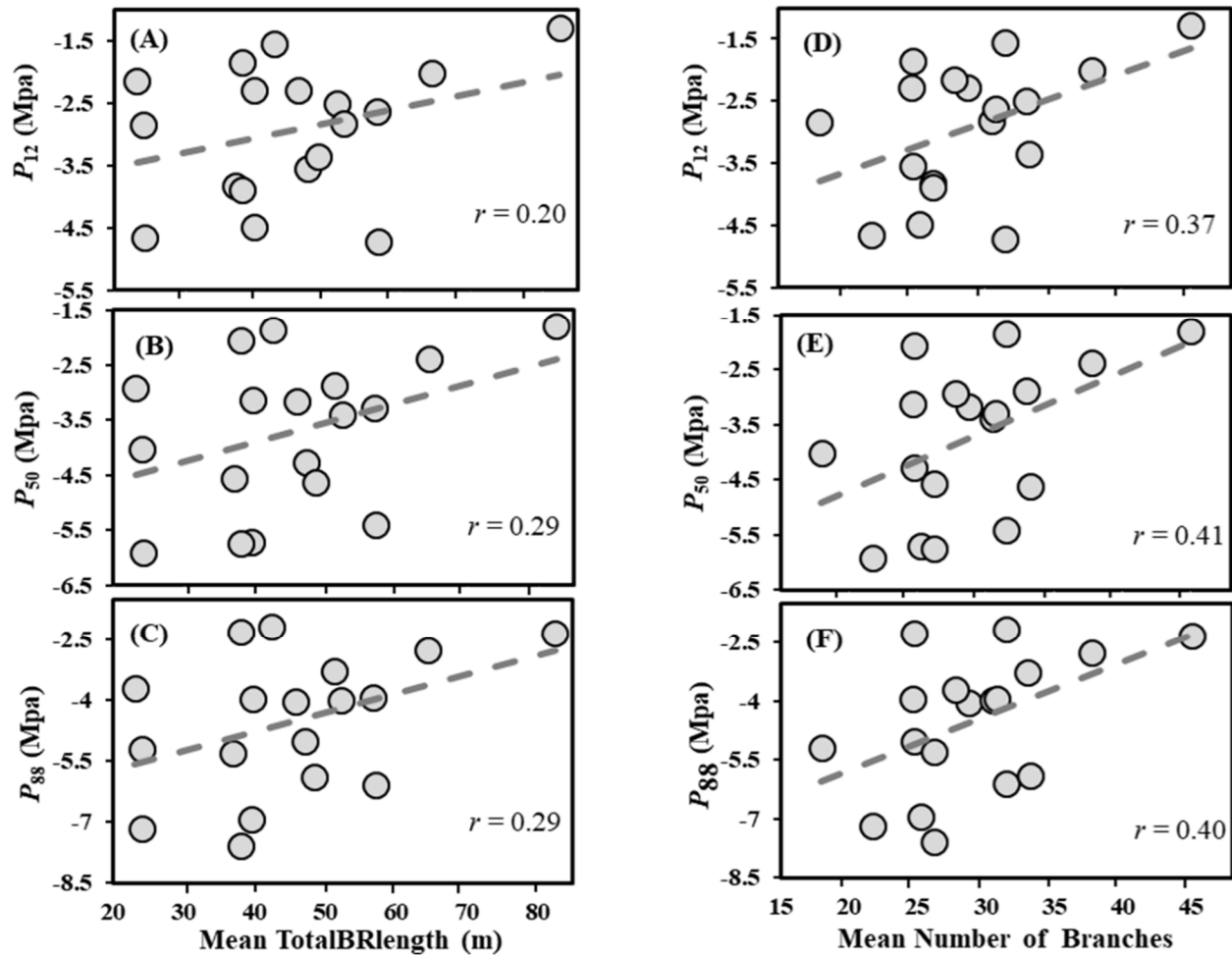


**Figure 4.8** Scatter plots of the three measures of xylem safety (**A**:  $P_{12}$ , **B**:  $P_{50}$ , **C**:  $P_{88}$ ; MPa) against total branch length (TotalBRLength [m]). Similarly, the scatterplots **(D)**, **(E)**, **(F)** show the relationship between xylem safety measures ( $P_{12}$ ,  $P_{50}$ ,  $P_{88}$ ) over the Mean Number of branches of all tree species, respectively. All the above data were available and analyzed for  $n = 18$  species of 71 tree individuals. Regression lines are shown as dashed grey lines to indicate non-significant relationships.

For the conventional measures of a tree structure, i.e., height and diameter at breast height, we also could not detect a relationship with  $P_{12}$ ,  $P_{50}$ , or  $P_{88}$  (Figure 4.9A-F).

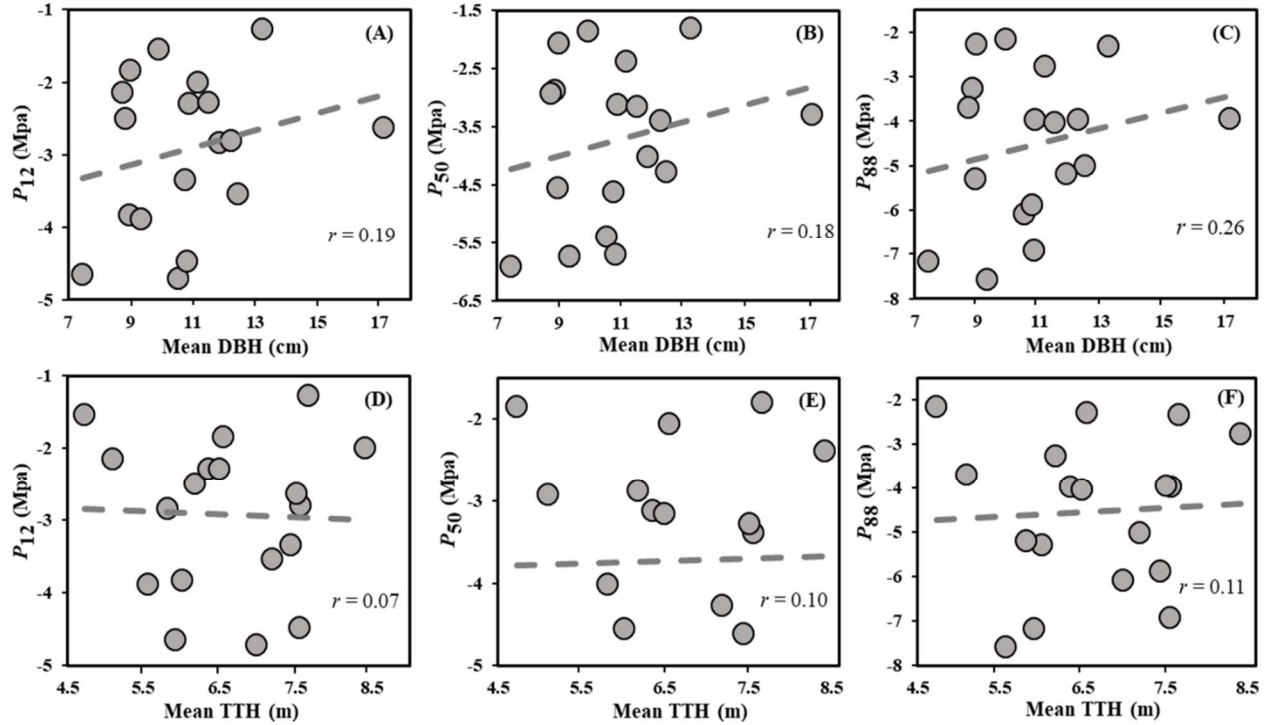


**Figure 4.9** Scatter plot of the three measures of xylem safety (**A**:  $P_{12}$ , **B**:  $P_{50}$ , **C**:  $P_{88}$ ; MPa) in dependence of the diameter at breast height (DBH [cm]) of all the study trees ( $n = 18$  species of 71 individuals). Similarly, the scatterplots **(D)**, **(E)** and **(F)** show correlations between different xylem pressure,  $P_{12}$ ,  $P_{50}$ ,  $P_{88}$ , in dependence of the total tree height (TTH [m]), respectively. The dashed grey lines show non-significant relationships.

#### 4.4 Discussion

Trees comprise a complex branching network, whereas resources need to travel across every part of this network. In the case of water conductance, the xylem network is responsible for the hydraulic conductivity of the system. The breakdown of this water transport system due to acute water deficit has been identified as a primary factor causing drought-induced tree mortality (Arend et al., 2021; Nolan et al., 2021; Hajek et al., 2022).

We set out to further our understanding of the relationship between tree architecture and drought tolerance of trees. To begin with, we hypothesized that trees' overall structural complexity would be directly related to their xylem safety (drought tolerance), and the findings of our study supported our first hypothesis. We found that the box-dimension ( $D_b$ ) as a holistic measure of tree architectural complexity showed a significant correlation with the three measures of xylem safety of the respective tree species, i.e., the water potentials

at 12%, 50% and 88% loss of hydraulic conductivity. In fact, the strongest observed relationship in our entire data was between  $D_b$  and xylem safety (compare  $r$  values of Figure 4.4 to all subsequent figures). It was stronger than that of other laser-based measures related to the sheer tree crown dimension (Figure 4.7). The laser-based measures describing the branching geometry (branching angles) also showed significant relationships with xylem safety, with correlation values up to 0.55 (Figure 4.6), thus partly supporting our second hypothesis. However, no significant relationship was observed for branch length. Finally, the third hypothesis was confirmed as the xylem safety units were more closely related to the laser-based measure of tree structural characteristics than to the conventional measures of tree size (n.s. for height and diameter at breast height (DBH); Figure 4.9).

Our data indicate that the higher the branch angles and more complex the architectural complexity of a tree species (i.e., higher  $D_b$  values), the lower is the xylem safety (ability to resist embolism formation). These findings are in line with several studies that observed a higher drought sensitivity for 'larger' trees (e.g., Bennett et al., 2015; Stovall et al., 2019). It has been argued that their physiological susceptibility in terms of water conductivity is the primary cause (Tyree & Zimmermann, 2002; Fajardo et al., 2021), leaving tall trees more susceptible to drought stress (McDowell & Allen, 2015). While large trees generally encounter more hydraulic challenges since they must move water to a greater height against gravity and greater path length-related resistance (Ryan et al., 2006; Bennett et al., 2015), our trees are likely smaller to observe such general patterns. Accordingly, no significant relationship between tree height or branch length and hydraulic failure risk could be observed.

Our data disentangle the importance of sheer tree size (height and DBH) as an important measure for large forest trees when compared to the structural complexity ( $D_b$ ) of a tree that already relates to hydraulic risk at very low tree heights investigated here (compare Figure 4.4 and Figure 4.9). We argue that two trees with the same height and DBH but different  $D_b$  would respond differently to drought stress. All other things being equal, a tree with higher  $D_b$  would suffer higher drought stress than a tree with lower  $D_b$  due to an increased crown network area and xylem vessel size in the more complex crown bearing a greater photosynthetic area, accordingly, greater hydraulic resistance in the system. However, our trees were all rather young (~12 years) and still rather small (<10 m in height),

which makes height-imposed increase in force and friction rather unlikely. While species-specific functional traits certainly result in different responses to drought stress because of varying vessel systems and branch sizes across the species (Olson et al., 2012; Hajek et al., 2014; Arseniou et al., 2021a), our findings indicate that across various species, the complexity of the hydraulic architecture and the greater photosynthetic area associated with a greater  $D_b$  (e.g., Seidel et al., 2019b), relate directly to an increased risk of hydraulic failure. A higher total leaf area consequently results in a greater demand for water, which is mirrored by the observed close positive relationship between branch hydraulic efficiency and the complexity of the crown. Across the similar-aged temperate trees of our sample, species with a more complex crown had branches with a higher specific hydraulic conductivity ( $K_s$ ) in order to support a greater total leaf area (cf. Seidel et al., 2019b) at the cost of xylem safety. The  $D_b$  integrates all architectural patterns, like the branch angles, branch numbers, branch length, crown surface area, crown volume, DBH, height, and many other tree architectural attributes and translates them into a single physiologically meaningful number (Seidel et al., 2019b). Conventional measures of tree size quantify this insufficiently, further supporting our third hypothesis. Our data indicate that future studies should focus on the complexity of the hydraulic system. The conductive path length and the complexity of the hydraulic system, described not only by the box-dimension (first hypothesis) but also by the branching angles (second hypothesis), were shown to be related to xylem safety. Hence, as indicated earlier, these complex tree architectural attributes, in particular  $D_b$ , in regular times contribute to higher vigor and strength of the trees (e.g., Seidel et al., 2019b). However, in times of severe droughts, they become a liability, as they result in greater water demand to sustain the ecophysiological processes. Overall, tree species with high structural complexity (high  $D_b$  values) developed an efficient but vulnerable xylem compared to species with lower structural complexity (low  $D_b$  values), which developed embolism-resistant xylem at the cost of hydraulic efficiency (Figure 4.4, 4.5). In this sense, future research could investigate whether species occurring in more water-stressed environments are then selected to evolve simpler architectural attributes.

It is important to stress that our data were obtained from trees growing in isolation (without competition for light or space). In closed forests, microclimate and shading might alter the effects observed here. However, some patterns observed here apply equally to forest

trees, for example, the observed relationship between the branch angles and hydraulic vulnerability. We argue that a reduced gravitational resistance exists when branches are more horizontal (flatter and lower angles). This helps explain why branching geometry plays a significant role not only in light interception but also in carbon and water fluxes between trees and the atmosphere (Iwasa et al., 1985; Enquist et al., 2009; Forrester et al., 2018; Dorji et al., 2021).

Finally, tree species (or provenances of the same species) of lower  $D_b$  might be favored for plantation in drought-prone regions (or provenances) rather than species with higher  $D_b$  because the latter might be vulnerable to more stress and disturbance when exposed to drought. This holds true if the architecture of the vessel system and other factors, such as the enzymatic control of water transport, are comparable.

#### **4.5 Conclusion**

Our findings shed new light on the relationship between tree architecture and hydraulic vulnerability. The combined use of TLS and fractal analysis provided a holistic measure of architectural complexity ( $D_b$ ). The  $D_b$  was shown to relate most strongly to the hydraulic vulnerability of our study trees. The branch xylem of tree species with a more complex crown, which most likely supports a higher total leaf area, appeared to be most vulnerable to drought-induced hydraulic failure. More difficult-to-access laser-based measures of detailed branching angles also related significantly to the hydraulic failure risk of the trees. However, these measures were also outperformed by the holistic measure, the  $D_b$ .

From our data, we can conclude that structurally complex trees are more vulnerable to drought-induced hydraulic failure than trees of simpler structures when growing in the open. It is important to note that our study trees were all growing without competition, in full exposure to the sun. In closed forest stands, microclimatic effects, soil moisture, and other stand-level parameters might be decisive and potentially result in a different picture. Our study is one of the first to clearly and empirically highlight the strong relationship between the architectural complexity of the hydraulic system and the hydraulic vulnerability of trees.

**Data and Materials Availability:** The data was made available at GRO (Göttingen Research Online) under the following DOI: <https://doi.org/10.25625/ZVPEJ4>

**Supplementary data:** None

**Conflict of Interest:** None declared

### **Funding**

We are grateful to the German Research Foundation for funding this research through grant SE2383/7-1 provided to Dominik Seidel.

### **Acknowledgments**

We acknowledge Klaus Körber and Andreas Lösch and everyone engaged in the "Klimabäume Stutel" project from the Bavarian State Institute for Viticulture and Horticulture, Veitshochheim, Germany, for allowing us access to the Stutel-Arboretum complex.

(<http://www.lwg.bayern.de/gartenbau/baumschule/101342/index.php/>).

### **Authors' Contribution**

Study conception and design by **YD, DS, BS**; Methodology Implementation by **YD, DS, EI, BS**; Experiment execution by **YD, DS, BS, EI**; Data collection by **YD, DS, EI**; Data analysis/Interpretation by **YD, DS, BS, EI, JS, PA, TT**; Manuscript writing/ revision by **YD, DS, BS, EI, JS, TT, PA**.



## 4.6 References

- Anderegg, W. R., Berry, J. A., Smith, D. D., Sperry, J. S., Anderegg, L. D., & Field, C. B. (2012). The roles of hydraulic and carbon stress in a widespread climate-induced forest die-off. *Proceedings of the National Academy of Sciences*, *109*(1), 233-237.
- Anderegg, W. R., Klein, T., Bartlett, M., Sack, L., Pellegrini, A. F., Choat, B., & Jansen, S. (2016). Meta-analysis reveals that hydraulic traits explain cross-species patterns of drought-induced tree mortality across the globe. *Proceedings of the National Academy of Sciences*, *113*(18), 5024-5029.
- Arend, M., Link, R. M., Patthey, R., Hoch, G., Schuldt, B., & Kahmen, A. (2021). Rapid hydraulic collapse as cause of drought-induced mortality in conifers. *Proceedings of the National Academy of Sciences*, *118*(16), e2025251118.
- Arseniou, G., & MacFarlane, D. W. (2021a). Fractal dimension of tree crowns explains species functional-trait responses to urban environments at different scales. *Ecological Applications*, *31*(4), e02297.
- Arseniou, G., MacFarlane, D. W., & Seidel, D. (2021b). Measuring the Contribution of Leaves to the Structural Complexity of Urban Tree Crowns with Terrestrial Laser Scanning. *Remote Sensing*, *13*(14), 2773.
- Bartlett, M. K., Scoffoni, C., & Sack, L. (2012). The determinants of leaf turgor loss point and prediction of drought tolerance of species and biomes: a global meta-analysis. *Ecology letters*, *15*(5), 393-405.
- Bennett, A. C., McDowell, N. G., Allen, C. D., & Anderson-Teixeira, K. J. (2015). Larger trees suffer most during drought in forests worldwide. *Nature plants*, *1*(10), 1-5.
- Bentley, L. P., Stegen, J. C., Savage, V. M., Smith, D. D., von Allmen, E. I., Sperry, J. S., ... & Enquist, B. J. (2013). An empirical assessment of tree branching networks and implications for plant allometric scaling models. *Ecology letters*, *16*(8), 1069-1078.
- Bittencourt, P. R., Oliveira, R. S., da Costa, A. C., Giles, A. L., Coughlin, I., Costa, P. B., ... & Rowland, L. (2020). Amazonia trees have limited capacity to acclimate plant hydraulic properties in response to long-term drought. *Global Change Biology*, *26*(6), 3569-3584.
- Britton, T. G., Brodribb, T. J., Richards, S. A., Ridley, C., & Hovenden, M. J. (2022). Canopy damage during a natural drought depends on species identity, physiology and stand composition. *New Phytologist*, *233*(5), 2058-2070.
- Borchert, R., & Slade, N. A. (1981). Bifurcation ratios and the adaptive geometry of trees. *Botanical gazette*, *142*(3), 394-401.
- Busov, V. B., Brunner, A. M., & Strauss, S. H. (2008). Genes for control of plant stature and form. *New Phytologist*, *177*(3), 589-607.
- Calders, K., Verbeeck, H., Burt, A., Origo, N., Nightingale, J., Malhi, Y., ... & Disney, M. (2022). Laser scanning reveals potential underestimation of biomass carbon in temperate forest. *Ecological Solutions and Evidence*.
- Chave, J., Andalo, C., Brown, S., Cairns, M. A., Chambers, J. Q., & Eamus, D. (2005). Fo lster H.; Fromard, F.; Higuchi N.; Kira, T.; Lescure, J. P., Nelson B., Ogawa H., Puig H., Riéra B. & Yamakura T, 87-99.
- Chen, S., Tang, D., Tao, S., Liu, P., & Mathews, J. P. (2021). Implications of the in situ stress distribution for coalbed methane zonation and hydraulic fracturing in multiple seams, western Guizhou, China. *Journal of Petroleum Science and Engineering*, *204*, 108755.
- Choat, B. (2013). Predicting thresholds of drought-induced mortality in woody plant species. *Tree physiology*, *33*(7), 669-671.
- Choat, B., Brodribb, T. J., Brodersen, C. R., Duursma, R. A., López, R., & Medlyn, B. E. (2018). Triggers of tree mortality under drought. *Nature*, *558*(7711), 531-539.
- Ciais, P., Reichstein, M., Viovy, N., Granier, A., Ogée, J., Allard, V., ... & Valentini, R. (2005). Europe-wide reduction in primary productivity caused by the heat and drought in 2003. *Nature*, *437*(7058), 529-533.

- Cochard, H. (2002). A technique for measuring xylem hydraulic conductance under high negative pressures. *Plant, Cell & Environment*, 25(6), 815-819.
- Cochard, H., Badel, E., Herbette, S., Delzon, S., Choat, B., & Jansen, S. (2013). Methods for measuring plant vulnerability to cavitation: a critical review. *Journal of Experimental Botany*, 64(15), 4779-4791.
- Cochard, H., Damour, G., Bodet, C., Tharwat, I., Poirier, M., & Améglio, T. (2005). Evaluation of a new centrifuge technique for rapid generation of xylem vulnerability curves. *Physiologia Plantarum*, 124(4), 410-418.
- Dassot, M., Constant, T., & Fournier, M. (2011). The use of terrestrial LiDAR technology in forest science: application fields, benefits and challenges. *Annals of forest science*, 68(5), 959-974.
- Dorji, Y., Annighöfer, P., Ammer, C., & Seidel, D. (2019). Response of beech (*Fagus sylvatica* L.) trees to competition—New insights from using fractal analysis. *Remote Sensing*, 11(22), 2656.
- Dorji, Y., Schuldt, B., Neudam, L., Dorji, R., Middleby, K., Isasa, E., ... & Seidel, D. (2021). Three-dimensional quantification of tree architecture from mobile laser scanning and geometry analysis. *Trees*, 35(4), 1385-1398.
- Enquist, B. J., West, G. B., & Brown, J. H. (2009). Extensions and evaluations of a general quantitative theory of forest structure and dynamics. *Proceedings of the National Academy of Sciences*, 106(17), 7046-7051.
- West, G. B., Enquist, B. J., & Brown, J. H. (2009). A general quantitative theory of forest structure and dynamics. *Proceedings of the National Academy of Sciences*, 106(17), 7040-7045.
- Fajardo, A., & Piper, F. I. (2021). How to cope with drought and not die trying: drought acclimation across tree species with contrasting niche breadth. *Functional Ecology*, 35(9), 1903-1913.
- Bittencourt, P. R., Oliveira, R. S., da Costa, A. C., Giles, A. L., Coughlin, I., Costa, P. B., ... & Rowland, L. (2020). Amazonia trees have limited capacity to acclimate plant hydraulic properties in response to long-term drought. *Global Change Biology*, 26(6), 3569-3584.
- Forrester, D. I., Ammer, C., Annighöfer, P. J., Barbeito, I., Bielak, K., Bravo-Oviedo, A., ... & Pretzsch, H. (2018). Effects of crown architecture and stand structure on light absorption in mixed and monospecific *Fagus sylvatica* and *Pinus sylvestris* forests along a productivity and climate gradient through Europe. *Journal of Ecology*, 106(2), 746-760.
- Gonzalez de Tanago, J., Lau, A., Bartholomeus, H., Herold, M., Avitabile, V., Raunonen, P., ... & Calders, K. (2018). Estimation of above-ground biomass of large tropical trees with terrestrial LiDAR. *Methods in Ecology and Evolution*, 9(2), 223-234.
- Hajek, P., Leuschner, C., Hertel, D., Delzon, S., & Schuldt, B. (2014). Trade-offs between xylem hydraulic properties, wood anatomy and yield in *Populus*. *Tree physiology*, 34(7), 744-756.
- Hajek, P., Link, R. M., Nock, C. A., Bauhus, J., Gebauer, T., Gessler, A., ... & Schuldt, B. (2022). Mutually inclusive mechanisms of drought-induced tree mortality. *Global Change Biology*, 28(10), 3365-3378.
- Halley, J. M., Hartley, S., Kallimanis, A. S., Kunin, W. E., Lennon, J. J., & Sgardelis, S. P. (2004). Uses and abuses of fractal methodology in ecology. *Ecology letters*, 7(3), 254-271.
- Hammond, W. M., Williams, A. P., Abatzoglou, J. T., Adams, H. D., Klein, T., López, R., ... & Allen, C. D. (2022). Global field observations of tree die-off reveal hotter-drought fingerprint for Earth's forests. *Nature communications*, 13(1), 1-11.
- Hastings, H. M., & Sugihara, G. (1993). Fractals. A user's guide for the natural sciences. *Oxford Science Publications*.
- Hollender, C. A., & Dardick, C. (2015). Molecular basis of angiosperm tree architecture. *New Phytologist*, 206(2), 541-556.
- Ishii, H. T., Tanabe, S. I., & Hiura, T. (2004). Exploring the relationships among canopy structure, stand productivity, and biodiversity of temperate forest ecosystems. *Forest Science*, 50(3), 342-355.

- Iwasa, Y. O. H., Cohen, D. A. N., & Leon, J. A. (1985). Tree height and crown shape, as results of competitive games. *Journal of theoretical Biology*, 112(2), 279-297.
- Klein, T., Torres-Ruiz, J. M., & Albers, J. J. (2022). Conifer desiccation in the 2021 NW heatwave confirms the role of hydraulic damage. *Tree physiology*, 42(4), 722-726.
- Kuuluvainen, T. (1992). Tree architectures adapted to efficient light utilization: is there a basis for latitudinal gradients? *Oikos*, 275-284.
- Liang, X., Hyypä, J., Kaartinen, H., Lehtomäki, M., Pyörälä, J., Pfeifer, N., ... & Wang, Y. (2018). International benchmarking of terrestrial laser scanning approaches for forest inventories. *ISPRS journal of photogrammetry and remote sensing*, 144, 137-179.
- Lewis, S. L., Brando, P. M., Phillips, O. L., Van Der Heijden, G. M., & Nepstad, D. (2011). The 2010 amazon drought. *Science*, 331(6017), 554-554.
- MacArthur, R. H., & MacArthur, J. W. (1961). On bird species diversity. *Ecology*, 42(3), 594-598.
- Malhi, Y., Jackson, T., Patrick Bentley, L., Lau, A., Shenkin, A., Herold, M., ... & Disney, M. I. (2018). New perspectives on the ecology of tree structure and tree communities through terrestrial laser scanning. *Interface Focus*, 8(2), 20170052.
- Mandelbrot, B. B. (1983). The fractal geometry of Nature WH Freeman and Company. *New York*, 8, 406-406.
- Martin-Ducup, O., Ploton, P., Barbier, N., Momo Takoudjou, S., Mofack, G., Kamdem, N. G., ... & Pélissier, R. (2020). Terrestrial laser scanning reveals convergence of tree architecture with increasingly dominant crown canopy position. *Functional Ecology*, 34(12), 2442-2452.
- McDowell, N. G., & Allen, C. D. (2015). Darcy's law predicts widespread forest mortality under climate warming. *Nature Climate Change*, 5(7), 669-672.
- McDowell, N. G., Sapes, G., Pivovarov, A., Adams, H. D., Allen, C. D., Anderegg, W. R., ... & Xu, C. (2022). Mechanisms of woody-plant mortality under rising drought, CO<sub>2</sub> and vapour pressure deficit. *Nature Reviews Earth & Environment*, 3(5), 294-308.
- Moore, J. R., & Maguire, D. A. (2008). Simulating the dynamic behavior of Douglas-fir trees under applied loads by the finite element method. *Tree physiology*, 28(1), 75-83.
- Nardini, A., Battistuzzo, M., & Savi, T. (2013). Shoot desiccation and hydraulic failure in temperate woody angiosperms during an extreme summer drought. *New Phytologist*, 200(2), 322-329.
- Neill, A. R., & Puettmann, K. J. (2013). Managing for adaptive capacity: thinning improves food availability for wildlife and insect pollinators under climate change conditions. *Canadian Journal of Forest Research*, 43(5), 428-440.
- Nepstad, D. C., Tohver, I. M., Ray, D., Moutinho, P., & Cardinot, G. (2007). Mortality of large trees and lianas following experimental drought in an Amazon forest. *Ecology*, 88(9), 2259-2269.
- Niinemets, Ü., & Kull, O. (1995). Effects of light availability and tree size on the architecture of assimilative surface in the canopy of *Picea abies*: variation in needle morphology. *Tree physiology*, 15(5), 307-315.
- Nolan, R. H., Gauthey, A., Losso, A., Medlyn, B. E., Smith, R., Chhajed, S. S., ... & Choat, B. (2021). Hydraulic failure and tree size linked with canopy die-back in eucalypt forest during extreme drought. *New Phytologist*, 230(4), 1354-1365.
- Ogle, K., Barber, J. J., Willson, C., & Thompson, B. (2009). Hierarchical statistical modeling of xylem vulnerability to cavitation. *New Phytologist*, 182(2), 541-554.
- Olson, M. E., & Rosell, J. A. (2013). Vessel diameter–stem diameter scaling across woody angiosperms and the ecological causes of xylem vessel diameter variation. *New phytologist*, 197(4), 1204-1213.

- Paligi, S. S., Link, R. M., Isasa, E., Bittencourt, P., Cabral, J. S., Jansen, S., ... & Schuldt, B. (2021). Accuracy of the pneumatic method for estimating xylem vulnerability to embolism in temperate diffuse-porous tree species. *bioRxiv*.
- Pammenter, N. V., & Van der Willigen, C. (1998). A mathematical and statistical analysis of the curves illustrating vulnerability of xylem to cavitation. *Tree physiology*, *18*(8-9), 589-593.
- Phillips, O. L., Van Der Heijden, G., Lewis, S. L., López-González, G., Aragão, L. E., Lloyd, J., ... & Vilanova, E. (2010). Drought–mortality relationships for tropical forests. *New Phytologist*, *187*(3), 631-646.
- Reichstein, M., Bahn, M., Ciais, P., Frank, D., Mahecha, M. D., Seneviratne, S. I., ... & Wattenbach, M. (2013). Climate extremes and the carbon cycle. *Nature*, *500*(7462), 287-295.
- Ribe, R. G. (2009). In-stand scenic beauty of variable retention harvests and mature forests in the US Pacific Northwest: The effects of basal area, density, retention pattern and down wood. *Journal of Environmental Management*, *91*(1), 245-260.
- Rousi, E., Kornhuber, K., Beobide-Arsuaga, G., Luo, F., & Coumou, D. (2022). Accelerated western European heatwave trends linked to more-persistent double jets over Eurasia. *Nature Communications*, *13*(1), 1-11.
- Rowland, L., da Costa, A. C., Galbraith, D. R., Oliveira, R. S., Binks, O. J., Oliveira, A. A., ... & Meir, P. (2015). Death from drought in tropical forests is triggered by hydraulics not carbon starvation. *Nature*, *528*(7580), 119-122.
- Ryan, M. G., Phillips, N., & Bond, B. J. (2006). The hydraulic limitation hypothesis revisited. *Plant, Cell & Environment*, *29*(3), 367-381.
- Saarinen, N., Calders, K., Kankare, V., Yrttimaa, T., Junttila, S., Luoma, V., ... & Verbeeck, H. (2021). Understanding 3D structural complexity of individual Scots pine trees with different management history. *Ecology and evolution*, *11*(6), 2561-2572.
- Sarkar, N., & Chaudhuri, B. B. (1994). An efficient differential box-counting approach to compute fractal dimension of image. *IEEE Transactions on systems, man, and cybernetics*, *24*(1), 115-120.
- Schneider, C. A., Rasband, W. S., & Eliceiri, K. W. (2012). NIH Image to ImageJ: 25 years of image analysis. *Nature methods*, *9*(7), 671-675.
- Schuldt, B., Buras, A., Arend, M., Vitasse, Y., Beierkuhnlein, C., Damm, A., ... & Kahmen, A. (2020). A first assessment of the impact of the extreme 2018 summer drought on Central European forests. *Basic and Applied Ecology*, *45*, 86-103.
- Scorza, R., Bassi, D., & Liverani, A. (2002). Genetic interactions of pillar (columnar), compact, and dwarf peach tree genotypes. *Journal of the American Society for Horticultural Science*, *127*(2), 254-261.
- Seidel, D. (2018). A holistic approach to determine tree structural complexity based on laser scanning data and fractal analysis. *Ecology and evolution*, *8*(1), 128-134.
- Seidel, D., Ehbrecht, M., Dorji, Y., Jambay, J., Ammer, C., & Annighöfer, P. (2019). Identifying architectural characteristics that determine tree structural complexity. *Trees*, *33*(3), 911-919.
- Seidel, D., Annighöfer, P., Stiers, M., Zemp, C. D., Burkardt, K., Ehbrecht, M., ... & Ammer, C. (2019). How a measure of tree structural complexity relates to architectural benefit-to-cost ratio, light availability, and growth of trees. *Ecology and evolution*, *9*(12), 7134-7142.
- Settle, J., Scholes, R., Betts, R. A., Bunn, S., Leadley, P., Nepstad, D., ... & Winter, M. (2015). Terrestrial and inland water systems. In *Climate change 2014 impacts, adaptation and vulnerability: Part A: Global and sectoral aspects* (pp. 271-360). Cambridge University Press.
- Skelton, R. P., West, A. G., & Dawson, T. E. (2015). Predicting plant vulnerability to drought in biodiverse regions using functional traits. *Proceedings of the National Academy of Sciences*, *112*(18), 5744-5749.
- Sperry, J. S., Nichols, K. L., Sullivan, J. E., & Eastlack, S. E. (1994). Xylem embolism in ring-porous, diffuse-porous, and coniferous trees of northern Utah and interior Alaska. *Ecology*, *75*(6), 1736-1752.

- Stovall, A. E., Shugart, H., & Yang, X. (2019). Tree height explains mortality risk during an intense drought. *Nature Communications*, *10*(1), 1-6.
- Torres-Ruiz, J. M., Jansen, S., Choat, B., McElrone, A. J., Cochard, H., Brodribb, T. J., ... & Delzon, S. (2015). Direct X-ray microtomography observation confirms the induction of embolism upon xylem cutting under tension. *Plant Physiology*, *167*(1), 40-43.
- Trenberth, K. E., Dai, A., Van Der Schrier, G., Jones, P. D., Barichivich, J., Briffa, K. R., & Sheffield, J. (2014). Global warming and changes in drought. *Nature Climate Change*, *4*(1), 17-22.
- Trugman, A. T., Anderegg, L. D., Shaw, J. D., & Anderegg, W. R. (2020). Trait velocities reveal that mortality has driven widespread coordinated shifts in forest hydraulic trait composition. *Proceedings of the National Academy of Sciences*, *117*(15), 8532-8538.
- Tyree, M. T., & Zimmermann, M. H. (2013). *Xylem structure and the ascent of sap*. Springer Science & Business Media.
- Valentine, H. T. (1985). Tree-growth models: derivations employing the pipe-model theory. *Journal of theoretical biology*, *117*(4), 579-585.
- West, G. B., Brown, J. H., & Enquist, B. J. (2001). A general model for ontogenetic growth. *Nature*, *413*(6856), 628-631.
- West, G. B., Enquist, B. J., & Brown, J. H. (2009). A general quantitative theory of forest structure and dynamics. *Proceedings of the National Academy of Sciences*, *106*(17), 7040-7045.
- Watt, M. S., Moore, J. R., & McKinlay, B. (2005). The influence of wind on branch characteristics of *Pinus radiata*. *Trees*, *19*(1), 58-65.
- White, F. M. (1991). Viscous fluid flow, mcgraw hill book company. *New York*, *19*(1), 400.
- Zande, D. V. D., Jonckheere, I., Stuckens, J., Verstraeten, W. W., & Coppin, P. (2008). Sampling design of ground-based lidar measurements of forest canopy structure and its effect on shadowing. *Canadian Journal of Remote Sensing*, *34*(6), 526-538.

# CHAPTER 5

---

## Synthesis

In the preceding chapters, the relationship between the tree architecture and competition aspects (Chapter 2), solar light angle, seed dispersal strategy, growth performance (Chapter 3), and drought stress tolerance (Chapter 4) was explored. Our data confirmed that the parameters mentioned above were indeed drivers (competition, solar light angle) and passengers (seed dispersal strategy, growth performance, drought stress tolerance) of tree architecture. Now, the following chapter will synthesize the findings and conclusions drawn from the three studies. Finally, based on the findings and results of chapters 2 to 4, limitations and suggestions to improve and consider will be discussed. The future scope and possibilities concerning this field will also be emphasized in conclusion, especially with regard to novel tools and methodologies (LiDAR system and fractal analysis).

### **5.1 The role of competition on the tree architecture complexity**

We explored if the branching pattern of beech trees responded to competition intensity, as indicated by earlier studies (Bayer et al., 2013; Juchheim et al., 2017). We extended this line of investigation by testing whether the overall structural complexity of a tree responds to competition as well. We hypothesized that the degree of competition influences the branching patterns and structural complexity of beech trees. Our findings provide substantial evidence in favour of this notion, showing that the target trees' branch lengths, branch angles, box-dimensions (structural complexity), and  $D_b$ -Intercept all significantly changed in response to the competition imposed on them by surrounding trees. However, other tree species may not be as affected by competition as beech, which can adapt and exhibit a range of physical characteristics in response to its environment. This has been observed and documented in earlier studies (Schröter et al., 2012; Valladares et al., 2017). For example, the paper by Bayer et al. (2013) presented the initial findings on modifications in the branch angles of beech depending on the neighbouring tree species. Juchheim et al. (2017)

used QSM model methods, which are also used in our current study. They found that the structure of the crown of European beech trees can vary significantly based on the competition they experience (either within their own or with other species). Our research findings contribute to understanding how beech tree architecture is generally impacted by the level of competition, regardless of the type of competition. Most notably, our research showed that competition has a negative effect on the overall tree architectural complexity. Relying solely on crown form and geometry to assess the impact of competition on trees may not provide a complete picture, as changes in the branching structure of a tree can alter the amount of light that passes through the crown and, ultimately, the canopy of a forest (as demonstrated by Oliver et al., 1996). These changes in light transmissivity are not taken into account when only considering the size of the crown. The use of fractal analysis in this study provides a more comprehensive evaluation of the tree's overall architecture (including both branches and stem) and how it may be affected by competition. This approach should capture any changes in the tree's structure caused by competition. In fact, we discovered that the box-dimension and  $D_b$ -intercept negatively correlated with the competition intensity (see Table 2.2 and Figure 2.5C, D in Chapter 2), confirming that competitive pressure lowers the structural complexity of beech trees.

We contend that the  $D_b$ -intercept functions as an indicator for the dimension of a tree's complexity-bearing portion, specifically the tree crown (comp. Figure 2.6, Chapter 2). This was reinforced by the positive association between the  $D_b$ -intercept and crown morphological attributes like crown radius and crown volume (as shown in Figure 2.6C, D of Chapter 2). However, the  $D_b$ -intercept was inversely linked with two traditional measures of tree size: diameter at breast height and total tree height. Although there was a significant correlation, the smoothing feature of the GAM model for the regression between DBH and  $D_b$ -intercept was not significant (as shown in Figure 2.6A, Chapter 2). This suggests that DBH alone is not necessarily a good metric of a tree's structural complexity, and trees with the same DBH can have remarkably varying levels of complexity.

In the current dataset employed here, we could not establish that the self-similarity measure is affected by competition. This may be due to the small sample size used in the study. While the rho-value of 0.31 (seen in Table 2.2, Chapter 2) suggests some association level,

it is not strong enough to make definitive conclusions. Future studies should further examine the relationship between self-similarity and competition.

TLS (terrestrial laser scanning) technology allows for detailed measurements of tree architecture, offering novel insights into how competition impacts tree anatomy and branching networks (as noted by Henning et al., 2006). This knowledge is vital for understanding the interactions between tree structure and productivity (Bayer et al., 2013; Seidel et al., 2019b), as well as structure-biodiversity linkages (Bazzaz et al., 1975; Tews et al., 2004). All of these relationships are influenced by the architecture of individual trees.

## **5.2 The relation between the tree architecture and solar light angle, seed dispersal strategy, and tree growth performance.**

### ***5.2.1 Tree architecture and solar light angle***

We hypothesized that tree species originating from different latitudes growing in the Stutel-Arboretum would exhibit crown designs that reflect adaptations to the solar elevation angles at the latitude of their species' native habitat. Based on 3D point cloud data acquired using MLS, our findings validate this hypothesis (Figure 3.5, Chapter 3). Even though the trees in this study were growing in the same geographic and climatic conditions, trees from species of different origins were inclined to have a relatively top-heavy crown when the latitude of their species origin was closer to the equator (lower latitude). Although the relationship between the origin latitude of the trees and their top-heavy geometry was not strong (as indicated by the  $R^2$  value of 0.052), it was still statistically significant, indicating the existence of genetic predisposition. Trees from higher latitudes developed deeper crowns with a lower Rel.Hmaxarea (Relative height of the maximum horizontal crown area) in order to effectively intercept light, compared to trees from lower latitudes that were exposed to greater solar light leading to higher Rel.Hmaxarea. We contend that, in the tropics at lower latitudes, the sun is always directly overhead, allowing tree to grow with wider horizontal crowns that maximizes light interception, and at the higher latitudes, the sun is at lower angle, meaning that a vertical crown shape is more efficient at collecting and absorbing light to optimize their photosynthetic process (Horn, 1971; Valadares et al 2007)



The empirical evidence from our findings (Chapter 3) corroborates earlier research theories that showed that there should be a quantifiable impact of the solar incidence angle on the morphology of trees (Whitmore, 1975; Hiura, 1998; Bomfleur et al., 2013). However, we only observed a weak influence of crown shape adaptation to the latitude of origin at our experimental location, which had identical growth environments for all study trees. It is worth noting that since precise information about a species' natural range is generally unavailable, the mid-point latitude of a species' origin can only be estimated. This may help to partially account for latitude's relatively weaker explanatory power for the Relative height of the maximum horizontal crown area (Figure 3.5, Chapter 3).

Additionally, we contend that the association is weak since tree architecture is influenced by various factors besides the angle of the sun's rays. The trees must balance numerous biological and physical elements following the optimum resource utilization strategy to achieve an optimal tree architectural design (Archibald & Bond, 2003; Minamino & Tateno, 2014). As a result, in recent years, the trees at the research location likewise adapted plastically to the local conditions, significantly diminishing the visible "legacy" in geometry. The literature suggests that there should be a link between the angle at which the sun's rays strike the earth at a particular latitude and the shape of the trees that grow there (Kuuluvainen, 1992).

By linking a tree's form to the latitude of the tree species native range, we were able to measure the genetic legacy effect of solar geometry. We hypothesize that the potential of a tree to modify its form to existing biotic and abiotic conditions may greatly surpass a tree's genetic propensity to develop a particular shape, which would explain the relationship's small impact size seen in Figure 3.5 of Chapter 3. To comprehensively understand the extent to which the solar light angle influences tree shape, it is necessary to explicitly link the latitude of a tree's origin (or the solar zenith angle at that latitude) with the trees' morphology. An in-depth and substantial point cloud of several trees from a diverse range of latitudes would be necessary to do this. The ability to establish a more direct link between solar geometry and tree shape, extending beyond the restriction of being able to investigate genetic legacy effects, would be made possible by combining a considerable number of georeferenced tree point clouds. Future research should emphasize global partnerships and data exchanges, in particular.

### ***5.2.2 Tree architecture and Seed dispersal strategy***

We were able to study the association between tree structural complexity ( $D_b$ ) and seed dispersal mechanism because several important parameters, such as temperature, water and nutrient availability, and competition, were identical and constant across all of our research trees.  $D_b$  is a metric for tree structure complexity that incorporates several topological dimensions of a tree, such as height, diameter, crown surface area, canopy width, branching patterns, and many others (Seidel et al., 2019a). Therefore, we proposed that  $D_b$  should be correlated with a species' seed dispersion strategies, considering reproduction and seed dispersal are important functions of tree form and structure (Malhi et al., 2018). In fact, we revealed that the tree structural complexity varied significantly between tree species that dispersed their seeds through wind and those that dispersed through animals. Therefore, our findings corroborate our second hypothesis (Figure 3.6). According to Malhi et al. (2018), there are variations between the tree structure and form of South Asian forests, where species mostly rely on wind dispersion, and the trees in central Africa and the Amazonia, where species primarily rely on animal dispersion strategy. Accordingly, our findings show that anemochorus tree species have higher  $D_b$  than the zoochorus tree species. We believe that simpler tree structures provide better animal access and aesthetic appeal. In contrast, trees with more complex crowns with numerous branches and larger total surface area, as shown by the higher  $D_b$ , could act as stronger wind barriers and thereby enhancing the wind velocity whenever wind rushes through the crowns. However, our sample trees were all young; therefore, further research is needed before drawing any firm conclusions.

### ***5.2.3 Tree architecture complexity and tree growth performance***

The findings corroborated our third hypothesis, which proposed that a greater  $D_b$  is correlated with a higher radial increment (Figure 3.7, Chapter 3). Previous research has also found these associations to be true for certain tree species in temperate and tropical regions (Seidel, 2018). While earlier research found linear correlations, the significant correlation in the present study appears to be non-linear, as indicated by the GAM model, showing more than 35% of explained variation. Until now, the argument for the association between  $D_b$  and the radial increment has been that a higher  $D_b$  is usually the outcome of less

competition, which leads to unconstrained development and hence an improved growth rate (e.g., Dorji et al., 2019). It was also established that a higher  $D_b$  was directly related to a better balance of the photosynthetic surface area to the volume of the woody tree, or rather, an efficient ratio between "productive" and "consuming" parts (Seidel et al., 2019b). We hypothesize that higher levels of tree structural complexity may lead to more significant improvements in productivity, which could be attributed to the fractal dimension of the tree. This means that as the tree's branches become more complex, with higher levels of branching networks, the tree will see a higher advantage in productivity. In simpler trees with less complexity, a larger 'investment' may be required in terms of wooden structure to generate additional surface area for capturing light since the branches must first extend to the outer portion of the crown where they can be exposed to sunlight. However, in more complex trees with numerous higher-order branches, these extra branches are already present (requiring less investment) to create additional light-capturing tissue surfaces in the canopy (Dorji et al., 2021). However, this is still a hypothesis until more research tackles the topic.

Nonetheless, we could establish that there appears to be a fundamental positive association between the  $D_b$  and productivity. A higher  $D_b$  is associated with a more beneficial tree structure, especially for temperate regions (Seidel et al., 2019a). Still, suppose a tree is genetically predisposed to grow with a dome-shaped crown well-suited for subtropical regions. In that case, it can only adapt to a limited extent to the environment in our Stutelarboretum. This means they will continue to carry the genetic imprint of their original home, despite being in a different environment. In addition to other factors such as adaptation to the soil, climate, and genetics, the lower growth rates of certain tree species can be attributed to their less optimized crown form compared to well-adapted tree species with an optimized crown. In the tropical regions, a high  $D_b$  would only be advantageous to trees that grow in underwood vegetation (receiving indirect solar radiation), as was the case with the trees studied in Seidel et al. (2019a), or trees that are mostly exposed to cloudy environments with considerable amounts of indirect light. High sunlight angle in the likes of tropical regions would otherwise lead to intensive self-shading, resulting in a contentious advantage from a broad, multi-layered, and complex tree crown as indicated by a high  $D_b$ .

In all of the abovementioned outcomes, the use of 3D data, in conjunction with topological geometry and fractal analysis, contributed significantly to converting the structural complexity of the tree into numerical values that enabled linking it to functional attributes. Due to the lack of 3D data in the past, it was extremely difficult to mathematically characterize the tree architecture (Borchert & Slade, 1981), which significantly hindered our progress in understanding the factors that influence the tree architectural complexity. According to recent studies, LiDAR offers a novel and unique approach to examining how tree form and functions relate to one another (Malhi et al., 2018; Calders et al., 2019). Therefore, it could be the most effective approach for developing functional-structural plant models that are necessary to understand better the performance of different forest stands (Bongers, 2020).

### **5.3 The linkage between tree architecture and hydraulic vulnerability**

We conducted this research to learn more about the linkages between tree structure and the ability of trees to withstand drought. We hypothesize that tree architectural complexity will be directly correlated with the xylem pressure of the trees, with more complex structures susceptible to drought stress, and our results supported this statement. We found that the box-dimension ( $D_b$ ), which reflects the overall complexity of a tree's structure, had a significant correlation with the tree's ability to maintain water potential during drought conditions, as measured by three different xylem safety, namely the water potentials at 12%, 50%, and 88% loss of hydraulic conductivity ( $P_{12}$ ,  $P_{50}$ ,  $P_{88}$ ). The strongest relationship across our entire data was between the box-dimension and drought tolerance (compare  $r$  values of Figure 4.4 to all other figures). It was stronger than other laser-based measures related to the sheer tree crown dimension (Figure 4.7, Chapter 4). The laser-based measures describing the branching geometry (branching angles) also showed significant relationships with xylem safety, with correlation values up to 0.55 (Figure 4.6, Chapter 4), thus partly supporting our second hypothesis. However, no significant relationship was observed for branch length. Finally, the third hypothesis was confirmed as the xylem safety units were more closely related to the laser-based measure of tree structural characteristics than to the conventional measures of tree size (n.s. for height and diameter at breast height (DBH); Figure 4.9, Chapter 4).

Our data indicate that the higher the branch angles and more complex the architectural complexity of a tree species (i.e., higher  $D_b$  values), the lower the xylem safety (ability to resist embolism formation). These findings align with several studies that observed a higher drought sensitivity for 'larger' trees (e.g., Benett et al., 2015; Stovall et al., 2019). It has been argued that their physiological susceptibility in terms of water conductivity is the primary cause (Tyree & Zimmermann, 2002; Fajardo et al., 2021), leaving tall trees more susceptible to drought stress (McDowell & Allen, 2015). While large trees generally encounter more hydraulic challenges since they must move water to a greater height against gravity and greater path length-related resistance (Ryan et al., 2006; Bennett et al., 2015), our trees are likely too small to observe such general patterns. Accordingly, no significant relationship between tree height or branch length and hydraulic failure risk could be observed.

Our data disentangle the importance of sheer tree size (height and DBH) as an important measure for large forest trees when compared to the structural complexity ( $D_b$ ) of a tree that already relates to hydraulic risk at very low tree heights investigated here (compare Figure 4.4 and Figure 4.9, Chapter 4). We argue that two trees with the same height and DBH but different  $D_b$  would respond differently to drought stress. All other things being equal, a tree with higher  $D_b$  would suffer higher drought stress than a tree with lower  $D_b$  due to an increased crown network area and xylem vessel size in the more complex crown bearing a greater photosynthetic area, accordingly, greater hydraulic resistance in the system. However, our trees were all rather young (~12 years) and still rather small (<10 m in height), which makes the height-imposed increase in force and friction rather unlikely. While species-specific functional traits certainly result in different responses to drought stress because of varying vessel systems and branch sizes across the species (Olson et al., 2012; Hajek et al., 2014; Arseniou et al., 2021a), our findings indicate that across various species, the complexity of the hydraulic architecture and the greater photosynthetic area associated with a greater  $D_b$  (e.g., Seidel et al., 2019b), relate directly to an increased risk of hydraulic failure. A higher total leaf area consequently results in a greater water demand, mirrored by the observed close positive relationship between branch hydraulic efficiency and the complexity of the crown. Across the similar-aged temperate trees of our sample, species with a more complex crown had branches with a higher specific hydraulic conduc-

tivity ( $K_s$ ) to support a greater total leaf area (cf. Seidel et al., 2019b) at the cost of xylem safety. The  $D_b$  integrates all architectural patterns, like the branch angles, branch numbers, branch length, crown surface area, crown volume, DBH, height, and many other tree architectural attributes, and translates them into a single physiologically meaningful number (Seidel et al., 2019b). Conventional measures of tree size quantify this insufficiently, further supporting our third hypothesis. Our data indicate that future studies should focus on the complexity of the hydraulic system. The conductive path length and the complexity of the hydraulic system, described not only by the box-dimension (first hypothesis) but also by the branching angles (second hypothesis), were shown to be related to xylem safety. Hence, as indicated earlier, these complex tree architectural attributes, in particular  $D_b$ , in regular times contribute to higher vigour and strength of the trees (e.g., Seidel et al., 2019b). However, in times of severe droughts, they become a liability, resulting in greater water demand to sustain the ecophysiological processes. Overall, tree species with high structural complexity (high  $D_b$  values) developed an efficient but vulnerable xylem compared to species with lower structural complexity (low  $D_b$  values), which developed embolism-resistant xylem at the cost of hydraulic efficiency (Figure 4.4, 4.5, Chapter 4). In this sense, future research could investigate whether species occurring in more water-stressed environments are then selected to evolve simpler architectural attributes.

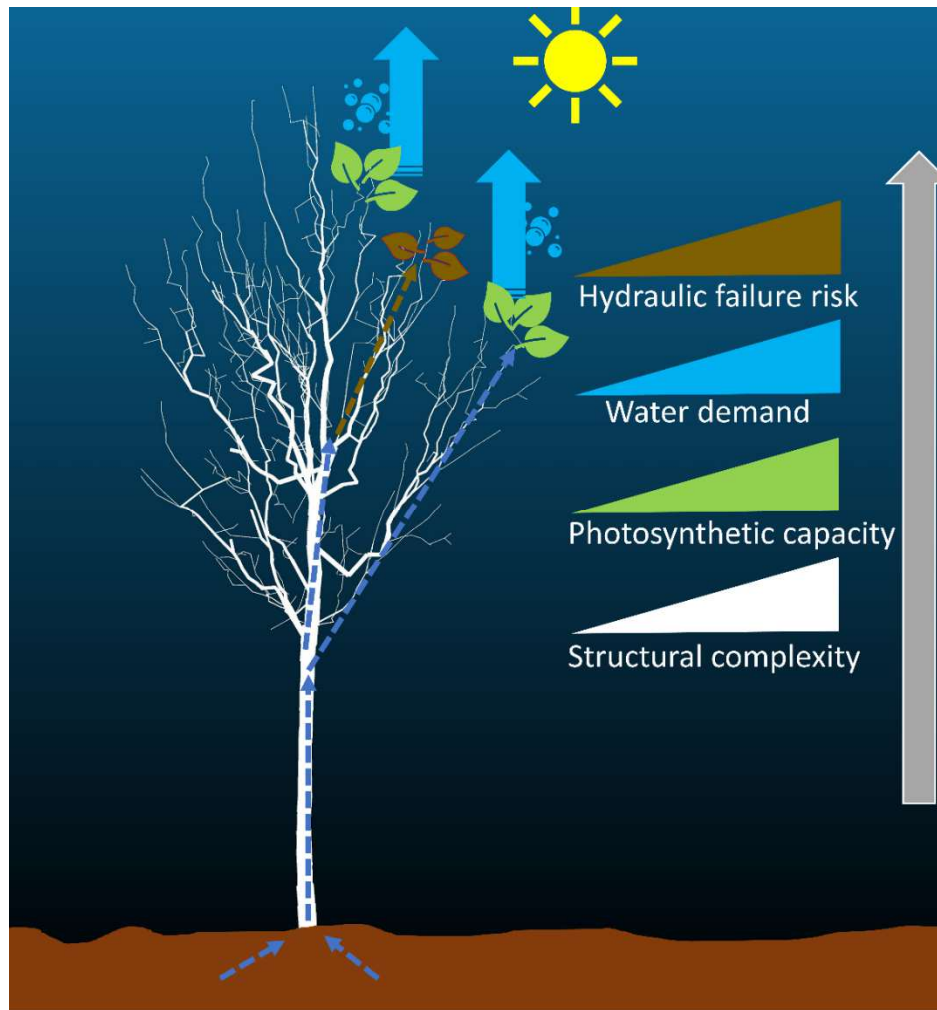


**Figure 5.1** Quantitative structure model of a real-world *Acer platanoides* tree obtained from terrestrial laser scanning (white tree skeleton) with schematic illustrations of water transport, the photosynthetic apparatus, an embolized branch, and the causal explanation for overall hydraulic failure risk (right).

It is important to stress that our data were obtained from trees growing in isolation (without competition for light or space). In closed forests, microclimate and shading might alter the effects observed here. However, some patterns observed here apply equally to forest trees, for example, the observed relationship between the branch angles and hydraulic vulnerability. We argue that a reduced gravitational resistance exists when branches are more horizontal (flatter and lower angles). This helps explain why branching geometry plays a

significant role not only in light interception but also in C and water flow between trees and the atmosphere (Enquist et al., 2009; Forrester et al., 2018).

Finally, tree species (or provenances of the same species) of lower  $D_b$  might be favoured for plantation in drought-prone regions (or provenances) rather than species with higher  $D_b$  because the latter might be vulnerable to more stress and disturbance when exposed to drought. This holds true if the architecture of the vessel system and other factors, such as the enzymatic control of water transport, are comparable.

#### **5.4 Limitations of LiDAR systems**

Laser scanning has become a popular tool for forestry applications, providing high-resolution, three-dimensional measurements of forest canopy structures. However, there are limitations to using LiDAR that should be considered when designing a study or interpreting results.

One of the main limitations of laser scanning in forestry is the occlusion effect (Daum et al., 2020). This is when trees or other vegetation block the laser beams from reaching their intended target. Nevertheless, with the development of mobile laser scanners, such effects have been minimized (Bauwens et al., 2016). The same is evident for ALS, where vertical side structures are not detected, and understory vegetation is occluded (Hilker et al., 2010). The use of TLS in dense forest blocks or "shadows" nearby trees, which increases the inaccuracy of tree exclusion at the forest boundary (Liu et al., 2018; Potter, 2019). However, a multi-scan can minimize this inaccuracy, but doing so requires more time and resources since targets must be defined beforehand, and co-registration of multiple scans is needed (Bauwens et al., 2016). Potter (2019) added that TLS has a limited sensor range and generates more noise as one gets further away from the scanner.

In addition to hardware limitations, weather conditions like precipitation (rain, fog, snow) and windy conditions lead to noisy data acquisition (Hilker et al., 2010). Hence it should only be employed in calm weather (Griebel et al., 2015).

In general, the LiDAR equipment and data processing cost can be expensive depending on specifications and its use for small or large areas (Tilley et al., 2004).



## 5.5 Conclusion and outlook

Fractal analysis is a mathematical method for analyzing the complexity and self-similarity of patterns found in nature and other systems (Mandelbrot 1977; Zeide & Gresham 1991). It has a vast potential to provide valuable insights into tree architecture. To fully understand how trees interact with their environment (biotic and abiotic), it is important to understand the complex and fractal-like nature of tree architecture. In all our studies (Chapters 2 to 4), we used the box-dimension approach of fractal analysis to translate the tree's structural complexity into single numbers and relate it with various parameters to further our understanding of the drivers and passengers of tree architecture. The details of the fractal analysis to derive box-dimension( $D_b$ ), self-similarity, and  $D_b$ -Intercept can be found in topic 2.2.4 of Chapter 2 (also see figure 2.4, Chapter 2); topic 3.2.7 of Chapter 3, and topic 4.2.4 of Chapter 4 of this dissertation.

Open-grown trees, which are not crowded by other vegetation, are the best subjects for studying the fractal-like architecture of trees (Arseniou & MacFarlane, 2021). Our experimental site at Stutel-arboretum had such settings (See figure 4.1, Chapter 4), where trees were grown in open exposure without competition (Paper 1 and paper 2). Our findings demonstrated that trees' structural complexity (fractal-like characteristics) are linked to their functional and inherent qualities and are influenced by the local as well as the original habitat environment (Dorji et al., 2021)

The use of TLS and MLS data has facilitated a deeper understanding of the complexity of tree architecture, including the role of various structural elements in creating intricate fractal designs and how the above-ground crown area is shaped (Seidel et al., 2019b, Neudam et al., 2022). This information has been valuable in improving our overall understanding of trees. However, due to the intricate nature of fractal analysis approaches, the innate complexity of tree structures, and the range of metrics that may be employed, it presents difficulties for future research (Murray et al., 2018). Contingent on the particular feature of tree architecture being investigated, the accuracy of the LiDAR data and the methods used to analyze them can considerably influence the reliability of tree models. Another challenge is interpreting the results of the analysis in a biological context (Arseniou et al., 2021b); While fractal analysis can provide useful insights into the structure of trees, it is important

to consider other factors, such as genetics, growth conditions, and functional characteristics, in order to fully understand the tree's architecture (Dorji et al., 2021). However, the expected advancement of new LiDAR systems and algorithms presents opportunities for enhancing the precision and effectiveness of tree modeling. Additionally, comparative research and multiscale analysis across various species, different growth conditions (such as managed and unmanaged stands), and various geographical regions can offer significant insights into the structure and function of trees (Dassot et al., 2011; Dorji et al., 2019). Another potential area of research is in forestry and conservation (Narine et al. 2019), such as forecasting forest growth and productivity, accurately projecting carbon storage (Calders et al., 2022), monitoring tree health, and exploring the impact of environmental changes on trees.

One significant outlook we can look forward to is in the field of thermodynamics, and its relation to the structural complexity of trees and forest stands. Seidel (2022) argues that considering thermodynamic theory into account in forest ecosystem research has enormous potential for providing a coherent interpretation of the effects of forest structural complexity. According to the paper, higher structural complexity is linked to increased photosynthetic capacity in forests, which is correlated with optimized thermodynamic processes. Given the challenges caused by climate change, an ecosystem's potential for adaptation has to be given more emphasis (Seidel, 2022). If an ecosystem's structural complexity can be defined and calculated, its potential for adaptation may be extrapolated and predicted. These potential linkages need to be corroborated by more studies, and that is where the LiDAR and fractal analysis can play significant roles in investigations and interpretation. Based on 3D LiDAR technology (terrestrial, mobile, and aerial laser scanning) and fractal analysis approach, it is now feasible to quantify the entire structural complexity of trees and forests (Atkins et al., 2018; Seidel et al., 2020; Ehbrecht et al., 2021, Neudam et al., 2022).

Overall, the combination of LiDAR technology and fractal analysis has the potential to revolutionize the way we study and understand tree architecture. By using LiDAR to accurately and efficiently measure tree structure and applying fractal analysis to quantify the complexity of that structure, we can gain a deeper understanding of how trees grow and func-

tion. This knowledge can be applied in a variety of fields, including forestry, agriculture, and ecology. Eventually, LiDAR and fractal analysis in tree architecture research will likely become widespread, significantly advancing our comprehension of tree architecture and leading to new insights and discoveries.

## 5.6 References

- Atkins, J. W., Bohrer, G., Fahey, R. T., Hardiman, B. S., Morin, T. H., Stovall, A. E., ... & Gough, C. M. (2018). Quantifying vegetation and canopy structural complexity from terrestrial LiDAR data using the `forestr` package. *Methods in Ecology and Evolution*, 9(10), 2057-2066.
- Archibald, S., & Bond, W. J. (2003). Growing tall vs growing wide: tree architecture and allometry of *Acacia karroo* in forest, savanna, and arid environments. *Oikos*, 102(1), 3-14.
- Arseniou, G., & MacFarlane, D. W. (2021a). Fractal dimension of tree crowns explains species functional-trait responses to urban environments at different scales. *Ecological Applications*, 31(4), e02297.
- Arseniou, G., MacFarlane, D. W., & Seidel, D. (2021b). Measuring the Contribution of Leaves to the Structural Complexity of Urban Tree Crowns with Terrestrial Laser Scanning. *Remote Sensing*, 13(14), 2773.
- Bauwens, S., Bartholomeus, H., Calders, K., & Lejeune, P. (2016). Forest inventory with terrestrial LiDAR: A comparison of static and hand-held mobile laser scanning. *Forests*, 7(6), 127.
- Bayer, D., Seifert, S., & Pretzsch, H. (2013). Structural crown properties of Norway spruce (*Picea abies* [L.] Karst.) and European beech (*Fagus sylvatica* [L.]) in mixed versus pure stands revealed by terrestrial laser scanning. *Trees*, 27(4), 1035-1047.
- Bazzaz, F. A. (1975). Plant species diversity in old-field successional ecosystems in southern Illinois. *Ecology*, 56(2), 485-488.
- Bennett, A. C., McDowell, N. G., Allen, C. D., & Anderson-Teixeira, K. J. (2015). Larger trees suffer most during drought in forests worldwide. *Nature plants*, 1(10), 1-5.
- Bomfleur, B., Decombeix, A. L., Escapa, I. H., Schwendemann, A. B., & Axsmith, B. (2013). Whole-plant concept and environment reconstruction of a *Telemachus conifer* (Voltziales) from the Triassic of Antarctica. *International Journal of Plant Sciences*, 174(3), 425-444.
- Bongers, F. J. (2020). Functional-structural plant models to boost understanding of complementarity in light capture and use in mixed-species forests. *Basic and Applied Ecology*, 48, 92-101.
- Borchert, R., & Slade, N. A. (1981). Bifurcation ratios and the adaptive geometry of trees. *Botanical gazette*, 142(3), 394-401.
- Calders, K., Phinn, S., Ferrari, R., Leon, J., Armston, J., Asner, G. P., & Disney, M. (2020). 3D imaging insights into forests and coral reefs. *Trends in ecology & evolution*, 35(1), 6-9.
- Dassot, M., Constant, T., & Fournier, M. (2011). The use of terrestrial LiDAR technology in forest science: application fields, benefits and challenges. *Annals of forest science*, 68(5), 959-974.
- Daum, A., Goetz, S., Köhl, M., & Koch, B. (2020). The occlusion effect of trees on laser scanning point clouds. *ISPRS International Journal of Geo-Information*, 9(3), 132.
- Dorji, Y., Annighöfer, P., Ammer, C., & Seidel, D. (2019). Response of beech (*Fagus sylvatica* L.) trees to competition—New insights from using fractal analysis. *Remote Sensing*, 11(22), 2656.
- Dorji, Y., Schuldt, B., Neudam, L., Dorji, R., Middleby, K., Isasa, E., ... & Seidel, D. (2021). Three-dimensional quantification of tree architecture from mobile laser scanning and geometry analysis. *Trees*, 35(4), 1385-1398.
- Ehbrecht, M., Seidel, D., Annighöfer, P., Kreft, H., Köhler, M., Zemp, D. C., ... & Ammer, C. (2021). Global patterns and climatic controls of forest structural complexity. *Nature communications*, 12(1), 1-12.
- Enquist, B. J., West, G. B., & Brown, J. H. (2009). Extensions and evaluations of a general quantitative theory of forest structure and dynamics. *Proceedings of the National Academy of Sciences*, 106(17), 7046-7051.
- Fajardo, A., & Piper, F. I. (2021). How to cope with drought and not die trying: drought acclimation across tree species with contrasting niche breadth. *Functional Ecology*, 35(9), 1903-1913.

- Forrester, D. I., Ammer, C., Annighöfer, P. J., Barbeito, I., Bielak, K., Bravo-Oviedo, A., ... & Pretzsch, H. (2018). Effects of crown architecture and stand structure on light absorption in mixed and monospecific *Fagus sylvatica* and *Pinus sylvestris* forests along a productivity and climate gradient through Europe. *Journal of Ecology*, *106*(2), 746-760.
- Griebel, A., Bennett, L. T., Culvenor, D. S., Newnham, G. J., & Arndt, S. K. (2015). Reliability and limitations of a novel terrestrial laser scanner for daily monitoring of forest canopy dynamics. *Remote Sensing of Environment*, *166*, 205-213.
- Hajek, P., Leuschner, C., Hertel, D., Delzon, S., & Schuldt, B. (2014). Trade-offs between xylem hydraulic properties, wood anatomy and yield in *Populus*. *Tree physiology*, *34*(7), 744-756
- Henning, J. G., & Radtke, P. J. (2006). Ground-based laser imaging for assessing three-dimensional forest canopy structure. *Photogrammetric Engineering & Remote Sensing*, *72*(12), 1349-1358.
- Hilker, T., van Leeuwen, M., Coops, N. C., Wulder, M. A., Newnham, G. J., Jupp, D. L., & Culvenor, D. S. (2010). Comparing canopy metrics derived from terrestrial and airborne laser scanning in a Douglas-fir dominated forest stand. *Trees*, *24*(5), 819-832.
- Horn, H. S. (1971). *The adaptive geometry of trees*. Princeton University Press.
- Ishii, H. T., Tanabe, S. I., & Hiura, T. (2004). Exploring the relationships among canopy structure, stand productivity, and biodiversity of temperate forest ecosystems. *Forest Science*, *50*(3), 342-355.
- Iwasa, Y. O. H., Cohen, D. A. N., & Leon, J. A. (1985). Tree height and crown shape, as results of competitive games. *Journal of theoretical Biology*, *112*(2), 279-297.
- Juchheim, J., Annighöfer, P., Ammer, C., Calders, K., Raunonen, P., & Seidel, D. (2017). How management intensity and neighborhood composition affect the structure of beech (*Fagus sylvatica* L.) trees. *Trees*, *31*(5), 1723-1735.
- Kuuluvainen, T. (1992). Tree architectures adapted to efficient light utilization: is there a basis for latitudinal gradients? *Oikos*, 275-284.
- Mandelbrot, B. (1977). *Fractals*. San Francisco: Freeman.
- Malhi, Y., Jackson, T., Patrick Bentley, L., Lau, A., Shenkin, A., Herold, M., ... & Disney, M. I. (2018). New perspectives on the ecology of tree structure and tree communities through terrestrial laser scanning. *Interface Focus*, *8*(2), 20170052.
- McDowell, N. G., & Allen, C. D. (2015). Darcy's law predicts widespread forest mortality under climate warming. *Nature Climate Change*, *5*(7), 669-672.
- Minamino, R., & Tateno, M. (2014). Tree branching: Leonardo da Vinci's rule versus biomechanical models. *PloS one*, *9*(4), e93535.
- Murray, J., Blackburn, G. A., Whyatt, J. D., & Edwards, C. (2018). Using fractal analysis of crown images to measure the structural condition of trees. *Forestry: An International Journal of Forest Research*, *91*(4), 480-491.
- Narine, L. L., Popescu, S., Neuenschwander, A., Zhou, T., Srinivasan, S., & Harbeck, K. (2019). Estimating aboveground biomass and forest canopy cover with simulated ICESat-2 data. *Remote Sensing of Environment*, *224*, 1-11.
- Neudam, L., Annighöfer, P., & Seidel, D. (2022). Exploring the Potential of Mobile Laser Scanning to Quantify Forest Structural Complexity. *Frontiers in Remote Sensing*, *3*.
- Oliver, C. D., & Larson, B. C. (1996). *Forest stand dynamics: Updated edition*. John Wiley and sons.
- Potter, T. L. (2019). *Mobile laser scanning in forests: Mapping beneath the canopy* (Doctoral dissertation, University of Leicester).

- Qian, C., Liu, H., Tang, J., Chen, Y., Kaartinen, H., Kukko, A., ... & Hyypä, J. (2016). An integrated GNSS/INS/LiDAR-SLAM positioning method for highly accurate forest stem mapping. *Remote Sensing*, 9(1), 3.
- Ryan, M. G., Phillips, N., & Bond, B. J. (2006). The hydraulic limitation hypothesis revisited. *Plant, Cell & Environment*, 29(3), 367-381.
- Schröter, M., Härdtle, W., & von Oheimb, G. (2012). Crown plasticity and neighborhood interactions of European beech (*Fagus sylvatica* L.) in an old-growth forest. *European Journal of Forest Research*, 131(3), 787-798.
- Seidel, D. (2018). A holistic approach to determine tree structural complexity based on laser scanning data and fractal analysis. *Ecology and evolution*, 8(1), 128-134.
- Seidel, D. (2022). Towards a causal understanding of the relationship between structural complexity, productivity and adaptability of forests based on principles of thermodynamics. *Authorea Preprints*.
- Seidel, D., Annighöfer, P., Ehbrecht, M., Magdon, P., Wöllauer, S., & Ammer, C. (2020). Deriving stand structural complexity from airborne laser scanning data—what does it tell us about a forest?. *Remote Sensing*, 12(11), 1854.
- Seidel, D., Annighöfer, P., Stiers, M., Zemp, C. D., Burkardt, K., Ehbrecht, M., ... & Ammer, C. (2019a). How a measure of tree structural complexity relates to architectural benefit-to-cost ratio, light availability, and growth of trees. *Ecology and evolution*, 9(12), 7134-7142.
- Seidel, D., Ehbrecht, M., Dorji, Y., Jambay, J., Ammer, C., & Annighöfer, P. (2019b). Identifying architectural characteristics that determine tree structural complexity. *Trees*, 33(3), 911-919.
- Stovall, A. E., Shugart, H., & Yang, X. (2019). Tree height explains mortality risk during an intense drought. *Nature Communications*, 10(1), 1-6.
- Tews, J., Brose, U., Grimm, V., Tielbörger, K., Wichmann, M. C., Schwager, M., & Jeltsch, F. (2004). Animal species diversity driven by habitat heterogeneity/diversity: the importance of keystone structures. *Journal of biogeography*, 31(1), 79-92.
- Tilley, B. K., Munn, I. A., Evans, D. L., Parker, R. C., & Roberts, S. D. (2004). Cost considerations of using LiDAR for timber inventory. *Southern Forest Economics Workers. Online papers*.
- Tyree, M. T., & Zimmermann, M. H. (2013). *Xylem structure and the ascent of sap*. Springer Science & Business Media.
- Valladares, F., & Niinemets, Ü. (2007). The architecture of plant crowns: from design rules to light capture and performance. In *Functional plant ecology* (pp. 101-150). CRC Press.
- Valladares, F., Gianoli, E., & Gómez, J. M. (2007). Ecological limits to plant phenotypic plasticity. *New phytologist*, 176(4), 749-763.
- Whitmore, T. C. (1984). *Tropical rain forests of the Par East*. Oxford. Clarendon Press.
- Williams, K., Olsen, M. J., Roe, G. V., & Glennie, C. (2013). Synthesis of transportation applications of mobile LiDAR. *Remote Sensing*, 5(9), 4652-4692.
- Zeide, B., & Gresham, C. A. (1991). Fractal dimensions of tree crowns in three loblolly pine plantations of coastal South Carolina. *Canadian Journal of Forest Research*, 21(8), 1208-1212.

## List of Tables

**Table 2.1.** Major characteristics of the 24 investigated beech trees (adapted from Metz et al. (2013). DBH = Diameter at breast height (1.3 m). HAI = Hainich Dün, SCH = Schorfheide Chorin, ALB = Swabian Alb.

**Table 2.2** All tested attributes of tree architecture and their relationship with competition strength.

**Table 3.1** Summary of all investigated trees, the number of samples per species/cultivar, mean box-dimension ( $D_b$ ), mean height, mean latitude of origin, respective seed dispersal strategy, and mean annual radial increment as a measure of growth. Abbreviation 'n.a.' refers to missing data. "Not included" indicates the species' seed dispersal strategy was not relying on a single mechanism or the mechanism could not be identified.

**Table 4.1** Summary of all investigated tree species: the number of individual trees in each species, mean box-dimension ( $D_b$ ), mean height (**TTH**), mean diameter at breast height (**DBH**), mean crown volume (**CV**), mean crown surface area (**CSA**), and total mean number of branches (1<sup>st</sup>, 2<sup>nd</sup>, and 3<sup>rd</sup> order branches). Measurement units are given within parentheses.

## List of Figures

**Figure 1.1** Hand-held mobile scanning device (ZEB HORIZON, GepSLAM, 2019) used in this study.

**Figure 1.2** A tripod-mounted Faro Focus 3D TLS (Faro Focus M70 Terrestrial Laser Scanner) that is placed 1.3 meters above the ground at the Stutel Arboretum.

**Figure 1.3** Shows the various box sizes, commencing with the largest box, which is the smallest bounding box encompassing the whole tree, and moving on to gradually smaller boxes.

**Figure 2.1.** Study areas within Germany (left side) and sampling design (right side).

**Figure 2.2** Example of a study tree point cloud (**left**), the corresponding quantitative structure model (**middle**) and a close-up of the quantitative structure model (**right**).

**Figure 2.3.** Exemplary three-dimensional tree point clouds with a high box-dimension (**left**:  $D_b$ : 2.02) and a low box-dimension (**right**:  $D_b$ : 1.50). Box-dimension is considered a measure of structural complexity.

**Figure 2.4** Explanatory graph on the calculation of the three tested measures from fractal analysis, namely box-dimension ( $D_b$ ), intercept of the regression line ( $D_b$ -intercept) and the coefficient of determination of the regression line (self-similarity).

**Figure 2.5** Scatterplots of architectural features (A = total length of 1<sup>st</sup> order branches; B = range of 2<sup>nd</sup> order branch angles; C = box dimension ( $D_b$ ); D = intercept of box dimension) with GAM and explained deviance (DevEx), respectively, of beech trees in dependence of competition strength as cumulative crown surface area (CCSA [ $m^2$ ]). Black solid lines show significant GAM models, the effective degrees of freedom (EDF) for all models was 1, suggesting linear within-data relationships.

**Figure 2.6** Scatterplots of  $D_b$ -Intercept against conventional measures of tree size (A = diameter at breast height (DBH (cm)); B = total tree height (TTH (m)) and crown morphology (C = Crown radius (m); D = Crown volume ( $m^3$ )) with GAM and explained deviance (DevEx), respectively, of beech trees. Black solid lines show significant GAM models; the dashed grey line shows insignificant model. The effective degree of freedom (EDF) for all models was 1, suggesting linear within data relationships.

**Figure 3.1.** Map of Germany with the location of the research site at Stutel arboretum, Würzburg, Germany, and an aerial view of the arboretum (Google Earth, 2013) with the three study plots chosen for our scanning campaign.

**Figure 3.2** Exemplary picture of trees of two rows after processing a mobile scan in GeoSlam Hub. The red line indicates the trajectory of the device during scanning with the loop being closed for each scan at the front left (start and end at beginning of row). Two tree rows were always scanned at a time by a zig-zagging walking path trajectory surrounding each tree in the two rows

**Figure 3.3** Exemplary cleaned and filtered 3D point cloud of an Elm tree (*Ulmus*) obtained from mobile laser scanning

**Figure 3.4** Example objects for box-dimension minimum (box-dimension: 1.0 = pole, topological dimension is also 1) and maximum (box-dimension: 3.0 = cube, topological dimension is also 3). For trees, examples are shown for 1.11 (lowest value observed in our study), 1.54, 1.86 and 2.29 (highest value observed in our study)



**Figure 3.5** Scatterplot of relative height of maximum horizontal crown area (Rel.Hmaxarea) over mean absolute latitude (latitudinal mid-point) of each species origin. The coefficient of determination ( $R^2$ ) was 0.052 but significant with  $p < 0.05$ ;  $n = 83$  species (mean values per species)

**Figure 3.6** Box-and-Whisker plot of trees of different seed dispersal strategies namely, wind ( $n = 192$ ) and animal ( $n = 130$ ) dispersed. The difference in means was significant at  $p < 0.001$  (animal-dispersed mean: 1.87; wind-dispersed mean: 1.95)

**Figure 3.7** Scatterplot of annual radial increment as a measure of growth over the box-dimension and GAM regression. The relationship is significant at  $p < 0.001$ ; adjusted  $R^2 = 0.364$ ; effective degrees of freedom (EDF) = 2.58. Growth data were available for  $n = 391$  tree individuals. Dev.ex. = deviation explained.

**Figure 4.1** Showing the map and location of the research site at Stutel, Wuerzburg, Germany, and a photograph depicting a section of the Stutel-Arboretum.

**Figure 4.2** Showing two-dimensional depiction of a 3D point cloud of a tree in Fig. 4.2A and the corresponding Quantitative Structure Model in Figure 4.2B. A close-up of QSM in Figure 4.2C and a cylindrical demonstration of colour-coded branching patterns on the right end in Figure 4.2D. Adapted and modified from Dorji et al., (2019).

**Figure 4.3** Two exemplary three-dimensional tree point clouds with the highest (left) and lowest (right) box-dimension ( $D_b$ ) values observed in our research study. On the left is a *Tilia cordata* tree ( $D_b = 2.04$ ); on the right is an individual of *Crataegus persimilis* ( $D_b = 1.55$ ).

**Figure 4.4** Scatter plots showing the correlation between the mean structural complexity of the tree species represented by the box-dimension ( $D_b$ ) and **(A)**  $P_{12}$  (MPa), **(B)**  $P_{50}$  (MPa), and **(C)**  $P_{88}$  (MPa). The data were available and analyzed for  $n = 18$  tree species (with a mean of 3-4 individuals per species). Regression lines are shown as solid black lines indicating significant relationships for all at  $p < 0.05$ , with Spearman's rank correlation ranging from  $r = 0.51$  to  $0.53$ .

**Figure 4.5** Results of simple species-level linear regressions of box-dimension ( $D_b$ ) in relation to **A)** Specific conductivity ( $K_s$ ,  $\text{kg m}^{-1} \text{MPa}^{-1} \text{s}^{-1}$ ) and **B)** Hydraulically-weighted vessel

diameter ( $D_h$ ,  $\mu\text{m}$ ). Shown are the species level averages with the model predictions  $\pm$  95% confidence bands.

**Figure 4.6** Scatter plot for the three measures of xylem safety ( $P_{12}$ ,  $P_{50}$ ,  $P_{88}$ ; MPa) over mean of mean branch angle (MeanBRangle [ $^\circ$ ]) of 1<sup>st</sup> order branches (**A**, **B**, **C**); MeanBRangle [ $^\circ$ ] of 2<sup>nd</sup> order branches (**D**, **E**, **F**) and 3<sup>rd</sup> order branches (**G**, **H**, **I**) of all species (shown as mean values). Black solid lines indicate significant relationships and dashed grey lines indicate non-significant relationships (**A**, **B**, **C**). Spearman's rank correlations ranged from  $r = 0.34$  to 0.55;  $n = 18$  Species.

**Figure 4.7** Scatter plots of the three measures of xylem safety (**A**:  $P_{12}$ , **B**:  $P_{50}$ , **C**:  $P_{88}$ ; MPa) against the Crown Surface Area (CSA, [ $\text{m}^2$ ]) of all the studied trees (mean per species). Similarly, the scatterplots (**D**), (**E**) and (**F**) show a correlation between different mean xylem pressure,  $P_{12}$ ,  $P_{50}$ , and  $P_{88}$ , with the Crown Volume (CV), respectively. Regression lines are shown as dashed lines indicating non-significant (N.S). The data were available and analyzed for  $n = 18$  species. Spearman's rank correlations ranged from  $r = 0.27$  to 0.44.

**Figure 4.8** Scatter plots of the three measures of xylem safety (**A**:  $P_{12}$ , **B**:  $P_{50}$ , **C**:  $P_{88}$ ; MPa) against total branch length (TotalBRlength [m]). Similarly, the scatterplots (**D**), (**E**), (**F**) show the relationship between xylem safety measures ( $P_{12}$ ,  $P_{50}$ ,  $P_{88}$ ) over the Mean Number of branches of all tree species, respectively. All the above data were available and analyzed for  $n = 18$  species of 71 tree individuals. Regression lines are shown as dashed grey lines to indicate non-significant relationships.

**Figure 4.9** Scatter plot of the three measures of xylem safety (**A**:  $P_{12}$ , **B**:  $P_{50}$ , **C**:  $P_{88}$ ; MPa) in dependence of the diameter at breast height (DBH [cm]) of all the study trees ( $n = 18$  species of 71 individuals). Similarly, the scatterplots (**D**), (**E**) and (**F**) show correlations between different xylem pressure,  $P_{12}$ ,  $P_{50}$ ,  $P_{88}$ , in dependence of the total tree height (TTH [m]), respectively. The dashed grey lines show non-significant relationships.

## Acknowledgment

I would first like to thank the members of my thesis committee: - Prof. Dr. Dominik Seidel, Prof. Dr. Peter Annighöfer, Prof. Dr. Christian Ammer and Prof. Dr. Holger Kreft for their constructive feedback, helpful suggestions, and valuable insights, which have greatly improved the quality of this work. Most of all, they made themselves available from their busy schedule whenever I called for meetings or sought guidance throughout my doctoral study. Their expertise, patience, and professionalism have been an inspiration to me.

I want to express my particular gratitude to my principal supervisor Prof. Dr. Dominik Seidel, for taking me in as his doctoral student. Thank you for your guidance and support throughout my Ph.D. journey. You have been like a family to me, Dendup and Yeshey, giving us a home away from home in Göttingen, Germany. I will treasure the opportunity I got to work with you; you are always there to offer your wisdom and insights and provide a safe and conducive environment for me to grow and learn. I will definitely take this quality of yours as a teacher and impart it to my students. I am truly grateful for all that you have done for me, and I am so proud to have come this far under your supervision. *Namey Samey Kadrinche* (Thank you beyond sky and earth)

I am deeply grateful to my friends and colleagues from the Department of Silviculture and Forest Ecology of the Temperate Zones and Dept. for Spatial Structures and Digitization of Forests, who were always so fun in everyday life and helpful in navigating academic life during my entire stay. In particular, I would like to thank my office mates, Liane, Kati, Vien, Laura, Katha, Amani, Kristen, Max, Ieva, Martin, Steffi and Ray, for their friendship, encouragement, and endless hours of discussions during coffee and lunch breaks. A special thanks to Silke Marks, who was always there to help navigate the administrative tasks and anything for that matter.

A big thanks go to my co-authors, Prof. Dr. Bernhard Schuldt and Emily, who helped me with the project and field works. Moreover, I would like to mention my friend and country-mate, Rinzin Dorji, who also provided great companionship throughout our stay.

I want to thank my Parents, brothers, and in-laws for their continuous moral and emotional support. A Special thanks to College of Natural Resources, the Royal University of Bhutan, for giving me Ph.D. study leave and accepting me back at my work as a teaching Faculty, which I love doing the most.

Last but not least, I would like to thank my wife, Yeshey Dema, for her unconditional love, support, and understanding throughout my studies. She has been there with me like a rock-solid in all walks of life, up or down. Her constant encouragement and belief in me have been a constant source of motivation and strength.

Finally, I would love to dedicate this work to my one and only daughter, Dendup Zangmo, a source of life and happiness for us. We love you!

# Curriculum Vitae

## PERSONAL INFORMATION

---

Name : Yonten Dorji  
Date of birth : 10.11.1983  
Place of birth : Wangduephodrang, Bhutan  
Academic degree : MSc. in Mountain Forestry  
Address : College of Natural Resources, 1264 Punakha, Bhutan  
Email: : yonten.dorji@uni-goettingen.de  
Phone: : +975 17919642

## Professional Experiences

---

03/2019 - 12/2022	<b>Ph.D. Candidate</b> Spatial Structures and Digitization of Forests, Göttingen University, Germany	Germany
03/2019 - 12/2020	<b>Research Associate</b> Silviculture and Forest Ecology of Temperate Zones, Göttingen University, Germany	Germany
10/2015 - 02/2019	<b>Head of the Department</b> Department of Forest Science, College of Natural Resources, Royal University of Bhutan	Bhutan
01/2010 - 09/2013	<b>Programme Leader</b> For Forest Science Programme, College of Natural Resources, Royal University of Bhutan	Bhutan
01/2009 - 09/2013	<b>Assistant Lecturer</b> Faculty of Forest Science, College of Natural Resources, Royal University of Bhutan	Bhutan

## ACADEMIC EDUCATION

---

04/2019 - today	Georg-August-University Spatial Structures and Digitization of Forest Ph.D. student in "Forest Sciences and Forest Ecology."	Germany
09/2013 - 10/2015	BOKU University, Vienna MSc. Mountain Forestry Institute of Forest Ecology	Austria
01/2005 - 03/2008	University of Queensland, Australia B.Sc. Environmental Botany Faculty of Biological Sciences	Australia

## PROJECTS

---

### 03/2019 - 03/2020 | Sorti-Scan

“Assessment of quality attributes and automated quality grading of standing trees through the use of mobile laser scanning”

Landwirtschaftliche Rentenbank (Göttingen, Lower Saxony, DE)

### 02/2018-02 to 11/2029 | CNR Grant

“Rapid assessment of roadside bird diversity in Punakha District, Bhutan.”

Royal University of Bhutan (Thimphu, BT)

### 07/2017 to 02/2019 | CNR Grant

“Assessment of nutrient from *Parthenium hysterphorus* compost using different inoculants”

Royal University of Bhutan (Thimphu, BT)

### 03/2017 to 04/2019 | AURG

“Coccinellidae diversity of Bhutan” (Insecta: Coleoptera)

Thimphu, Bhutan, BT

### 02/2017 to 04/2018 | AURG

“Assessment of Biomass, Carbon Stock and Climate Change Mitigation Potentials of *Bambusa balcooa* Bamboo.”

Royal University of Bhutan (Thimphu, Bhutan, BT)

### 09/2013 - 10/2015 | BCCAP Project | APPEAR Grant

Bhutan Climate Change Adaptation Program

Master Thesis

BOKU University (Vienna, Austria)

## SKILLS

---

Languages:           Dzongkha, Nation Language of Bhutan  
                          English, Professional command  
                          Hindi, Communication Skill  
                          Nepali, Communication Skill

Software skills:     R software, SPSS, MS Office, Faro Scene, Cloud compare, CompuTree

## PUBLICATION LIST

---

Dorji, Y., Schuldt, B., Neudam, L. *et al.* (2021) Three-dimensional quantification of tree architecture from mobile laser scanning and geometry analysis. *Trees* **35**, 1385–1398. <https://doi.org/10.1007/s00468-021-02124-9>

Sacha, N., Dorji, Y., Nepal, N., Choden, S., Ghally, TB., Dendup, KC. (2021) Regeneration status and soil nutrient content in blue pine forest in Thimphu, Western Bhutan. *Indonesian Journal of Social and Environmental Issues (IJSEI)*, 2 (1), 48-58. <https://doi.org/10.47540/ijsei.v2i1.201>

Sherub. K, Jambay. J, Dorji. Y, Gyelpo. T, Wangda. L. (2020) A pictorial guide to roadside Avifauna of Punakha District, Bhutan - A field guide. College of Natural Resources, Royal University of Bhutan

**Dorji Y**, Annighöfer P, Ammer C, Seidel D (2019): Response of beech (*Fagus sylvatica* L.) trees to competition- new insights from using fractal analysis. *Remote Sensing* 11 (22): 2656. DOI: 10.3390 / rs11222656

Seidel D, Ehbrecht M, **Dorji Y**, Jambay J, Ammer C, Annighöfer P (2019) Identifying architectural characteristics that determine tree structural complexity. *Trees* 33: 911-919. DOI: 10.1007 / s00468-019-01827-4

Wangdi N, **Dorji Y**, Om K, Nirola MP (2018). Reducing the Vulnerability of Bhutan's Forests to the Expected Impacts of Climate Change. Policy Brief. UWICER Policy Brief Series 2018: No.1, Ministry of Agriculture and Forestry, Bhutan.

Yonten S, **Dorji Y**. Influence of forest fire frequency on nest-site selection and nest-use by White-bellied heron (*Ardea insignis*) at Athang Gewog under Wangdiphodrang Dzongkhag (2017). Royal Society for Protection of Nature, Bhutan.

**Dorji Y**, Godbold, DL (2016). The Effects of Experimental Drought on the Fine Root Biomass of Two Different Altitudinal Forests of Bhutan. Master's Dissertation. University of Natural Resources and Life Sciences (BOKU), Vienna, Austria.